

**EXPERIMENT ON SLIDING AND FLOATING OF
WOODEN BLOCKS IN SWASH ZONE ON SAND
BEACH**

BY

XAVIER CHÁVEZ CÁRDENAS AND NOBUHISA KOBAYASHI

RESEARCH REPORT NO. CACR-15-08
NOVEMBER 2015



CENTER FOR APPLIED COASTAL RESEARCH

Ocean Engineering Laboratory
University of Delaware
Newark, Delaware 19716

ACKNOWLEDGMENTS

During a 9-month Ph.D. study at the University of Delaware, X. Chavez Cardenas was supported by the Mexican Scholarship Program CONACYT. This study was partially supported by the U.S. Army Corps of Engineers under Cooperative Agreement No. W912HZ-15-2-0028. The authors would like to thank Rebecca Quan for her contribution to this experiment at the beginning of this study.

TABLE OF CONTENTS

LIST OF TABLES	vi
LIST OF FIGURES	xiv
ABSTRACT	xix
1 INTRODUCTION	1
2 EXPERIMENT	3
2.1 Experimental Setup	3
2.1.1 Wave Tank and Wave Maker	3
2.1.2 Sediment Characteristics and Profile	3
2.1.3 Measurement Instruments	4
2.1.3.1 Hydrodynamics	5
2.1.3.2 Profile Evolution and Block Locations	6
2.1.3.3 Overtopping and Overwash	6
2.2 Blocks	8
2.2.1 Friction Coefficient	9
2.3 Eight Tests	12
2.3.1 Test Procedures	14
2.4 Similitude	17
3 DATA ANALYSIS	19
3.1 Blocks on Ground	20
3.1.1 Hydrodynamics	20
3.1.2 Overtopping and Overwash	32
3.1.3 Profile Evolution	34
3.1.4 Foreshore and Berm Accretion or Erosion	35
3.1.5 Block Movement	44
3.2 Blocks on Long Pilings	53
3.2.1 Hydrodynamics	53
3.2.2 Overtopping and Overwash	66
3.2.3 Profile Evolution	69

3.2.4	Foreshore and Berm Accretion or Erosion	69
3.2.5	Block Movement	78
3.3	Blocks on Short Pilings	92
3.3.1	Hydrodynamics.....	92
3.3.2	Overtopping and Overwash.....	101
3.3.3	Profile Evolution	102
3.3.4	Foreshore and Berm Accretion or Erosion.....	103
3.3.5	Block Movement	109
3.4	Block Effects on Hydrodynamics.....	119
4	BLOCK MOVEMENT ANALYSIS.....	125
4.1	Block Elevation Above Still Water Level.....	125
4.2	Block Sliding and Floating Probabilities.....	129
5	CONCLUSIONS	145
	REFERENCES	147
	Appendix	149
	ADDITIONAL DATA	149

LIST OF TABLES

Table 2.1.	Sediment characteristics.	4
Table 2.2.	Wave gauge locations (WG1-WG8) and velocimeter locations (ADV; Red-Vectrino, RV; and Blue-Vectrino, BV).	5
Table 2.3.	Block characteristics.	9
Table 2.4.	Friction coefficients.	11
Table 2.5.	Eight tests and three test series.	14
Table 2.6.	Model vs Prototype.	18
Table 3.1.	Incident wave characteristics, LG.	21
Table 3.2.	Incident wave characteristics, MG.	22
Table 3.3.	Incident wave characteristics, HG.	22
Table 3.4.	Mean free-surface elevation $\bar{\eta}$ (cm) at 7 wave gauge locations, LG.	23
Table 3.5.	Mean free-surface elevation $\bar{\eta}$ (cm) at 7 wave gauge locations, MG.	23
Table 3.6.	Mean free-surface elevation $\bar{\eta}$ (cm) at 7 wave gauge locations, HG.	24
Table 3.7.	Free-surface standard deviation σ_{η} (cm) at 7 wave gauge locations, LG.	24
Table 3.8.	Free-surface standard deviation σ_{η} (cm) at 7 wave gauge locations, MG.	25
Table 3.9.	Free-surface standard deviation σ_{η} (cm) at 7 wave gauge locations, HG.	25
Table 3.10.	Wet probability P_w , its mean free-surface elevation $\bar{\eta}$ (cm), and free-surface standard deviation σ_{η} (cm) for WG8, LG.	26
Table 3.11.	Wet probability P_w , its mean free-surface elevation $\bar{\eta}$ (cm), and free-surface standard deviation σ_{η} (cm) for WG8, MG.	27
Table 3.12.	Wet probability P_w , its mean free-surface elevation $\bar{\eta}$ (cm), and free-surface standard deviation σ_{η} (cm) for WG8, HG.	28

Table 3.13.	Mean cross-shore \bar{u} and standard deviation σ_u of the 2D ADV co-located with WG4 at $x = 8.30$ m, Red Vectrino co-located with WG5 at $x = 12.90$ m and Blue Vectrino co-located with WG6 at $x = 15.50$ m, LG. .	29
Table 3.14.	Mean cross-shore \bar{u} and standard deviation σ_u of the 2D ADV co-located with WG4 at $x = 8.30$ m, Red Vectrino co-located with WG5 at $x = 12.90$ m and Blue Vectrino co-located with WG6 at $x = 15.50$ m, MG.	30
Table 3.15.	Mean cross-shore \bar{u} and standard deviation σ_u of the 2D ADV co-located with WG4 at $x = 8.30$ m, Red Vectrino co-located with WG5 at $x = 12.90$ m and Blue Vectrino co-located with WG6 at $x = 15.50$ m, HG. .	31
Table 3.16.	Measured sediment overwash rate q_{bs} , water overtopping rate q_o , and their ratio q_{bs}/q_o , LG.	32
Table 3.17.	Measured sediment overwash rate q_{bs} , water overtopping rate q_o , and their ratio q_{bs}/q_o , MG.	33
Table 3.18.	Measured sediment overwash rate q_{bs} , water overtopping rate q_o , and their ratio q_{bs}/q_o , HG.	33
Table 3.19.	Cumulative volume changes (cm^3/cm): eroded V_e , and deposited V_d sand volumes, net volume change V_c , cumulative sand overwash volume V_o , offshore sand loss volume V_l as well as the ratios $V_l/ V_c $ and $V_o/ V_c $ for the zone $x = 16$ to 19.9 m, LG.	36
Table 3.20.	Maximum erosion depth and deposition height at cross-shore location x , and bottom elevation change Δz_b at WG7 and WG8 locations, LG.	36
Table 3.21.	Cumulative volume changes (cm^3/cm): eroded V_e , and deposited V_d sand volumes, net volume change V_c , cumulative sand overwash volume V_o , offshore sand loss volume V_l as well as the ratios $V_l/ V_c $ and $V_o/ V_c $ for the zone $x = 16$ to 19.9 m, MG.	38
Table 3.22.	Maximum erosion depth and deposition height at cross-shore location x , and bottom elevation change Δz_b at WG7 and WG8 locations, MG.	38
Table 3.23.	Cumulative volume changes (cm^3/cm): eroded V_e , and deposited V_d sand volumes, net volume change V_c , cumulative sand overwash volume V_o , offshore sand loss volume V_l as well as the ratios $V_l/ V_c $ and $V_o/ V_c $ for the zone $x = 16$ to 19.9 m, HG.	40
Table 3.24.	Maximum erosion depth and deposition height at cross-shore location x , and bottom elevation change Δz_b at WG7 and WG8 locations, HG.	40

Table 3.25.	Block response during each of 10 runs in test LG.....	46
Table 3.26.	Location of 10 blocks during test LG with initial still water shoreline location $x_{SWL} = 17.88$ m.....	46
Table 3.27.	Block response during each of 10 runs in test MG.	49
Table 3.28.	Location of 10 blocks during test MG with initial still water shoreline location $x_{SWL} = 18.13$ m.....	49
Table 3.29.	Block response during each of 5 runs in test HG.	51
Table 3.30.	Location of 10 blocks during test HG with initial still water shoreline location $x_{SWL} = 18.40$ m.....	52
Table 3.31.	Incident wave characteristics, LL.....	54
Table 3.32.	Incident wave characteristics, ML.....	55
Table 3.33.	Incident wave characteristics, HL.	55
Table 3.34.	Mean free-surface elevation $\bar{\eta}$ (cm) at 7 wave gauge locations, LL.	56
Table 3.35.	Mean free-surface elevation $\bar{\eta}$ (cm) at 7 wave gauge locations, ML.	56
Table 3.36.	Mean free-surface elevation $\bar{\eta}$ (cm) at 7 wave gauge locations, HL.....	57
Table 3.37.	Free-surface standard deviation σ_{η} (cm) at 7 wave gauge locations, LL.	57
Table 3.38.	Free-surface standard deviation σ_{η} (cm) at 7 wave gauge locations, ML.	58
Table 3.39.	Free-surface standard deviation σ_{η} (cm) at 7 wave gauge locations, HL.	58
Table 3.40.	Wet probability P_w , its mean free-surface elevation $\bar{\eta}$ (cm), and free- surface standard deviation σ_{η} (cm) for WG8, LL.	59
Table 3.41.	Wet probability P_w , its mean free-surface elevation $\bar{\eta}$ (cm), and free- surface standard deviation σ_{η} (cm) for WG8, ML.	60
Table 3.42.	Wet probability P_w , its mean free-surface elevation $\bar{\eta}$ (cm), and free- surface standard deviation σ_{η} (cm) for WG8, HL.	61

Table 3.43.	Mean cross-shore \bar{u} and standard deviation σ_u of the 2D ADV co-located with WG4 at $x = 8.30$ m, Red Vectrino co-located with WG5 at $x = 12.90$ m and Blue Vectrino co-located with WG6 at $x = 15.50$ m, LL...	63
Table 3.44.	Mean cross-shore \bar{u} and standard deviation σ_u of the 2D ADV co-located with WG4 at $x = 8.30$ m, Red Vectrino co-located with WG5 at $x = 12.90$ m and Blue Vectrino co-located with WG6 at $x = 15.50$ m, ML..	64
Table 3.45.	Mean cross-shore \bar{u} and standard deviation σ_u of the 2D ADV co-located with WG4 at $x = 8.30$ m, Red Vectrino co-located with WG5 at $x = 12.90$ m and Blue Vectrino co-located with WG6 at $x = 15.50$ m, HL. .	65
Table 3.46.	Measured sediment overwash rate q_{bs} , water overtopping rate q_o , and their ratio q_{bs}/q_o , LL.	67
Table 3.47.	Measured sediment overwash rate q_{bs} , water overtopping rate q_o , and their ratio q_{bs}/q_o , ML.	67
Table 3.48.	Measured sediment overwash rate q_{bs} , water overtopping rate q_o , and their ratio q_{bs}/q_o , HL.	68
Table 3.49.	Cumulative volume changes (cm^3/cm): eroded V_e , and deposited V_d sand volumes, net volume change V_c , cumulative sand overwash volume V_o , offshore sand loss volume V_l as well as the ratios $V_l/ V_c $ and $V_o/ V_c $ for the zone $x = 16$ to 19.9 m, LL.	70
Table 3.50.	Maximum erosion depth and deposition height at cross-shore location x , and bottom elevation change Δz_b at WG7 and WG8 locations, LL.....	70
Table 3.51.	Cumulative volume changes (cm^3/cm): eroded V_e , and deposited V_d sand volumes, net volume change V_c , cumulative sand overwash volume V_o , offshore sand loss volume V_l as well as the ratios $V_l/ V_c $ and $V_o/ V_c $ for the zone $x = 16$ to 19.9 m, ML.	72
Table 3.52.	Maximum erosion depth and deposition height at cross-shore location x , and bottom elevation change Δz_b at WG7 and WG8 locations, ML.	72
Table 3.53.	Cumulative volume changes (cm^3/cm): eroded V_e , and deposited V_d sand volumes, net volume change V_c , cumulative sand overwash volume V_o , offshore sand loss volume V_l as well as the ratios $V_l/ V_c $ and $V_o/ V_c $ for the zone $x = 16$ to 19.9 m, HL.	74
Table 3.54.	Maximum erosion depth and deposition height at cross-shore location x , and bottom elevation change Δz_b at WG7 and WG8 locations, HL.	74

Table 3.55.	Block response during each of 10 runs in test LL.	81
Table 3.56.	Location of 10 blocks during test LL with initial still water shoreline location $x_{SWL} = 17.86$ m.....	81
Table 3.57.	Clearance C (cm) during each run, LL.	83
Table 3.58.	Block response during each of 10 runs in test ML.....	85
Table 3.59.	Location of 10 blocks during test ML with initial still water shoreline location $x_{SWL} = 18.19$ m.....	85
Table 3.60.	Clearance C (cm) during each run, ML.....	87
Table 3.61.	Block response during each of 10 runs in test HL.....	89
Table 3.62.	Location of 10 blocks during test HL with initial still water shoreline location $x_{SWL} = 18.40$ m.....	89
Table 3.63.	Clearance C (cm) during each run, HL.....	91
Table 3.64.	Incident wave characteristics, LS.	93
Table 3.65.	Incident wave characteristics, MS.	93
Table 3.66.	Mean free-surface elevation $\bar{\eta}$ (cm) at 7 wave gauge locations, LS.	94
Table 3.67.	Mean free-surface elevation $\bar{\eta}$ (cm) at 7 wave gauge locations, MS.....	94
Table 3.68.	Free-surface standard deviation σ_{η} (cm) at 7 wave gauge locations, LS.	95
Table 3.69.	Free-surface standard deviation σ_{η} (cm) at 7 wave gauge locations, MS.	95
Table 3.70.	Wet probability P_w , its mean free-surface elevation $\bar{\eta}$ (cm), and free- surface standard deviation σ_{η} (cm) for WG8, LS.....	96
Table 3.71.	Wet probability P_w , its mean free-surface elevation $\bar{\eta}$ (cm), and free- surface standard deviation σ_{η} (cm) for WG8, MS.	97
Table 3.72.	Mean cross-shore \bar{u} and standard deviation σ_u of the 2D ADV co-located with WG4 at $x = 8.30$ m, Red Vectrino co-located with WG5 at $x =$ 12.90 m and Blue Vectrino co-located with WG6 at $x = 15.50$ m, LS. ..	99

Table 3.73.	Mean cross-shore \bar{u} and standard deviation σ_u of the 2D ADV co-located with WG4 at $x = 8.30$ m, Red Vectrino co-located with WG5 at $x = 12.90$ m and Blue Vectrino co-located with WG6 at $x = 15.50$ m, MS.100	
Table 3.74.	Measured sediment overwash rate q_{bs} , water overtopping rate q_o , and their ratio q_{bs}/q_o , LS.	101
Table 3.75.	Measured sediment overwash rate q_{bs} , water overtopping rate q_o , and their ratio q_{bs}/q_o , MS.	102
Table 3.76.	Cumulative volume changes (cm^3/cm): eroded V_e , and deposited V_d sand volumes, net volume change V_c , cumulative sand overwash volume V_o , offshore sand loss volume V_l as well as the ratios $V_l/ V_c $ and $V_o/ V_c $ for the zone $x = 16$ to 19.9 m, LS.	104
Table 3.77.	Maximum erosion depth and deposition height at cross-shore location x , and bottom elevation change Δz_b at WG7 and WG8 locations, LS.....	104
Table 3.78.	Cumulative volume changes (cm^3/cm): eroded V_e , and deposited V_d sand volumes, net volume change V_c , cumulative sand overwash volume V_o , offshore sand loss volume V_l as well as the ratios $V_l/ V_c $ and $V_o/ V_c $ for the zone $x = 16$ to 19.9 m, MS.	106
Table 3.79.	Maximum erosion depth and deposition height at cross-shore location x , and bottom elevation change Δz_b at WG7 and WG8 locations, MS.....	106
Table 3.80.	Block response during each of 10 runs in test LS.	112
Table 3.81.	Location of 10 blocks during test LS with initial still water shoreline location $x_{SWL} = 17.84$ m.....	112
Table 3.82.	Clearance C (cm) during each run, LS.	114
Table 3.83.	Block response during each of 7 runs in test MS.	116
Table 3.84.	Location of 10 blocks during test MS with initial still water shoreline location $x_{SWL} = 18.20$ m.....	116
Table 3.85.	Clearance C (cm) during each run, MS.	118
Table 4.1.	Bottom elevation z_b (cm) above SWL at $t = 0$	126
Table 4.2.	Clearance C (cm) at $t = 0$	126

Table 4.3.	Block bottom elevation E (cm) above SWL at $t = 0$	127
Table 4.4.	Blocks characteristics used for block floating and sliding.	132
Table 4.5.	Floating and sliding depths calculated for clearance $C = 0$ to 4 cm.....	133
Table 4.6.	Sliding depth h_s (cm) calculated using measured C , LL.....	133
Table 4.7.	Sliding depth h_s (cm) calculated using measured C , ML.....	134
Table 4.8.	Sliding depth h_s (cm) calculated using measured C , HL.	134
Table 4.9.	Sliding depth h_s (cm) calculated using measured C , LS.....	135
Table 4.10.	Sliding depth h_s (cm) calculated using measured C , MS.....	135
Table 4.11.	Floating depth h_f (cm) calculated using measured C , LL.....	136
Table 4.12.	Floating depth h_f (cm) calculated using measured C , ML.....	136
Table 4.13.	Floating depth h_f (cm) calculated using measured C , HL.	137
Table 4.14.	Floating depth h_f (cm) calculated using measured C , LS.....	137
Table 4.15.	Floating depth h_f (cm) calculated using measured C , MS.....	138
Table A. 1.	Still water shoreline location (m) for 8 tests: before run 1 (X_{S0}), after run 5 (X_{S5}) and after run 10 (X_{S10}).	149
Table A. 2.	Wetting probability P_c , sliding probability P_s , and floating probability P_f of blocks 3 and 4, LG.	154
Table A. 3.	Wetting probability P_c , sliding probability P_s , and floating probability P_f of blocks 3 and 4, MG.	155
Table A. 4.	Wetting probability P_c , sliding probability P_s , and floating probability P_f of blocks 3 and 4, HG.	156
Table A. 5.	Wetting probability P_c , sliding probability P_s , and floating probability P_f of blocks 3 and 4, LL.	157
Table A. 6.	Wetting probability P_c , sliding probability P_s , and floating probability P_f of blocks 3 and 4, ML.	158

Table A. 7.	Wetting probability P_c , sliding probability P_s , and floating probability P_f of blocks 3 and 4, HL.	159
Table A. 8.	Wetting probability P_c , sliding probability P_s , and floating probability P_f of blocks 3 and 4, LS.	160
Table A. 9.	Wetting probability P_c , sliding probability P_s , and floating probability P_f of blocks 3 and 4, MS.	161

LIST OF FIGURES

Figure 1.1.	Wave runup beneath elevated buildings at Scituate, MA, during the December 1992 nor'easter storm. Source: Jim O'Connell, Coastal Construction Manual, fourth edition, FEMA P-55, Vol. I, August 2011..	2
Figure 2.1.	Experimental setup scheme: top view of the entire wave tank (top) and cross section view of the wave flume.....	7
Figure 2.2.	Painted and numbered blocks (a), block dimensions (b), dry mass (c), block volume (d), submerged blocks (e), and wet mass (f).....	8
Figure 2.3.	Pulling apparatus used to estimate the friction coefficient.....	10
Figure 2.4.	Block on pilings: schematic definition (left) and adjustment to ensure horizontal block surface (right).	12
Figure 2.5.	Initial block locations: top view of block placement (top); side view for test LL (middle); and side view for test LG (bottom).	13
Figure 2.6.	Profile construction (left) and surface patterns demonstrating the alongshore uniformity (middle and right)	15
Figure 2.7.	Initial block locations before tests: HG with block 1 floating and block 2 at floating limit (left), ML (middle), and MS (right).....	15
Figure 2.8.	Block zone after test LL with blocks 1, 2, and 3 removed (left) and local scour depth (right).	16
Figure 2.9.	Blocks 5 and 6 with clearance decreasing landward and buried rear pilings after run 1 of test LS (left) and pilings of blocks 5 and 6 after test LS (right).	17
Figure 3.1.	Cross-shore variations of mean $\bar{\eta}$ and standard deviation σ_{η} of free surface elevation η above SWL together with wet probability P_w for tests LG, MG, and HG.....	28
Figure 3.2.	Cross-shore variations of mean \bar{u} and standard deviation σ_u of cross-shore velocity u for tests LG, MG, and HG.	31
Figure 3.3.	Temporal variations of wave overtopping rate q_o and sand overwash rate q_{bs} for tests LG (blue), MG (red), and HG (black).	34
Figure 3.4.	Profile evolution during tests LG, MG, and HG.	35

Figure 3.5. Bottom elevation difference between initial profile and profile measured after run 5 and 10 in test LG.....	37
Figure 3.6. Bottom elevation difference between initial profile and profile measured after run 5 and 10 in test MG.....	39
Figure 3.7. Bottom elevation difference between initial profile and profile measured after run 5 in test HG.	41
Figure 3.8. Beach profile evolution for series of tests LG, MG, and HG.....	42
Figure 3.9. Comparison of beach profile evolution for tests LG, MG, and HG.	43
Figure 3.10. Swash and block interactions in each of 10 runs, along with initial and final block photos, LG.	45
Figure 3.11. Laser line scanner images during test LG: initial (left), after run 5 (right-top), and final (right-bottom).....	47
Figure 3.12. Swash and block interactions in each of 10 runs, along with initial and final block photos, MG.....	48
Figure 3.13. Laser line scanner images during test MG: initial (left), after run 5 (right-top), and final (right-bottom).....	50
Figure 3.14. Swash and block interactions in each of 5 runs, along with initial and final block photos, HG.	51
Figure 3.15. Laser line scanner images during test HG: initial (left) and final (right-bottom).	52
Figure 3.16. Response (floated, slid, and wet) of 10 blocks on ground in each run for tests LG, MG, and HG.....	53
Figure 3.17. Cross-shore variations of mean $\bar{\eta}$ and standard deviation σ_{η} of free surface elevation η above SWL together with wet probability P_w for tests LL, ML, and HL.	62
Figure 3.18. Cross-shore variations of mean \bar{u} and standard deviation σ_u of cross-shore velocity u for tests LL, ML, and HL.	66
Figure 3.19. Temporal variations of wave overtopping rate q_o and sand overwash rate q_{bs} for tests LL (blue), ML (red), and HL (black).	68
Figure 3.20. Profile evolution during tests LL, ML, and HL.....	69

Figure 3.21. Bottom elevation difference between initial profile and profile measured after run 5 and 10 in test LL.	71
Figure 3.22. Bottom elevation difference between initial profile and profile measured after run 5 and 10 in test ML.	73
Figure 3.23. Bottom elevation difference between initial profile and profile measured after run 5 and 10 in test HL.	75
Figure 3.24. Beach profile evolution for series of tests LL, ML, and HL.	76
Figure 3.25. Comparison of beach profile evolution for tests LL, ML, and HL.	77
Figure 3.26. Swash and block interactions in each of 10 runs, along with initial and final block photos, LL.	80
Figure 3.27. Laser line scanner images during test LL: initial (top), after run 5 (middle), and final (bottom).	82
Figure 3.28. Swash and block interactions in each of 10 runs, along with initial and final block photos, ML.	84
Figure 3.29. Laser line scanner images during test ML: initial (top), after run 5 (middle), and final (bottom).	86
Figure 3.30. Swash and block interactions in each of 10 runs, along with initial and final block photos, HL.	88
Figure 3.31. Laser line scanner images during test HL: initial (top), after run 5 (middle), and final (bottom).	90
Figure 3.32. Response (fell, wet, and dry) of 10 blocks on long pilings in each run for tests LL, ML, and HL.	91
Figure 3.33. Cross-shore variations of mean $\bar{\eta}$ and standard deviation σ_{η} of free surface elevation η above SWL together with wet probability P_w for tests LS and MS.	98
Figure 3.34. Cross-shore variations of mean \bar{u} and standard deviation σ_u of cross-shore velocity u for tests LS, and MS.	100
Figure 3.35. Temporal variations of wave overtopping rate q_o and sand overwash rate q_{bs} for tests LS (blue), and MS (red).	102
Figure 3.36. Profile evolution during tests LS and MS.	103

Figure 3.37. Bottom elevation difference between initial profile and profile measured after run 5 and 10 in test LS.	105
Figure 3.38. Bottom elevation difference between initial profile and profile measured after run 5 and 7 in test MS.	107
Figure 3.39. Beach profile evolution for series of tests LS and MS.	108
Figure 3.40. Comparison of beach profile evolution for tests LS and MS.	109
Figure 3.41. Swash and block interactions in each of 10 runs, along with initial and final block photos, LS.	111
Figure 3.42. Laser line scanner images during test LS: initial (top), after run 5 (middle), and final (bottom).	113
Figure 3.43. Swash and block interactions in each of 7 runs, along with initial and final block photos, MS.	115
Figure 3.44. Laser line scanner images during test MS: initial (top), and after run 5 (bottom).	117
Figure 3.45. Responce (fell, wet, and dry) of 10 blocks on short pilings in each run for tests LS and MS.	118
Figure 3.46. Comparisons of q_o and q_{bs} for tests with low (L), medium (M), and high (H) water levels.	120
Figure 3.47. Beach profile evolution for 8 tests: tests G (LG, MG, and HG), tests L (LL, ML, and HL), and tests S (LS, and MS).	121
Figure 3.48. Beach profile evolution for 8 tests: tests L (LG, LL, and LS), tests M (MG, ML, and MS), and tests H (HG, and HL).	122
Figure 3.49. Cross-shore variations of the mean (left top) and standard deviation (left middle) of free surface elevation η , wet probability P_w (left bottom), and cross-shore variations of the mean (right top) and standard deviation (right bottom) of the cross-shore velocity u at the three velocimeters for the 8 tests using the average values of each test.	123
Figure 4.1. Comparisons of response (damaged, wet, and dry) of 10 blocks in each run for the 8 tests together using block elevation E above SWL normalized by incident wave height H_{m0}	127

Figure 4.2. Comparisons of response (damaged, wet, and dry) of 10 blocks in each run for tests with low, medium, and high water levels using block elevation E above SWL normalized by incident wave height H_{m0} 128

Figure 4.3. Estimated floating (P_f), sliding (P_s), and wetting (P_c) probabilities for blocks 3 and 4 (left), and slope change (right) during test LG..... 138

Figure 4.4. Estimated floating (P_f), sliding (P_s), and wetting (P_c) probabilities for blocks 3 and 4 (left), and slope change (right) during test MG..... 139

Figure 4.5. Estimated floating (P_f), sliding (P_s), and wetting (P_c) probabilities for blocks 3 and 4 (left), and slope change (right) during test HG. 139

Figure 4.6. Estimated floating (P_f), sliding (P_s), and wetting (P_c) probabilities for blocks 3 and 4 (left), and slope change (right) during the test LL. 140

Figure 4.7. Estimated floating (P_f), sliding (P_s), and wetting (P_c) probabilities for blocks 3 and 4 (left), and slope change (right) during test ML. 140

Figure 4.8. Estimated floating (P_f), sliding (P_s), and wetting (P_c) probabilities for blocks 3 and 4 (left), and slope change (right) during test HL..... 141

Figure 4.9. Estimated floating (P_f), sliding (P_s), and wetting (P_c) probabilities for blocks 3 and 4 (left), and slope change (right) during test LS. 141

Figure 4.10. Estimated floating (P_f), sliding (P_s), and wetting (P_c) probabilities for blocks 3 and 4 (left), and slope change (right) during test MS. 142

Figure 4.11. Estimated floating (P_f), sliding (P_s), and wetting (P_c) probabilities for blocks 3 and 4 for tests LG, MG, and HG (blocks 3 and 4 floated in run 1), for tests LS, MS, and HL (blocks 3 and 4 fell in run 1), and for tests LL and ML (blocks 3 and 4 did not fall during run 1-10)..... 143

Figure 4.12. Estimated probabilities (P_f for blocks on ground and P_s for blocks on pilings) compared with normalized block elevation E/H_{m0} for blocks 3 and 4. 144

ABSTRACT

A laboratory experiment consisting of eight tests was conducted in a wave flume with a sand beach to examine the movement of ten wooden blocks (idealized houses) on the foreshore and berm as well as on short and long pilings. The still water level was varied to create accretional and erosional profile changes on the foreshore and berm. The cross-shore wave transformation on the beach and the wave overtopping and overwash of the berm were measured in 71 400-s runs of irregular waves. The initial block elevation above the sand surface is shown to have little effect on the hydrodynamics, sediment transport, and profile evolution in this experiment with widely-spaced blocks. The block floating and sliding on the sand surface and the block falling from the pilings depended partly on the block elevation above the still water level but on the swash hydrodynamics and block clearance above the foreshore and berm whose profile varied during each test. A probabilistic model is developed to estimate the wetting, sliding, and floating probabilities for the block in the swash zone using the water depth measured in the vicinity of the block. The estimated probabilities are used to explain the observed block floating and falling.

Chapter 1

INTRODUCTION

The proposed research aims to improve our capabilities in predicting the interactions among storm tide, wind waves, currents, bottom sediment, and structures near and above the mean sea level (coastal hazards zone) for the measured or computed storm tide (sum of storm surge and tide) and wind waves in water depth of about 10 m. The hydrodynamics, sediment and structure interactions determine the severity and extent of beach erosion and structure damage and the consequences of a severe storm. The accurate prediction of the consequences of various severe storms is prerequisite for coastal flood risk assessment and infrastructure planning and design. The field survey of the Texas coast after Hurricane Ike by Edge *et al.* (2010) indicated the importance of structure elevation for its survival (Figure 1.1). Wooden houses with floor joists below wave crests suffered significant damage or destruction. Tomiczek, Kennedy and Rogers (2014) examined collapse limit state fragilities of wood-framed houses after Hurricane Ike. The housing freeboard and construction date as well as the wave height and current velocity were found to be important factors. On the other hand, Walling *et al.* (2014) surveyed three New Jersey coastal communities after Hurricane Sandy. One of the three communities was protected by a wide beach and high dune and suffered the least amount of flooding and structure damage. The post-storm field surveys are valuable in assessing the consequences of the severe storms but do not reveal the time-varying interactions among storm tide, wind waves, currents, sand beaches, and structures during the storms.

An experiment was performed in a wave flume to measure the time-varying interactions among the hydrodynamics, sand beach and wooden blocks (idealized wooden houses). The blocks were placed in the swash zone near and above the still water shoreline. Wave runup on the foreshore of a beach is the landward limit of the swash zone and may be predicted empirically and numerically if the foreshore profile is known (*e.g.*, Kobayashi, Pietropaolo, and Melby, 2013). However, the foreshore profile change during a storm modifies the swash hydrodynamics and block movement. Consequently, both the hydrodynamics and beach profile evolution are expected to influence the block movement in the swash zone. The experiment consisted of eight tests using ten wooden blocks on no, short and long pilings for three different water levels in the wave flume. The following sections present the experimental setup and measurements, the data analysis for the blocks placed at three different elevations above the initial beach profile, and the block movement analysis.



Figure 1.1. Wave runup beneath elevated buildings at Scituate, MA, during the December 1992 nor'easter storm. Source: Jim O'Connell, Coastal Construction Manual, fourth edition, FEMA P-55, Vol. I, August 2011.

Chapter 2

EXPERIMENT

This chapter describes the experiment conducted in the sand tank of the University of Delaware.

2.1 Experimental Setup

The initial setup of the entire wave tank is shown in Figure 2.1 and described in the followings subsections (Wave tank and wave maker, Sediment characteristic and profile, and Measurement instruments). This experimental setup was constructed by Figlus *et al.* (2011) for their dune overwash experiment.

2.1.1 Wave Tank and Wave Maker

The tests were performed in a 23 m long, 1.15 m wide flume section of the entire 30 m long, 2.5 m wide and 1.5 m high wave tank. The flume section was built with a dividing wall along the length of the middle of the wave tank to reduce the amount of fine sand, the water level change caused by wave overtopping, and seiche development in the wave tank. A piston-type wave maker generated a 400-s burst of irregular waves corresponding to a TMA spectrum. The wave maker has no capability of absorbing waves reflected from the beach. The spectral significant wave height and peak period were approximately 18 cm and 2.6 s, respectively.

2.1.2 Sediment Characteristics and Profile

The characteristics of the sand used in the experiment are summarized in Table 2.1.

Table 2.1. Sediment characteristics.

Unified Soil Classification System (USCS)	SP (poorly graded sand)
Color	Light brown
Grain shape	Subangular to subrounded
d_{16}, d_{50}, d_{84}	0.124 mm, 0.183 mm, 0.221 mm
d_{10}, d_{30}, d_{60}	0.117 mm, 0.146 mm, 0.194 mm
Uniformity coefficient, C_u , and coefficient of curvature C_c	1.7, 0.9
Specific gravity, s ; porosity, n_p ; and average fall velocity, w_f	2.6, 0.4, 2.0 cm/s

The sand was placed on a plywood bottom of a 1/30 slope in order to reduce the quantity of sand required to build the beach. The initial beach profile (Figure 2.1) was a semi-equilibrium beach profile in the surf zone after preliminary tests before the experiment. The foreshore with an approximate 1/8 slope and the berm were deformed during each test. The placed sand was moistened and compacted after the beach and berm profile was rebuilt. This profile represents a barrier beach with no dune.

A rock embankment at the far end of the tank reduced wave reflection and seiching development in the wave tank.

2.1.3 Measurement Instruments

The instruments used to measure the hydrodynamics, profile evolution, and block locations as well as wave overtopping and overwash are explained in the following.

2.1.3.1 Hydrodynamics

Free surface elevations above the still water level (SWL) were measured by eight capacitance wave gauges (WG1-WG8) located along the center line in the 1.15-m wide wave flume as listed in Table 2.2. Where x = onshore coordinate with $x = 0$ at WG1 and y = alongshore coordinate with $y = 0$ along the flume center line. WG1, WG2, and WG3 situated well outside the surf zone were used to separate incident and reflected waves as well as to monitor the repeatability of 400-s runs. WG4 was in the breaker zone. WG5, WG6, and WG7 were in the surf zone. WG8 on the foreshore was in the swash zone.

Table 2.2. Wave gauge locations (WG1-WG8) and velocimeter locations (ADV; Red-Vectrino, RV; and Blue-Vectrino, BV).

Wave Gauge	WG1	WG2	WG3	WG4	WG5	WG6	WG7	WG8
x (m)	0.00	0.25	0.95	8.30	12.90	15.50	17.10	18.60
y (m)	0.00	0.00	0.00	0.00	0.00	0.00	0.00	0.00
Velocity Gauge				ADV	RV	BV		
x (m)				8.30	12.90	15.50		
y (m)				0.15	0.15	0.12		
z (m)				$-2d/3$	$-2d/3$	$-2d/3$		

d = local water depth at the start of each run.

z = vertical coordinate with $z = 0$ at SWL.

Fluid velocities were recorded by three acoustic Doppler velocimeters (one 2D ADV and two 3D Vectrinos) at the location indicated in Table 2.2 and Figure 2.1. The velocimeters were adjusted vertically after each 400-s run to measure the velocities at an elevation of one-third of the local water depth above the bottom which varied with time.

2.1.3.2 Profile Evolution and Block Locations

A laser line scanner mounted on a motorized cart was used to record alongshore transects at 2-cm cross-shore intervals with a vertical accuracy of ± 1 mm, yielding three-dimensional bathymetry of the surface bed in the zone of $x = 5$ to 19.9 m after lowering the water level.

An array of three submerged ultrasonic transducers was used to record three cross-shore transects for the submerged portion of the sand bed ($x = 0$ to 5 m).

The block locations were obtained scanning in detail the block zone by alongshore transects at 2 mm cross-shore intervals, in contrast to 2 cm for the case of the entire beach profile.

2.1.3.3 Overtopping and Overwash

A practical system consisting of a collection basin, a sand trap, a wave gauge (WG9), and an automatic pump with a flow meter allowed the measurement of the overtopping rate and overwash rate averaged over each 400-s run. The mixture of water and sand transported over the impermeable vertical wall located at $x = 19.9$ m during each 400-s run was separated by the sand trap. The trap was made of a polyester fabric mesh that retained sediment diameter exceeding 0.074 mm. The increased water volume in the collection basin was measured using both WG9 and a mechanical float. The water recirculation system maintained a constant water volume in the tank during each test.

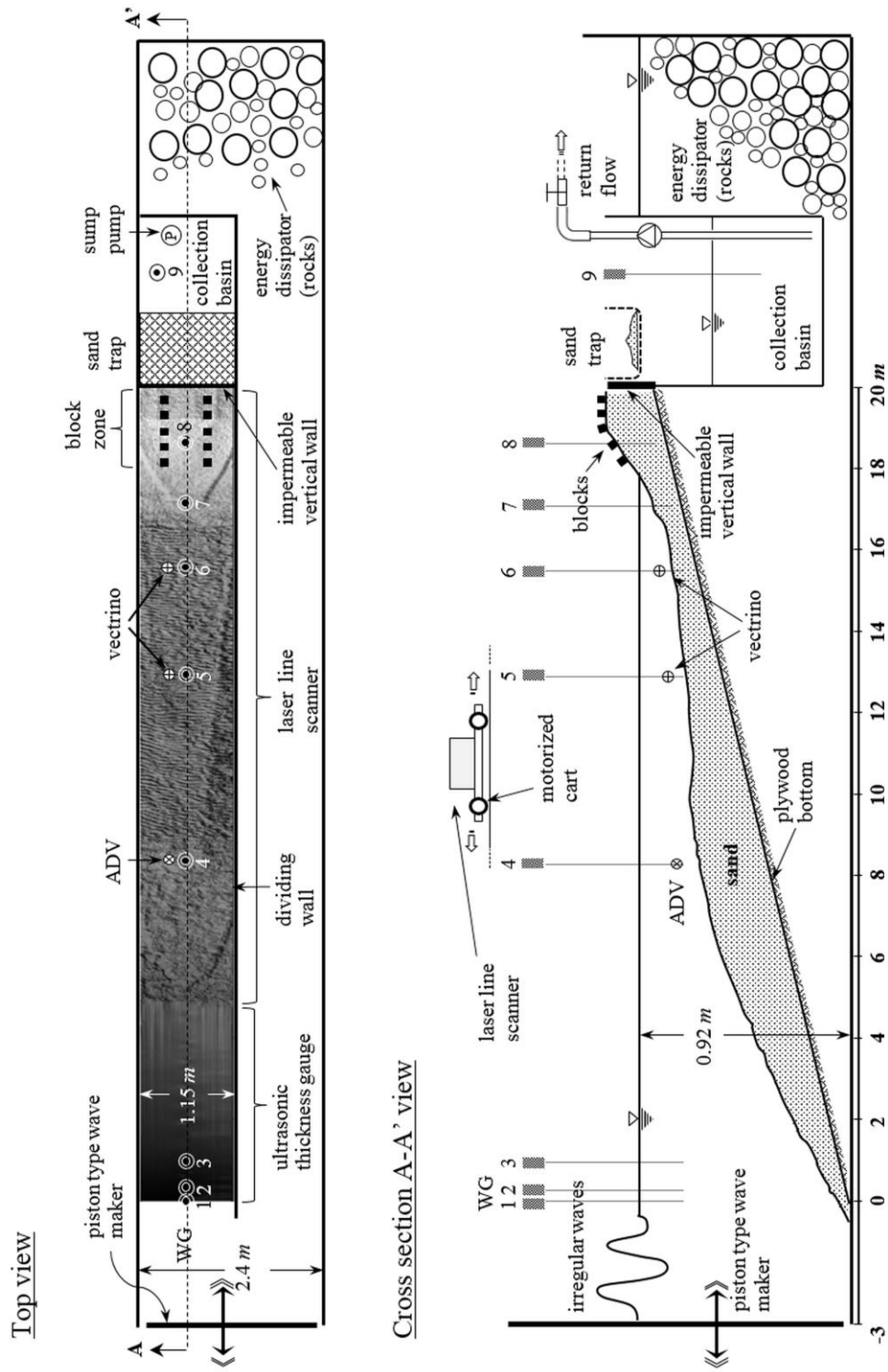


Figure 2.1. Experimental setup scheme: top view of the entire wave tank (top) and cross section view of the wave flume.

2.2 Blocks

Ten wooden blocks were used as model houses. These blocks were created sawing approximately 8.3-cm long sections from a wooden beam of 8.9 cm width and 3.8 cm thickness. In order to differentiate the blocks, each block was colored differently and numbered on its top face. An arrow was drawn on each block to indicate its seaward side facing wave uprush.

The alongshore width B , cross-shore length L , thickness T , and dry mass M_d of each block were measured to detect the slight variations of the ten block characteristics (Figure 2.2 and Table 2.3). The average values were $B = 8.9$ cm, $L = 8.3$ cm, $T = 3.8$ cm, and $M_d = 118$ g. The block volume $V = BLT$ was found to be the same as the displaced water volume of each block submerged in water briefly. The ten blocks were submerged in water with density $\rho = 1.0$ g/cm³ for a day to estimate the degree of water absorption (Figure 2.2e). The wet mass M_w of each block was measured and the average value was $M_w = 157$ g. The characterization sequence, shown in Figure 2.2, finished with the calculation of the block porosity.

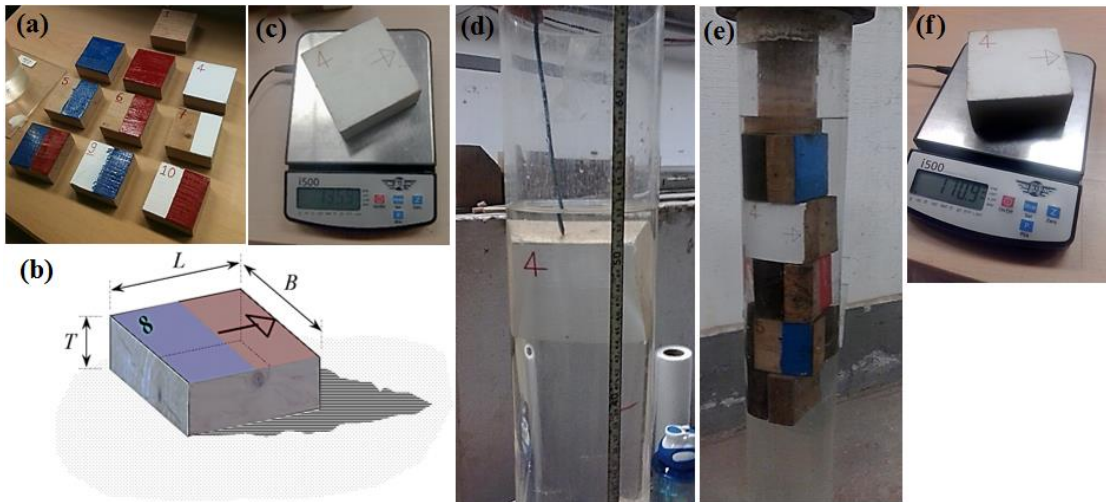


Figure 2.2. Painted and numbered blocks (a), block dimensions (b), dry mass (c), block volume (d), submerged blocks (e), and wet mass (f).

The porosity of each block was estimated as the ratio between the absorbed water volume $(M_w - M_d)/\rho$ and the block volume V . The average porosity was 0.15.

The block characterization results are presented in the following table.

Table 2.3. Block characteristics.

Color	Block	T (cm)	B (cm)	L (cm)	M_d (g)	V (cm³)	M_w (g)	Porosity
no color	1	3.9	8.9	8.2	127.4	271.8	150.8	0.09
all blue	2	3.9	8.9	8.1	127.2	263.3	149.4	0.08
all red	3	3.8	8.8	8.3	96.2	263.3	148.6	0.20
all white	4	3.8	8.8	8.2	135.9	263.3	170.9	0.13
blue+no color	5	3.9	9.0	8.3	130.6	271.8	155.8	0.09
red+no color	6	3.9	8.9	8.2	128.6	271.8	154.1	0.09
white+no color	7	3.9	8.9	8.1	137.7	254.8	173.3	0.14
blue+red	8	3.8	8.8	8.4	98.8	263.3	162.1	0.24
blue+white	9	3.7	8.8	8.5	97.0	263.3	153.3	0.21
red+white	10	3.8	8.8	8.4	98.4	263.3	153.5	0.21
average		3.8	8.9	8.3	118.0	265.0	157.2	0.15

2.2.1 Friction Coefficient

The friction coefficient C_f for block sliding in the cross-shore direction was measured by pulling each block horizontally on the compacted sand in a container. A simple pulling apparatus consisted of a thread tied to the block at one end and tied to a cup at the other end. The cup was hanging vertically from a pulley in the middle of the thread to change the force direction (Figure 2.3). Dry sand was added in the cup

incrementally to initiate the block sliding. The value of C_f was measured for the dry blocks and wet blocks. The degree of saturation S of the sand underneath the block, defined as the ratio between the water and pore volumes, was varied as $S = 0, 1/3, 2/3,$ and 1. The friction coefficients for the ten dry blocks were measured before the blocks were submerged in water for a day. The measured values of C_f for the dry and wet blocks were somewhat variable for $S = 0$ and $1/3$ but practically constant for $S = 2/3$ and 1. The averaged value of C_f for $S = 2/3$ and 1 was 0.73 for the dry blocks and 0.78 for the wet blocks (Table 2.4).



Figure 2.3. Pulling apparatus used to estimate the friction coefficient.

Cylindrical wooden dowels were used as model pilings. The diameter and length of each dowel were 0.9 and 15 cm, respectively. These dowels were used by Ayat and Kobayashi (2015) as tree stems to investigate the dowel density and toppling effects on dune erosion and overwash in the flume depicted in Figure 2.1. Four dowels were

hammered into the sand vertically with cross-shore and alongshore spacing of 7 cm to support each block at its four corners. The tops of the four dowels were adjusted to ensure that the placed block was horizontal. The friction coefficient C_f for each block sliding on the tops of the four dowels was measured using the same pulling apparatus. The average value of C_f was 0.80 for the dry blocks and 0.96 for the wet blocks (Table 2.4).

Table 2.4. Friction coefficients.

Block	Dry blocks					Wet blocks				
	S				Pilings	S				Pilings
	0	1/3	2/3	1		0	1/3	2/3	1	
1	0.83	0.76	0.74	0.72	0.70	0.78	0.87	0.74	0.78	1.05
2	0.79	0.73	0.70	0.69	0.72	0.78	0.82	0.78	0.79	0.99
3	0.91	0.83	0.75	0.74	1.02	0.78	0.89	0.79	0.78	1.06
4	0.81	0.76	0.71	0.72	0.83	0.71	0.86	0.81	0.79	0.92
5	0.82	0.74	0.70	0.71	0.77	0.78	0.80	0.80	0.77	0.96
6	0.79	0.70	0.68	0.72	0.78	0.80	0.85	0.76	0.78	0.93
7	0.87	0.46	0.75	0.79	0.74	0.72	0.79	0.79	0.80	0.92
8	0.94	0.76	0.74	0.76	0.82	0.83	0.85	0.77	0.79	0.94
9	1.05	0.74	0.72	0.76	0.86	0.76	0.85	0.75	0.78	0.86
10	0.97	0.77	0.69	0.73	0.76	0.81	0.84	0.78	0.78	0.97
average	0.88	0.73	0.72	0.73	0.80	0.78	0.84	0.78	0.78	0.96

Considering the differences between the dry and wet blocks, only the wet blocks were used in the following eight tests. The ten blocks were submerged in water for a day before each test. The wet blocks were exposed to water during the test. Digital videos and photographs were used to record the movement of the ten blocks.

2.3 Eight Tests

The SWL and the block bottom elevation above the initial sand surface were varied in the eight tests. The incident waves, the initial beach profile, and horizontal block locations were kept the same in the eight tests.

Eight tests were conducted for low (L), medium (M) and high (H) water levels and for ten blocks on ground (G), short pilings (S) and long pilings (L). The three water levels corresponded to 92, 94 and 96 cm water depths above the flume bottom at the wave maker. The initial clearance C of the blocks (Figure 2.4) was 0, 2, and 4 cm for the 10 blocks in the G, S, and L tests, respectively. The blocks were placed horizontally on the four pilings (Figure 2.5).

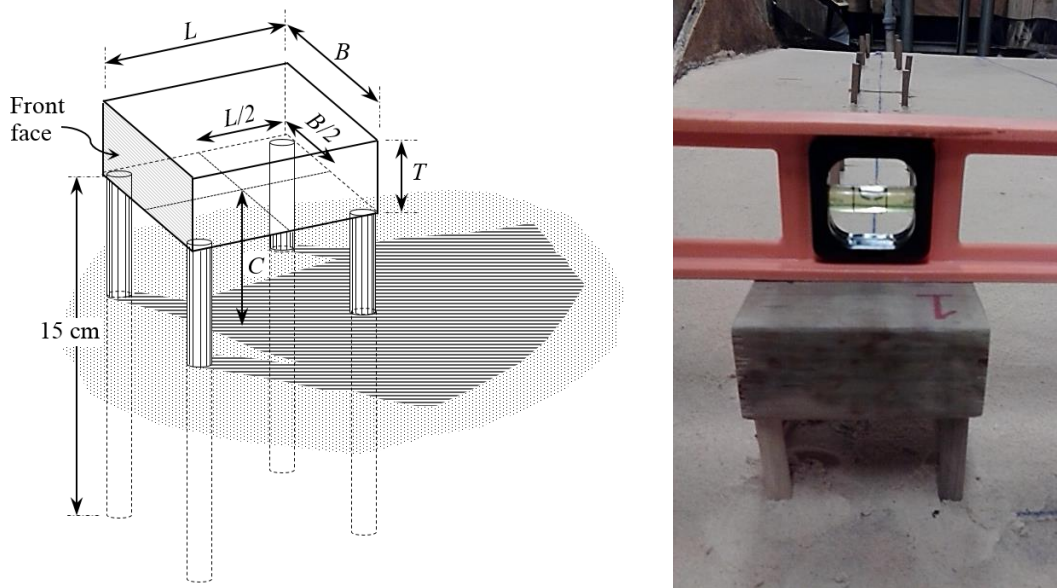


Figure 2.4. Block on pilings: schematic definition (left) and adjustment to ensure horizontal block surface (right).

The initial block locations in the cross-shore and alongshore coordinate (x , y) determined after conducting preliminary tests in order to guarantee damage to the 10

blocks on the foreshore and berm. Five rows of two blocks with an alongshore distance of 0.55 m were placed at a cross-shore interval of 0.33 m (Figure 2.5).

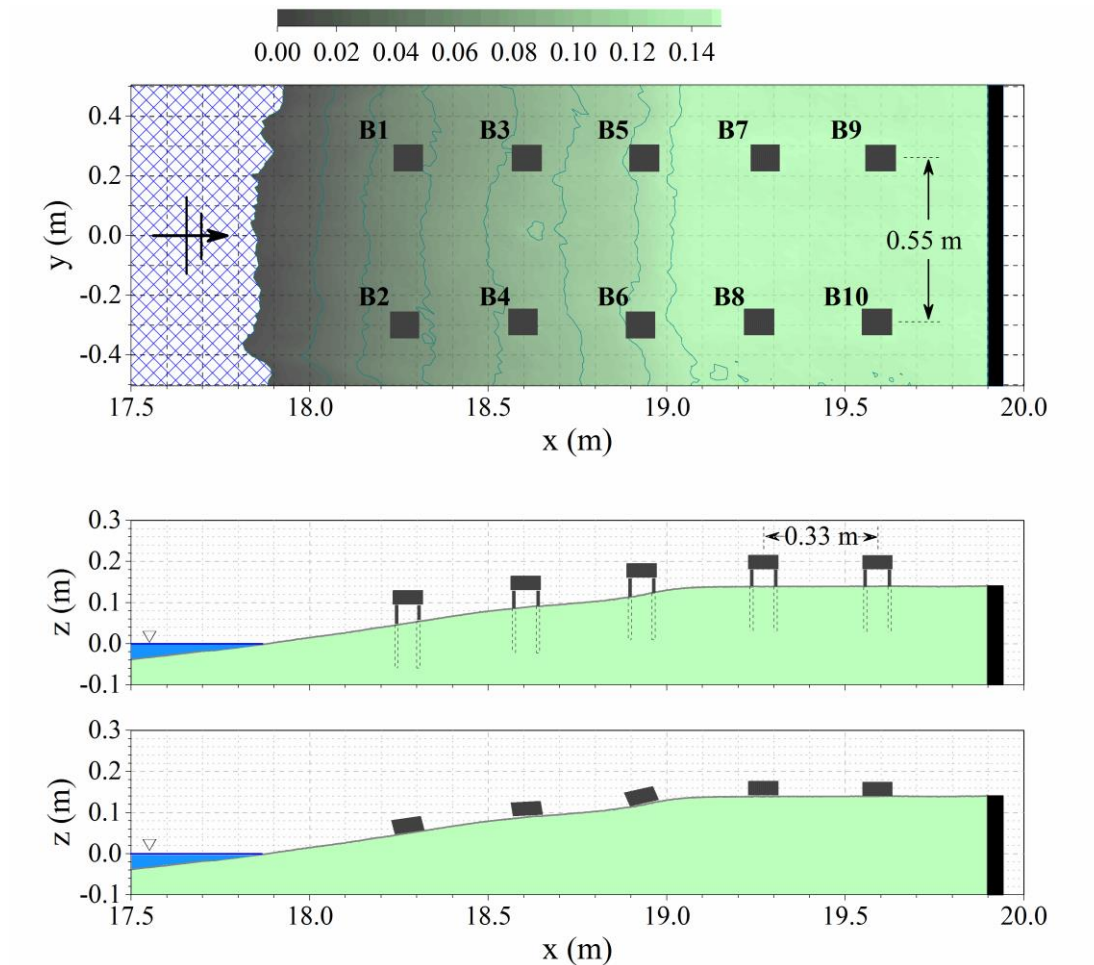


Figure 2.5. Initial block locations: top view of block placement (top); side view for test LL (middle); and side view for test LG (bottom).

The experimental sequence is summarized in Table 2.5. Each test consisted of 10 runs except for test HG (10 blocks damage after run 5) and test MS (wave maker malfunction). Each run corresponded to the 400-s burst of irregular waves with the spectral significant wave height and peak period of 18 cm and 2.6 s, respectively.

Table 2.5. Eight tests and three test series.

Tests	SWL	Blocks on:	Number of runs	Notes
LG	Low	Ground	10	Initial beach construction
MG	Medium	Ground	10	Wave maker malfunction during run 10
HG	High	Ground	5	Damage to 10 blocks
LL	Low	Long pilings	10	Rebuilding initial beach
ML	Medium	Long pilings	10	Recording file of run 3 was ruined
HL	High	Long pilings	10	
LS	Low	Short pilings	10	Rebuilding initial beach
MS	Medium	Short pilings	7	Wave maker malfunction during run 7

2.3.1 Test Procedures

The same initial profile was built before the tests LG, LL and LS. The alongshore uniformity of the beach profile was necessary in this wave flume experiment. Surface patterns (Figures 2.6 and 2.8) and pilings (Figure 2.9) were checked during each test to confirm the alongshore uniformity. During each run the free surface elevation and velocity data were collected. At the end of each run the increased water level in the collection basin and the pumped water volume as well as the collected sand mass were measured to calculate the average overtopping and overwash rate, respectively, during each run.



Figure 2.6. Profile construction (left) and surface patterns demonstrating the alongshore uniformity (middle and right)

The block interactions with wave uprush and downrush were recorded using digital videos and photographs during each run to register their responses (dry, wet, slid, floated or fell).

For the test with blocks on ground, floated blocks including those transported over the impermeable vertical wall were removed, after each run. For the blocks on pilings, fallen blocks during the run were removed to minimize block collision. The blocks were placed in their initial positions at the beginning of each test (Figure 2.7).

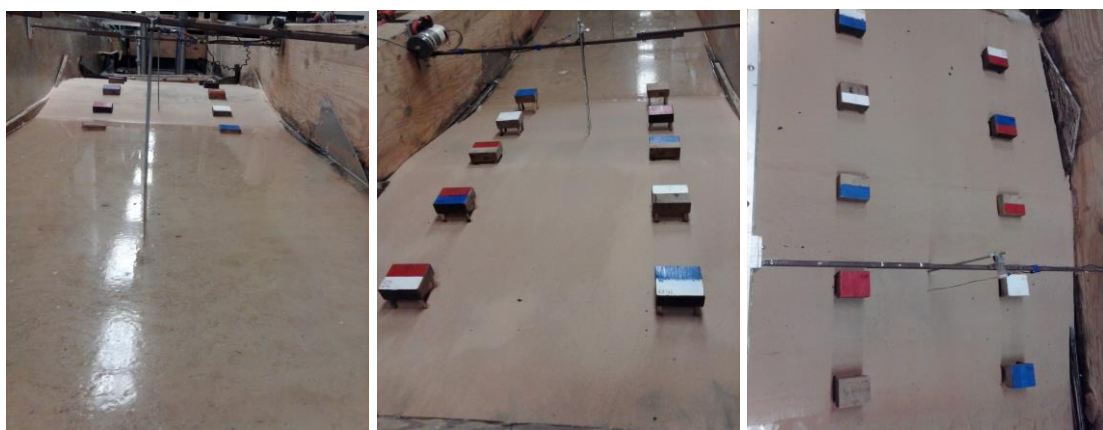


Figure 2.7. Initial block locations before tests: HG with block 1 floating and block 2 at floating limit (left), ML (middle), and MS (right).

For the tests with blocks on pilings, the clearance C was measured for all the blocks including the fallen blocks to check the profile change in the vicinity of the pilings. The block bottom elevation (or pilings top) was measured at the seaward and landward locations in the middle of the block. The local scour of about 1.0-cm depth around the four pilings occurred for some pilings (Figure 2.8). The local scour was not included in the measured clearance.



Figure 2.8. Block zone after test LL with blocks 1, 2, and 3 removed (left) and local scour depth (right).

After test LS the pilings of blocks 5 and 6 (at $x = 18.9$ m) were buried (Figure 2.9). Sand was removed to place the blocks on the pilings at the beginning of test MS. This slight adjustment modified the initial profile of test MS in the vicinity of blocks 5 and 6 somewhat.



Figure 2.9. Blocks 5 and 6 with clearance decreasing landward and buried rear pilings after run 1 of test LS (left) and pilings of blocks 5 and 6 after test LS (right).

2.4 Similitude

This experiment is not based on a specific prototype but might be regarded as a model experiment based on Froude similitude with a length ratio of the order of $1/25$ (model/prototype). The comparison of the model and prototype based on the $1/25$ ratio are presented in Table 2.6.

Table 2.6. Model vs Prototype.

Parameter	Model (cm)	Prototype (m)	Note
Water depth	92	23	offshore depth
Berm height above SWL	16	4	berm elevation
Wave height	18	4.5	storm waves
Wave period	2.6	13	storm period
Houses	8.9x8.3x3.8	2.1x2.1x0.9	small mobile houses or huts
sand			
Size	0.18 mm	4.5 mm	bed load
Fall velocity	2 cm/s (0.18 mm)	10 cm/s (0.7 mm)	suspended load

We cannot satisfy the similitude for both bed load and suspended load (4.5 mm \neq 0.7 mm) but the fine sand used in this experiment might correspond to prototype coarse sand. The wooden blocks might be regarded as small mobile houses or wooden huts. The purpose of the experiment is to investigate the time-varying interactions among the swash hydrodynamics, sand beach and berm, along with floatable objects.

Chapter 3

DATA ANALYSIS

The data collected during the experiment is presented following the sequence of the eight tests and three test series: blocks on ground; blocks on long pilings; and blocks on short pilings. For each test series: hydrodynamics, overtopping and overwash, profile evolution, foreshore and berm accretion and erosion, and block movement are presented in sequence.

The synchronized 400-s time series sampled at 20 Hz measured by the eight wave gauges and the three velocimeters were reduced by removing the initial 20-s transition period before the data analysis. The statistics are represented by the mean free surface elevation $\bar{\eta}$, the corresponding standard deviation σ_{η} , and the wet probability P_w as well as the mean cross-shore velocity \bar{u} and the velocity standard deviation σ_u . The time series from WG1 to WG3 were used to separate incident and reflected waves at the location $x = 0.0$ m of WG1. The incident waves are represented by the spectral significant wave height H_{m0} and peak period T_p as well as the zero-crossing wave parameters: the significant wave height H_s and the significant wave period T_s . The reflection coefficient R is defined as the ratio between the values of H_{m0} for the reflected and incident waves. The data from the sediment trap and the collection basin are used to obtain the sediment transport rate q_{bs} and the water overtopping rate q_o .

The profile elevation z_b was found by analyzing the laser and acoustic measurements. The measured bottom elevations were averaged alongshore to obtain the beach profile as a function of x at time t with $t = 0$ s at the beginning of each test. The vertical coordinate z is positive upward with $z = 0$ m at SWL. Each profile is identified

by its run number starting from run number 0 for the initial profile. The run number is affixed to the test name.

3.1 Blocks on Ground

Runs LG1-10, MG1-10, and HG1-5 for tests LG, MG and HG are presented in the following.

3.1.1 Hydrodynamics

Tables 3.1, 3.2, and 3.3 list the incident wave characteristics at the location $x = 0$ m of WG1. The average values of H_{m0} and T_p changed slightly probably because of the water depth change and wave generator signal adjustment. The slight variation of R is related to the foreshore slope in the three tests. The average value of R for test LG was smaller than that of test MG.

Tables 3.4 to 3.12 list the mean $\bar{\eta}$ and standard deviation σ_η of the free surface elevation η above SWL as well as the wet probability P_w at the eight wave gauges for all the runs for tests LG, MG, and HG. Figure 3.1 plots the values in the Tables 3.4 to 3.12. The gray scale is used to differentiate the values measured from run 1 (black) to run 10 (light gray) in these and subsequent figures. The measured values of $\bar{\eta}$ were negative (wave setdown) at WG1 to WG3 outside the surf zone and WG4 near the breaker zone. The value of $\bar{\eta}$ were positive (wave setup) at WG5 to WG7 in the inner surf zone and WG8 in the swash zone. The averaging for WG8 buried partially in the sand above SWL was performed for the wet duration only. The decrease of the bottom elevation at the location of WG8 contributed to the decrease of $\bar{\eta}$ during test HG. The local significant wave height is estimated at $H_{m0} = 4\sigma_\eta$. The cross-shore variation of σ_η is related to the wave height decay due to irregular wave breaking. P_w is defined as

the ratio between the wet and total duration where $P_w = 1$ at WG1 to WG7. The values of σ_η and P_w at WG8 fixed at $x = 18.6$ m increased with the increase of SWL by 2 cm (4 cm) from test LG to test MG (HG). The swash action on a fixed object increases with the decrease of the object's distance from the still water shoreline.

Figure 3.2 shows the mean \bar{u} and standard deviation σ_u of the measured cross-shore velocity u for all the runs in tests LG, MG, and HG which are listed in Tables 3.13, 3.14, and 3.15. The measured alongshore and vertical velocities were small in comparison with the cross-shore velocities in this experiment. The negative values of \bar{u} represent the offshore return current. The positive value of σ_u is related to the wave-induced oscillatory velocity. The return current and wave velocity decreased from the breaker zone to the inner surf zone. It is noted that the velocimeters could not measure the velocities in shallower depth because of its emergence in air during the 400-s run.

Table 3.1. Incident wave characteristics, LG.

Run	H_{mo} (cm)	H_{rms} (cm)	H_s (cm)	T_p (s)	T_s (s)	R
LG1	17.55	12.41	16.93	2.62	2.06	0.13
LG2	17.90	12.66	17.14	2.62	2.05	0.13
LG3	18.03	12.75	17.37	2.62	2.05	0.13
LG4	18.08	12.78	17.38	2.62	2.06	0.13
LG5	18.04	12.76	17.30	2.62	2.04	0.13
LG6	17.84	12.61	17.22	2.62	2.08	0.13
LG7	18.22	12.88	17.42	2.62	2.05	0.13
LG8	18.36	12.98	17.54	2.62	2.03	0.13
LG9	18.44	13.04	17.72	2.62	2.05	0.13
LG10	18.48	13.07	17.78	2.62	2.05	0.13
Average	18.09	12.79	17.38	2.62	2.05	0.13

Table 3.2. Incident wave characteristics, MG.

Run	H_{mo} (cm)	H_{rms} (cm)	H_s (cm)	T_p (s)	T_s (s)	R
MG1	17.67	12.50	17.06	2.64	2.14	0.16
MG2	18.17	12.85	17.48	2.64	2.10	0.19
MG3	18.30	12.94	17.62	2.64	2.09	0.18
MG4	18.45	13.04	17.89	2.64	2.11	0.20
MG5	18.37	12.99	17.60	2.64	2.10	0.18
MG6	18.05	12.76	17.30	2.64	2.10	0.18
MG7	18.25	12.91	17.49	2.64	2.11	0.18
MG8	18.26	12.91	17.65	2.64	2.12	0.16
MG9	18.23	12.89	17.58	2.64	2.12	0.17
MG10	NR	NR	NR	NR	NR	NR
Average	18.20	12.87	17.52	2.64	2.11	0.18

NR implies "not reliable" data.

Table 3.3. Incident wave characteristics, HG.

Run	H_{mo} (cm)	H_{rms} (cm)	H_s (cm)	T_p (s)	T_s (s)	R
HG1	17.78	12.57	17.07	2.57	2.09	0.15
HG2	18.03	12.75	17.32	2.57	2.12	0.15
HG3	18.19	12.86	17.39	2.57	2.11	0.15
HG4	18.25	12.91	17.36	2.57	2.07	0.15
HG5	18.25	12.90	17.46	2.57	2.08	0.15
Average	18.10	12.80	17.32	2.57	2.09	0.15

Table 3.4. Mean free-surface elevation $\bar{\eta}$ (cm) at 7 wave gauge locations, LG.

Run	WG1	WG2	WG3	WG4	WG5	WG6	WG7
LG1	-0.14	-0.21	-0.14	-0.16	0.26	0.38	0.36
LG2	-0.13	-0.16	-0.14	-0.16	0.32	0.41	0.40
LG3	-0.10	-0.15	-0.15	-0.16	0.35	0.42	0.42
LG4	-0.14	-0.12	-0.14	-0.14	0.35	0.44	0.42
LG5	-0.12	-0.13	-0.14	-0.13	0.34	0.44	0.44
LG6	-0.16	-0.16	-0.13	-0.19	0.26	0.34	0.37
LG7	-0.15	-0.16	-0.14	-0.12	0.33	0.43	0.45
LG8	-0.11	-0.12	-0.14	-0.20	0.34	0.45	0.49
LG9	-0.12	-0.12	-0.15	-0.14	0.34	0.42	0.49
LG10	-0.12	-0.12	-0.15	-0.12	0.35	0.49	0.50
Average	-0.13	-0.15	-0.14	-0.15	0.32	0.42	0.43

Table 3.5. Mean free-surface elevation $\bar{\eta}$ (cm) at 7 wave gauge locations, MG.

Run	WG1	WG2	WG3	WG4	WG5	WG6	WG7
MG1	-0.04	-0.14	-0.11	-0.20	0.15	0.34	0.31
MG2	-0.16	-0.14	-0.13	-0.20	0.21	0.33	0.39
MG3	-0.15	-0.13	-0.13	-0.18	0.24	0.35	0.42
MG4	-0.15	-0.12	-0.15	-0.17	0.24	0.34	0.43
MG5	-0.14	-0.13	-0.13	-0.13	0.24	0.35	0.42
MG6	-0.06	-0.14	-0.12	-0.18	0.17	0.33	0.35
MG7	-0.14	-0.14	-0.13	-0.14	0.22	0.34	0.35
MG8	-0.11	-0.13	-0.14	-0.18	0.24	0.38	0.34
MG9	-0.11	-0.10	-0.12	-0.16	0.24	0.35	0.35
MG10	NR	NR	NR	NR	NR	NR	NR
Average	-0.12	-0.13	-0.13	-0.17	0.22	0.35	0.37

NR implies "not reliable" data.

Table 3.6. Mean free-surface elevation $\bar{\eta}$ (cm) at 7 wave gauge locations, HG.

Run	WG1	WG2	WG3	WG4	WG5	WG6	WG7
HG1	-0.29	-0.25	-0.15	-0.28	-0.01	0.17	0.23
HG2	-0.18	-0.26	-0.16	-0.24	0.12	0.24	0.19
HG3	-0.17	-0.22	-0.16	-0.24	0.11	0.20	0.15
HG4	-0.16	-0.22	-0.16	-0.24	0.12	0.25	0.23
HG5	-0.16	-0.22	-0.17	-0.25	0.12	0.23	0.18
Average	-0.19	-0.23	-0.16	-0.25	0.09	0.22	0.20

Table 3.7. Free-surface standard deviation σ_{η} (cm) at 7 wave gauge locations, LG.

Run	WG1	WG2	WG3	WG4	WG5	WG6	WG7
LG1	4.30	4.29	4.46	3.91	2.71	2.38	2.24
LG2	4.39	4.38	4.55	3.92	2.72	2.39	2.27
LG3	4.42	4.41	4.58	3.94	2.74	2.40	2.31
LG4	4.43	4.43	4.58	3.97	2.74	2.41	2.32
LG5	4.43	4.43	4.59	3.95	2.73	2.41	2.33
LG6	4.40	4.38	4.50	4.04	2.80	2.51	2.36
LG7	4.51	4.48	4.58	4.07	2.82	2.51	2.37
LG8	4.54	4.51	4.62	4.08	2.82	2.49	2.36
LG9	4.56	4.53	4.64	4.07	2.83	2.51	2.34
LG10	4.57	4.54	4.65	4.11	2.82	2.50	2.33
Average	4.46	4.44	4.58	4.01	2.77	2.45	2.32

Table 3.8. Free-surface standard deviation σ_η (cm) at 7 wave gauge locations, MG.

Run	WG1	WG2	WG3	WG4	WG5	WG6	WG7
MG1	4.44	4.41	4.54	4.26	3.08	2.93	2.68
MG2	4.59	4.53	4.69	4.31	3.08	2.92	2.69
MG3	4.67	4.55	4.71	4.34	3.08	2.92	2.69
MG4	4.76	4.58	4.72	4.32	3.08	2.93	2.67
MG5	4.69	4.58	4.69	4.33	3.08	2.91	2.67
MG6	4.60	4.55	4.63	4.27	3.12	2.95	2.70
MG7	4.63	4.59	4.67	4.30	3.11	2.94	2.69
MG8	4.66	4.61	4.69	4.27	3.11	2.92	2.70
MG9	4.63	4.59	4.65	4.28	3.11	2.93	2.71
MG10	NR						
Average	4.63	4.55	4.67	4.30	3.09	2.93	2.69

NR implies "not reliable" data.

Table 3.9. Free-surface standard deviation σ_η (cm) at 7 wave gauge locations, HG.

Run	WG1	WG2	WG3	WG4	WG5	WG6	WG7
HG1	4.36	4.40	4.50	4.22	3.16	3.03	2.65
HG2	4.43	4.47	4.55	4.30	3.17	3.04	2.63
HG3	4.48	4.50	4.59	4.30	3.16	3.02	2.63
HG4	4.50	4.51	4.59	4.31	3.17	3.02	2.64
HG5	4.52	4.52	4.59	4.34	3.19	3.02	2.64
Average	4.46	4.48	4.56	4.29	3.17	3.03	2.64

Table 3.10. Wet probability P_w , its mean free-surface elevation $\bar{\eta}$ (cm), and free-surface standard deviation σ_η (cm) for WG8, LG.

Run	t (s)	P_w	Z_b (cm)	\bar{h} (cm)	$\bar{\eta}$ (cm)	σ_η (cm)
	0		8.84			
LG1	200	0.31	8.81	0.91	9.72	0.62
LG2	600	0.30	8.76	0.96	9.72	0.66
LG3	1000	0.29	8.71	0.92	9.63	0.66
LG4	1400	0.31	8.66	0.84	9.50	0.65
LG5	1800	0.29	8.62	0.77	9.39	0.68
	2000		8.59			
LG6	2200	0.30	8.60	0.77	9.37	0.66
LG7	2600	0.29	8.62	0.77	9.39	0.67
LG8	3000	0.30	8.64	0.73	9.37	0.67
LG9	3400	0.27	8.65	0.85	9.50	0.71
LG10	3800	0.24	8.67	0.83	9.50	0.74
	4000		8.68			
Average		0.29		0.83	9.51	0.67

Table 3.11. Wet probability P_w , its mean free-surface elevation $\bar{\eta}$ (cm), and free-surface standard deviation σ_η (cm) for WG8, MG.

Run	t (s)	P_w	Z_b (cm)	\bar{h} (cm)	$\bar{\eta}$ (cm)	σ_η (cm)
	0		6.49			
MG1	200	0.53	6.42	1.28	7.70	0.82
MG2	600	0.50	6.28	1.15	7.43	0.85
MG3	1000	0.54	6.14	1.18	7.32	0.87
MG4	1400	0.50	6.00	1.32	7.32	0.85
MG5	1800	0.49	5.86	1.23	7.09	0.88
	2000		5.79			
MG6	2200	0.52	5.76	1.28	7.04	0.91
MG7	2600	0.53	5.71	1.30	7.02	0.92
MG8	3000	0.55	5.67	1.37	7.04	0.94
MG9	3400	0.56	5.62	1.45	7.07	0.96
MG10	3800	NR	5.57	NR	NR	NR
	4000		5.55			
Average		0.52		1.28	7.22	0.89

NR implies "not reliable" data.

Table 3.12. Wet probability P_w , its mean free-surface elevation $\bar{\eta}$ (cm), and free-surface standard deviation σ_η (cm) for WG8, HG.

Run	t (s)	P_w	Z_b (cm)	\bar{h} (cm)	$\bar{\eta}$ (cm)	σ_η (cm)
	0		3.26			
HG1	200	0.72	2.98	2.10	5.08	1.34
HG2	600	0.75	2.41	1.93	4.34	1.44
HG3	1000	0.78	1.85	2.29	4.14	1.53
HG4	1400	0.81	1.28	2.43	3.71	1.60
HG5	1800	0.84	0.71	2.53	3.24	1.67
	2000		0.43			
Average		0.78		2.26	4.10	1.52

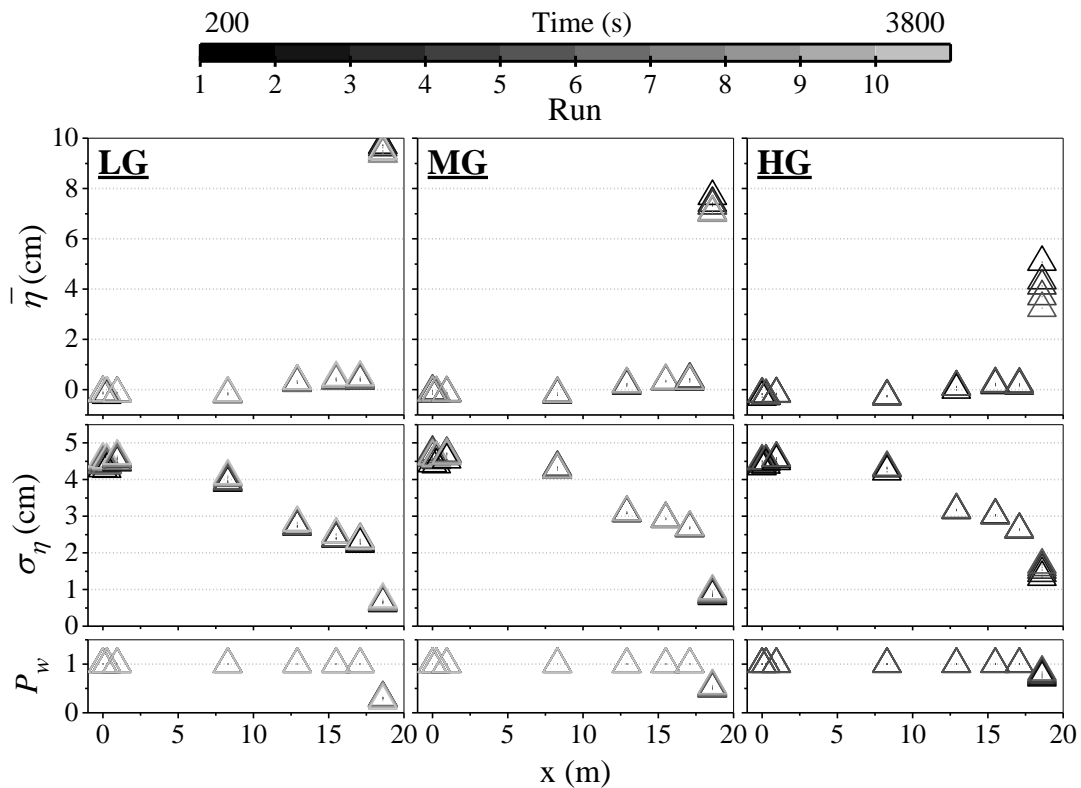


Figure 3.1. Cross-shore variations of mean $\bar{\eta}$ and standard deviation σ_η of free surface elevation η above SWL together with wet probability P_w for tests LG, MG, and HG.

Table 3.13. Mean cross-shore \bar{u} and standard deviation σ_u of the 2D ADV co-located with WG4 at $x = 8.30$ m, Red Vectrino co-located with WG5 at $x = 12.90$ m and Blue Vectrino co-located with WG6 at $x = 15.50$ m, LG.

Run	2D ADV at WG4		Red Vectrino at WG5		Blue Vectrino at WG6	
	\bar{u} (cm/s)	σ_u (cm/s)	\bar{u} (cm/s)	σ_u (cm/s)	\bar{u} (cm/s)	σ_u (cm/s)
LG1	-6.29	21.00	-4.59	15.71	-3.96	17.47
LG2	-7.17	21.10	-4.68	15.47	-3.59	17.56
LG3	-7.05	20.95	-4.07	15.88	-3.67	17.61
LG4	-6.72	20.80	-3.70	15.78	-3.33	17.40
LG5	-6.35	20.99	NR	NR	-3.36	17.43
LG6	-6.59	20.79	-3.51	15.77	-3.33	17.40
LG7	-6.78	20.96	-4.29	15.80	-3.55	17.27
LG8	-7.13	21.37	-4.23	15.69	-3.65	17.22
LG9	-6.54	21.14	NR	NR	-3.51	17.41
LG10	-6.19	21.04	-4.06	15.86	-3.13	17.39
Average	-6.68	21.01	-4.14	15.75	-3.51	17.42

NR implies "not reliable" data.

Table 3.14. Mean cross-shore \bar{u} and standard deviation σ_u of the 2D ADV co-located with WG4 at $x = 8.30$ m, Red Vectrino co-located with WG5 at $x = 12.90$ m and Blue Vectrino co-located with WG6 at $x = 15.50$ m, MG.

Run	2D ADV at WG4		Red Vectrino at WG5		Blue Vectrino at WG6	
	\bar{u} (cm/s)	σ_u (cm/s)	\bar{u} (cm/s)	σ_u (cm/s)	\bar{u} (cm/s)	σ_u (cm/s)
MG1	-5.92	20.88	-3.29	16.72	-4.65	17.35
MG2	-6.09	21.05	-4.23	16.58	-3.95	17.22
MG3	-6.39	21.10	-2.51	16.68	-3.94	17.37
MG4	-6.93	21.10	-3.03	16.81	-4.32	17.35
MG5	-6.87	21.16	NR	NR	NR	NR
MG6	-5.97	21.19	-3.83	17.01	-3.68	17.24
MG7	-7.14	21.05	NR	NR	-3.96	17.16
MG8	-6.25	20.68	-3.77	16.81	NR	NR
MG9	-6.30	20.94	-4.21	16.78	-3.64	17.03
MG10	NR	NR	NR	NR	NR	NR
Average	-6.43	21.02	-3.55	16.77	-4.02	17.25

NR implies "not reliable" data.

Table 3.15. Mean cross-shore \bar{u} and standard deviation σ_u of the 2D ADV co-located with WG4 at $x = 8.30$ m, Red Vectrino co-located with WG5 at $x = 12.90$ m and Blue Vectrino co-located with WG6 at $x = 15.50$ m, HG.

Run	2D ADV at WG4		Red Vectrino at WG5		Blue Vectrino at WG6	
	\bar{u} (cm/s)	σ_u (cm/s)	\bar{u} (cm/s)	σ_u (cm/s)	\bar{u} (cm/s)	σ_u (cm/s)
HG1	-4.82	20.88	NR	NR	-4.21	17.21
HG2	-5.51	21.28	-3.52	17.31	-4.56	17.36
HG3	-5.58	21.37	-3.26	17.18	-4.17	17.41
HG4	-4.55	21.22	-4.43	17.00	-3.59	17.24
HG5	-5.18	21.07	-3.42	16.94	-3.62	17.39
Average	-5.13	21.16	-3.66	17.11	-4.03	17.32

NR implies “not reliable” data.

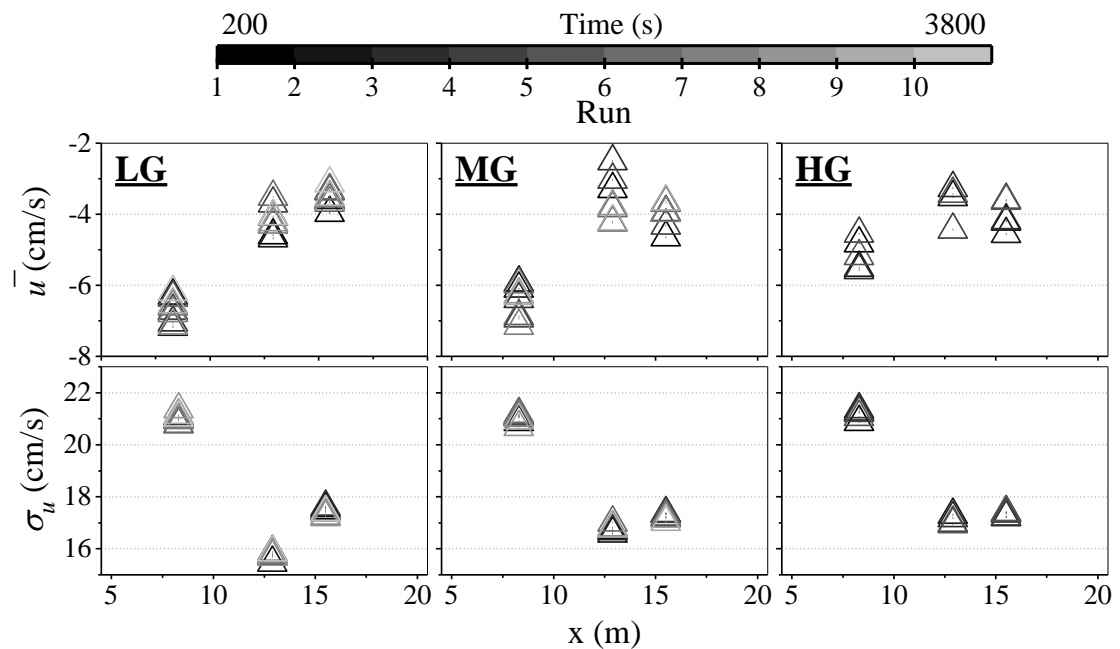


Figure 3.2. Cross-shore variations of mean \bar{u} and standard deviation σ_u of cross-shore velocity u for tests LG, MG, and HG.

3.1.2 Overtopping and Overwash

The volumes of water and sand transported over the impermeable vertical wall were used to obtain the water overtopping rate q_o , sand overwash rate q_{bs} , and their ratio q_{bs}/q_o per unit width averaged over each 400-s run as listed in Tables 3.16, 3.17, and 3.18. Figure 3.3 shows the temporal variations of q_o and q_{bs} for all the runs in tests LG, MG, and HG. The average rates are plotted at time t corresponding to the middle of each run where $t = 0$ at the start of each test. The overtopping rate and overwash rate did not change much during each test but increased significantly with the increase of SWL. The height of the vertical wall crest above SWL was 14, 12, and 10 cm for tests LG, MG, and HG, respectively.

Table 3.16. Measured sediment overwash rate q_{bs} , water overtopping rate q_o , and their ratio q_{bs}/q_o , LG.

Run	q_{bs} (cm²/s)	q_o (cm²/s)	q_{bs}/q_o
LG1	0.0004	0.083	0.005
LG2	0.0019	0.211	0.009
LG3	0.0023	0.190	0.012
LG4	0.0020	0.157	0.013
LG5	0.0020	0.185	0.011
LG6	0.0018	0.118	0.015
LG7	0.0022	0.143	0.015
LG8	0.0021	0.145	0.014
LG9	0.0018	0.135	0.014
LG10	0.0015	0.131	0.012

Table 3.17. Measured sediment overwash rate q_{bs} , water overtopping rate q_o , and their ratio q_{bs}/q_o , MG.

Run	q_{bs} (cm²/s)	q_o (cm²/s)	q_{bs}/q_o
MG1	0.0040	0.383	0.010
MG2	0.0090	0.489	0.018
MG3	0.0096	0.463	0.021
MG4	0.0101	0.486	0.021
MG5	0.0093	0.464	0.020
MG6	0.0102	0.472	0.022
MG7	0.0111	0.485	0.023
MG8	0.0103	0.471	0.022
MG9	0.0098	0.410	0.024
MG10	0.0134	0.420	0.032

Table 3.18. Measured sediment overwash rate q_{bs} , water overtopping rate q_o , and their ratio q_{bs}/q_o , HG.

Run	q_{bs} (cm²/s)	q_o (cm²/s)	q_{bs}/q_o
HG1	0.0638	1.916	0.033
HG2	0.0716	2.055	0.035
HG3	0.0744	2.317	0.032
HG4	0.0827	2.619	0.032
HG5	0.0953	2.711	0.031

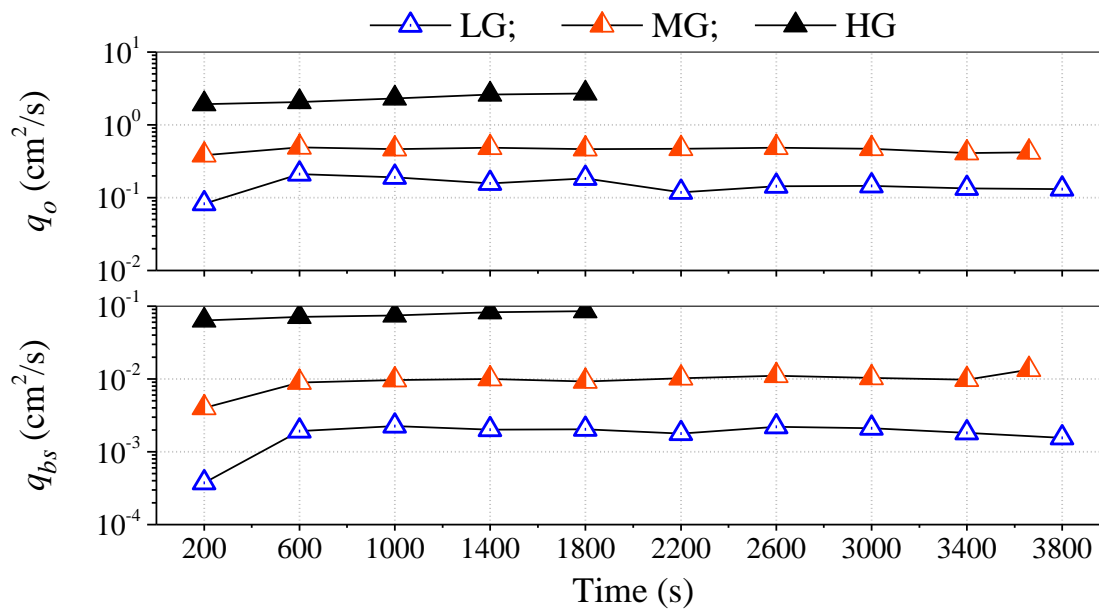


Figure 3.3. Temporal variations of wave overtopping rate q_o and sand overwash rate q_{bs} for tests LG (blue), MG (red), and HG (black).

3.1.3 Profile Evolution

The entire profile evolutions for the tests with blocks on ground are displayed in Figure 3.4. The final profiles LG10 and MG10 are practically the same as the initial profiles MG0 and HG0, respectively. The profiles in the foreshore and berm zone of $x = 16$ to 19.9 m of noticeable profile changes are presented in Figures 3.5, 3.6, and 3.7.

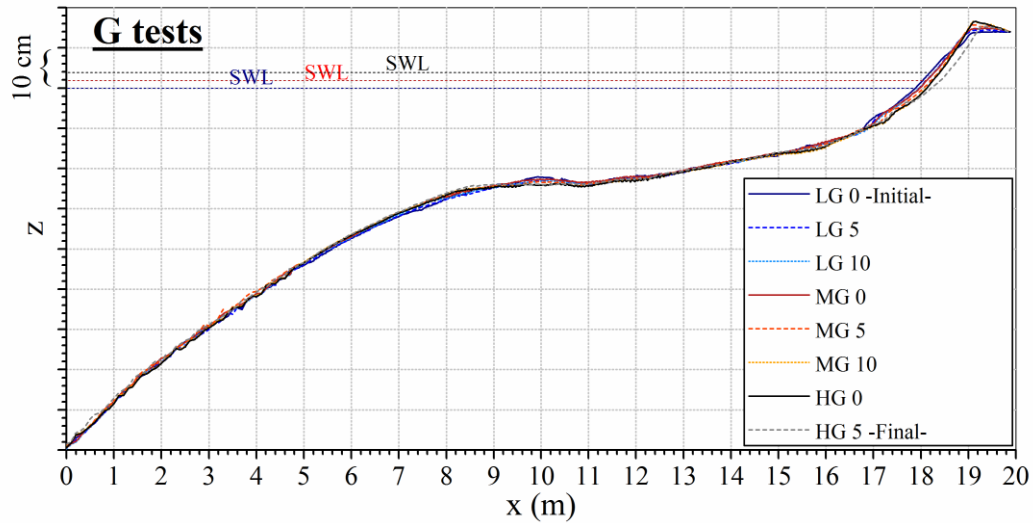


Figure 3.4. Profile evolution during tests LG, MG, and HG.

3.1.4 Foreshore and Berm Accretion or Erosion

The foreshore slope was eroded and became slightly steeper during test LG. Some of the eroded sand was deposited on the berm and transported over the vertical wall located at $x = 19.9$ m. A sediment budget analysis for the zone of $x = 16 - 19.9$ m indicated that some of the eroded sand was also dispersed offshore from $x = 16$ m. However, the deposited sand was not detectable from the profile measurement of ± 1 -mm uncertainty. After the 2-cm increase of SWL in test MG, the trend of foreshore erosion and berm accretion continued. The additional 2-cm increase of SWL in test HG caused the upward increase of foreshore erosion with no berm accretion, which resulted in the foreshore slope decrease. The sediment budget is examined by the volumetric changes (cm^3 per 1-cm alongshore length) during each test as listed in Tables 3.19, 3.21, and 3.23 for tests LG, MG, and HG, respectively. The eroded sand volume V_e (–) and deposited sand volume V_d (+) are related to the net volume change $V_c = V_e + V_d$. The cumulative sand overwash volume V_o is calculated from the measured q_{bs} . The offshore

sand loss volume is estimated as $V_l = |V_c| - V_o$. The ratios $V_l/|V_c|$ and $V_o/|V_c|$ indicate the degree of the offshore loss and onshore loss contributing to the erosion in the zone of $x = 16 - 19.9$ m.

Tables 3.20, 3.22, and 3.24 list the maximum erosion depth (negative) and deposition height (positive) and their cross-shore locations as well as the bottom elevation change Δz_d (negative for erosion) at WG7 and WG8 on the basis of Figures 3.5, 3.6, and 3.7 for tests LG, MG, and HG, respectively.

Table 3.19. Cumulative volume changes (cm^3/cm): eroded V_e , and deposited V_d sand volumes, net volume change V_c , cumulative sand overwash volume V_o , offshore sand loss volume V_l as well as the ratios $V_l/|V_c|$ and $V_o/|V_c|$ for the zone $x = 16$ to 19.9 m, LG.

Run	V_e	V_d	V_c	V_o	V_l	$V_l/ V_c $	$V_o/ V_c $
LG5	-360.32	110.24	-250.08	5.74	244.34	0.98	0.02
LG10	-425.19	171.22	-253.96	12.03	241.93	0.95	0.05

Table 3.20. Maximum erosion depth and deposition height at cross-shore location x , and bottom elevation change Δz_b at WG7 and WG8 locations, LG.

RUN	max erosion		max deposition		WG7	WG8
	depth (cm)	x (m)	height (cm)	x (m)	Δz_b (cm)	Δz_b (cm)
LG5	-1.50	16.92	1.74	18.86	-0.41	-0.25
LG10	-1.96	17.02	1.84	18.91	-1.19	-0.15

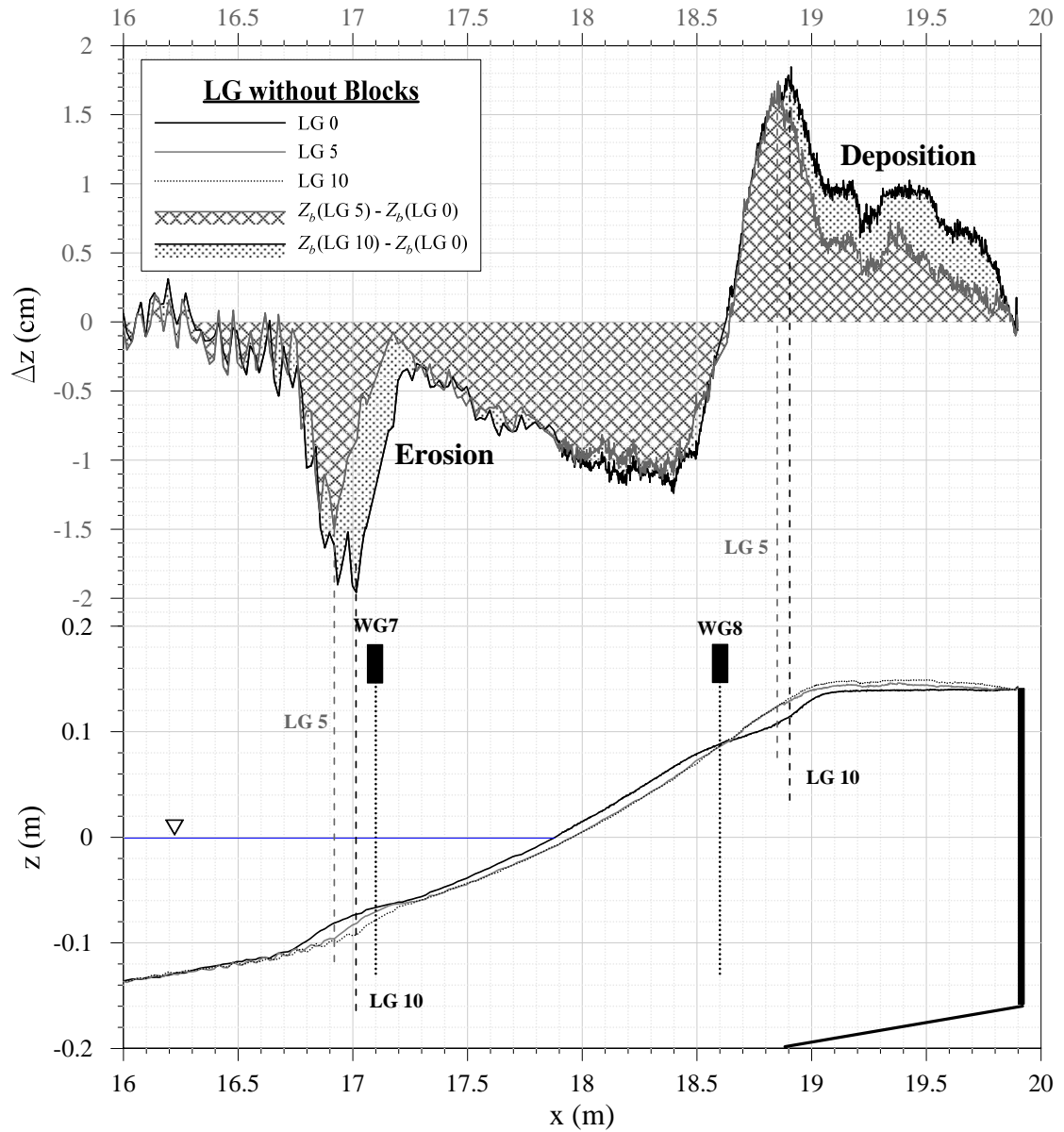


Figure 3.5. Bottom elevation difference between initial profile and profile measured after run 5 and 10 in test LG.

Table 3.21. Cumulative volume changes (cm^3/cm): eroded V_e , and deposited V_d sand volumes, net volume change V_c , cumulative sand overwash volume V_o , offshore sand loss volume V_l as well as the ratios $V_l/|V_c|$ and $V_o/|V_c|$ for the zone $x = 16$ to 19.9 m, MG.

Run	V_e	V_d	V_c	V_o	V_l	$V_l/ V_c $	$V_o/ V_c $
MG5	-426.43	78.10	-348.33	27.94	320.39	0.92	0.08
MG10	-947.53	85.87	-861.66	61.36	800.30	0.93	0.07

Table 3.22. Maximum erosion depth and deposition height at cross-shore location x , and bottom elevation change Δz_b at WG7 and WG8 locations, MG.

RUN	max erosion		max deposition		WG7	WG8
	depth (cm)	x (m)	height (cm)	x (m)	Δz_b (cm)	Δz_b (cm)
MG5	-1.60	17.16	1.06	19.05	-1.25	-0.70
MG10	-2.70	17.20	1.88	19.10	-1.61	-0.94

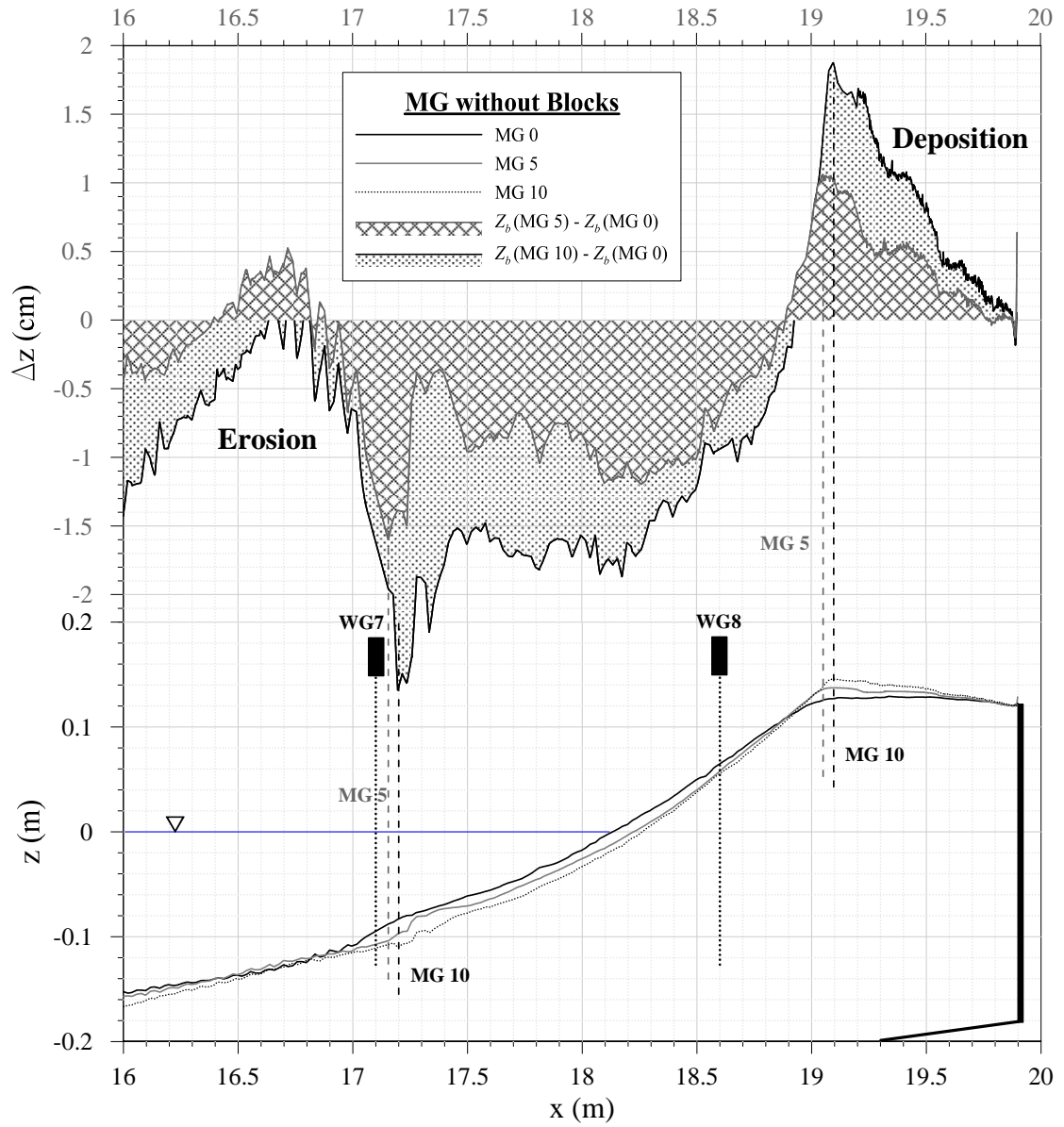


Figure 3.6. Bottom elevation difference between initial profile and profile measured after run 5 and 10 in test MG.

Table 3.23. Cumulative volume changes (cm^3/cm): eroded V_e , and deposited V_d sand volumes, net volume change V_c , cumulative sand overwash volume V_o , offshore sand loss volume V_l as well as the ratios $V_l/|V_c|$ and $V_o/|V_c|$ for the zone $x = 16$ to 19.9 m, HG.

Run	V_e	V_d	V_c	V_o	V_l	$V_l/ V_c $	$V_o/ V_c $
HG5	-862.42	99.64	-762.77	251.87	510.90	0.67	0.33

Table 3.24. Maximum erosion depth and deposition height at cross-shore location x , and bottom elevation change Δz_b at WG7 and WG8 locations, HG.

RUN	max erosion		max deposition		WG7	WG8
	depth (cm)	x (m)	height (cm)	x (m)	Δz_b (cm)	Δz_b (cm)
HG5	-4.12	19.04	1.37	17.52	0.38	-2.83

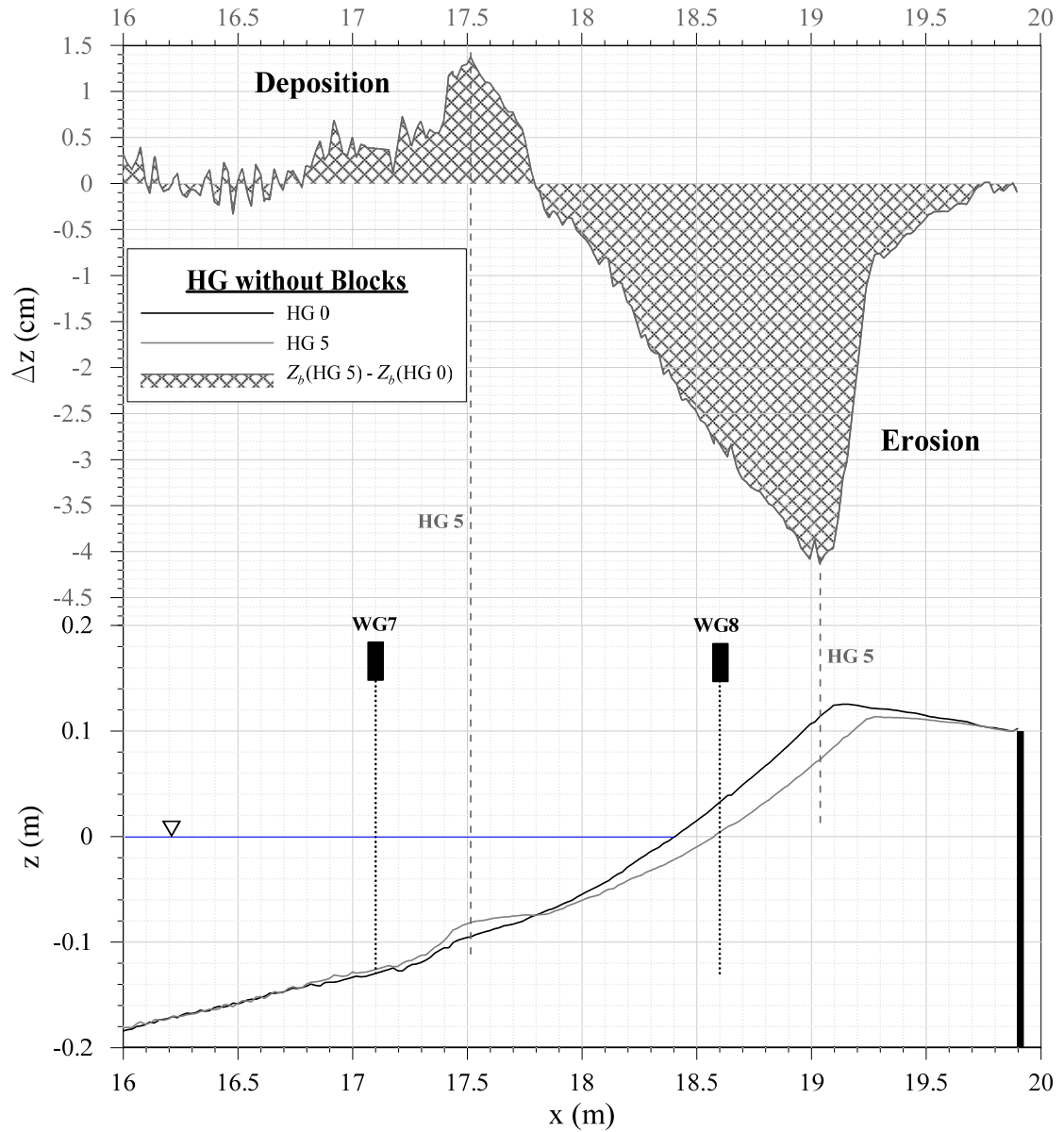


Figure 3.7. Bottom elevation difference between initial profile and profile measured after run 5 in test HG.

The profile evolution differences among the three tests (Figures 3.8 and 3.9) may be related to the different rates of q_o and q_{bs} shown in Figure 3.3 but detailed sediment dynamics is uncertain. The values of q_o and q_{bs} remained approximately constant in

spite of the temporal change of the berm elevation during each test. This constancy may be explained by the increase (decrease) of the foreshore slope coupled with the increase (decrease) of the berm elevation in tests LG and MG (HG).

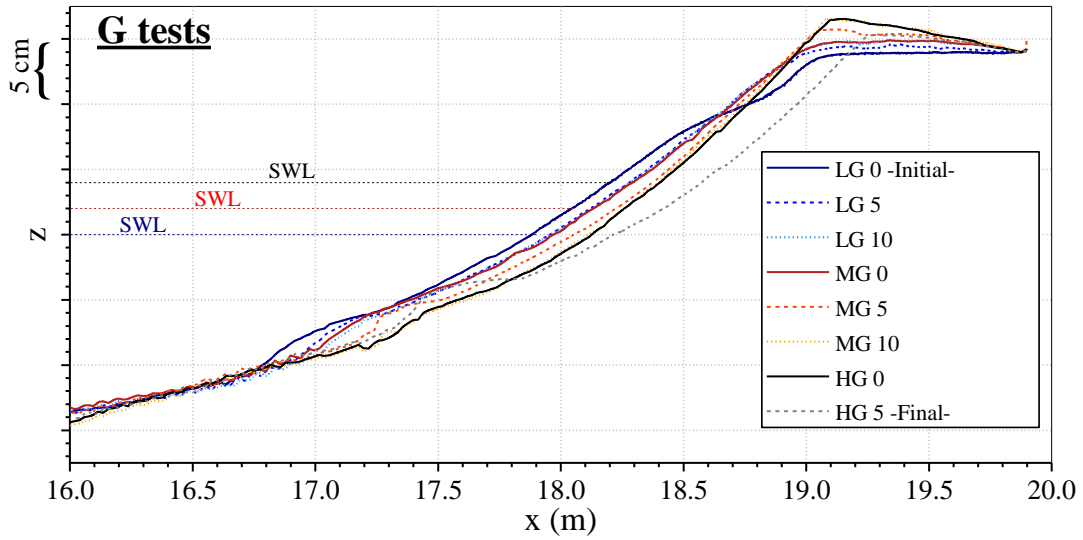


Figure 3.8. Beach profile evolution for series of tests LG, MG, and HG.

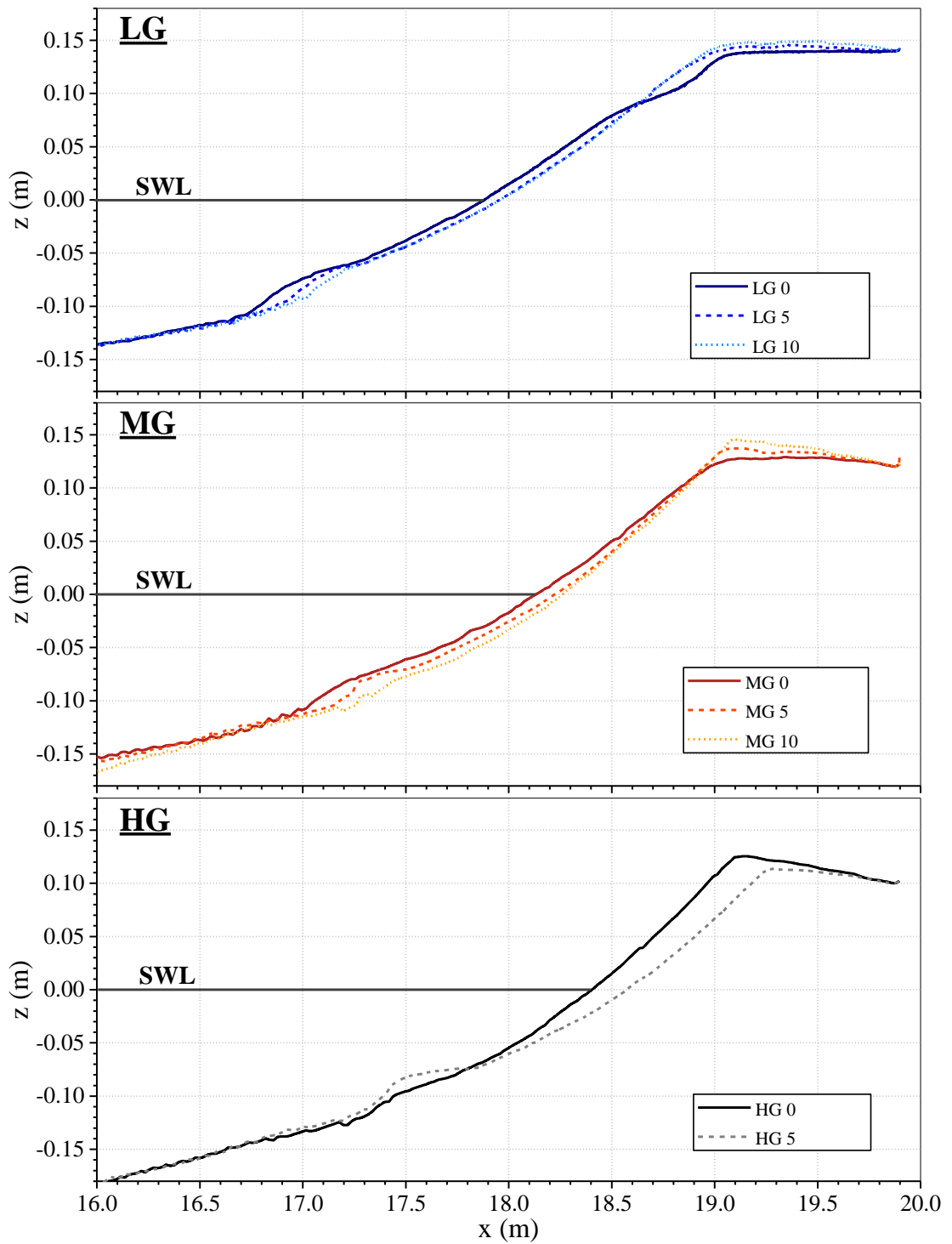


Figure 3.9. Comparison of beach profile evolution for tests LG, MG, and HG.

3.1.5 Block Movement

Figures 3.10, 3.12, and 3.14 show the photos of the blocks before and after tests LG, MG, and HG as well as during each of their runs. The responses of the 10 blocks to wave uprush and downrush during each run for the three tests are summarized in Tables 3.25, 3.27, and 3.29. The block locations before and after the test as well as after runs 5 are listed in Tables 3.26, 3.28, and 3.30. In addition, these block locations can be visualized in Figures 3.11, 3.13 and 3.15 based on the three-dimensional laser line scanner images. The block number in these figures increases landward and from the left to the right.

Figure 3.16 summarizes the reaction (floated, slid, and wet) of the 10 blocks in tests LG, MG and HG. The initial block location x is used to identify the 10 blocks because the block reaction was mostly uniform alongshore. The middle time t of each run is used to indicate the test progression. The 2-cm increase of SWL in test MG resulted in the landward shift of the block floating and sliding zones. For test HG with the additional 2-cm increase of SWL, blocks 8 and 10 slid over the vertical wall during run 2 and are not shown for runs 3 to 5. Test HG was terminated after run 5 because block 7 (the only block remaining) slid and reached the vertical wall at $x = 19.9$ m.

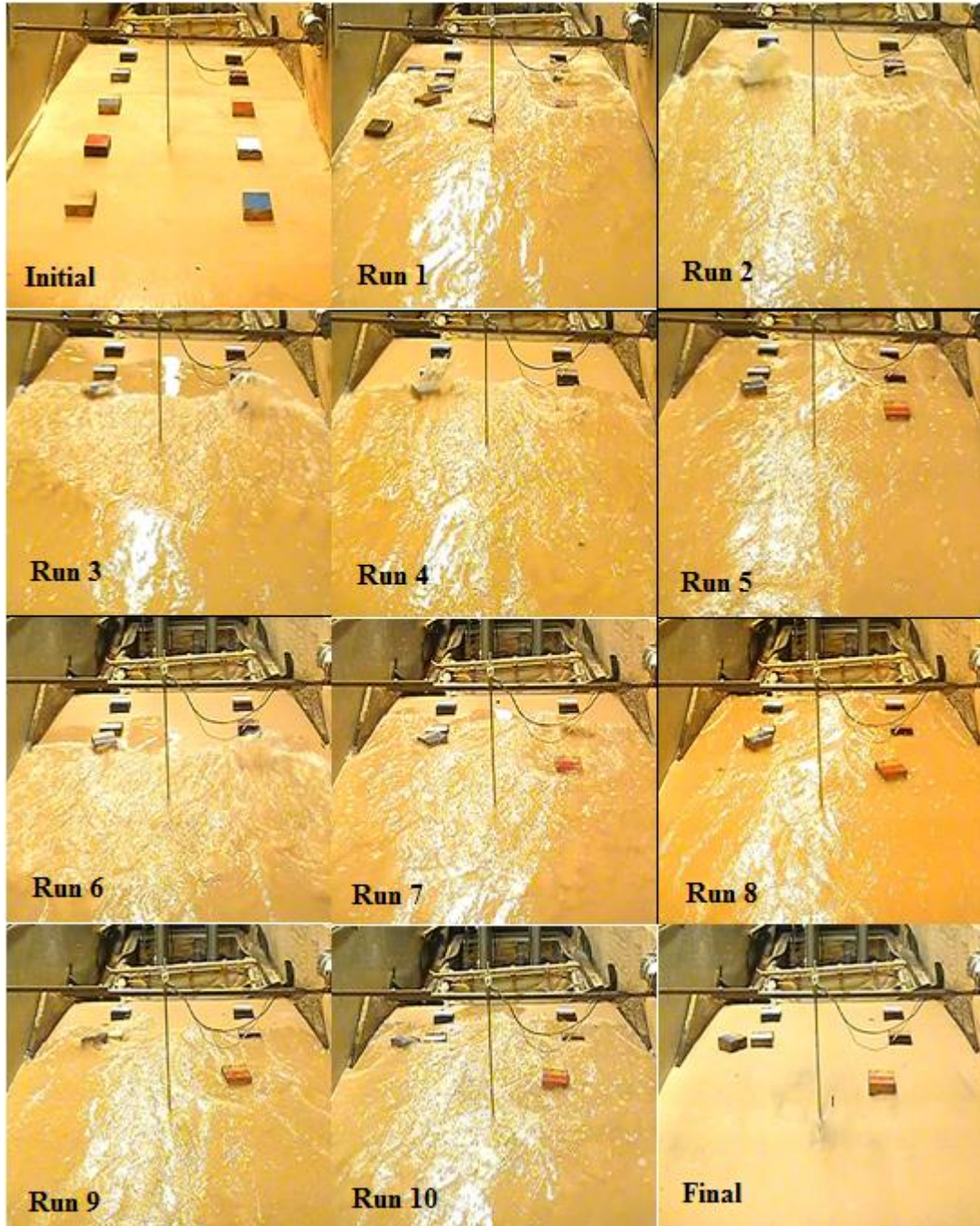


Figure 3.10. Swash and block interactions in each of 10 runs, along with initial and final block photos, LG.

Table 3.25. Block response during each of 10 runs in test LG.

Run	Block number									
	1	2	3	4	5	6	7	8	9	10
LG1	floated	floated	floated	floated	slid	slid	wet	wet	wet	wet
LG2	no	no	no	no	wet	wet	wet	wet	wet	wet
LG3	no	no	no	no	wet	wet	wet	wet	wet	wet
LG4	no	no	no	no	wet	wet	wet	wet	wet	wet
LG5	no	no	no	no	slid	wet	wet	wet	wet	wet
LG6	no	no	no	no	slid	slid	wet	wet	wet	wet
LG7	no	no	no	no	slid	slid	wet	wet	wet	wet
LG8	no	no	no	no	slid	slid	wet	wet	wet	wet
LG9	no	no	no	no	slid	slid	wet	wet	wet	wet
LG10	no	no	no	no	wet	slid	wet	wet	wet	wet

no implies “removed block”.

Table 3.26. Location of 10 blocks during test LG with initial still water shoreline location $x_{SWL} = 17.88$ m.

Block No.	1	2	3	4	5	6	7	8	9	10
Initial location										
x_b (m)	18.28	18.28	18.60	18.61	18.93	18.94	19.26	19.26	19.59	19.59
y_b (m)	0.26	-0.29	0.26	-0.29	0.26	-0.29	0.26	-0.29	0.26	-0.29
Location after run 5										
x_b (m)	-	-	-	-	19.09	18.92	19.26	19.26	19.59	19.59
y_b (m)	-	-	-	-	0.27	-0.28	0.26	-0.29	0.26	-0.29
Final location										
x_b (m)	-	-	-	-	19.22	18.85	19.26	19.26	19.59	19.59
y_b (m)	-	-	-	-	0.38	-0.19	0.26	-0.29	0.26	-0.29

- implies “removed block”.

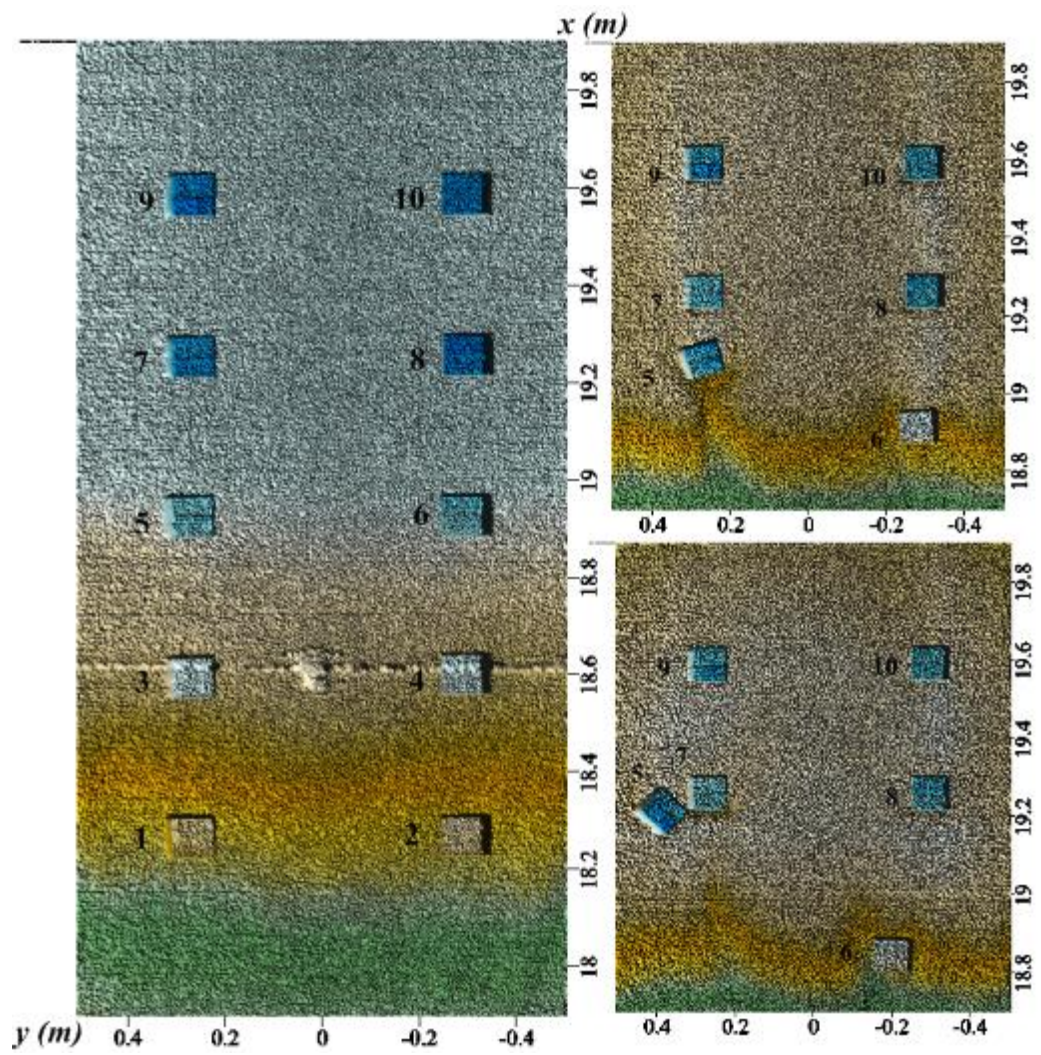


Figure 3.11. Laser line scanner images during test LG: initial (left), after run 5 (right-top), and final (right-bottom).

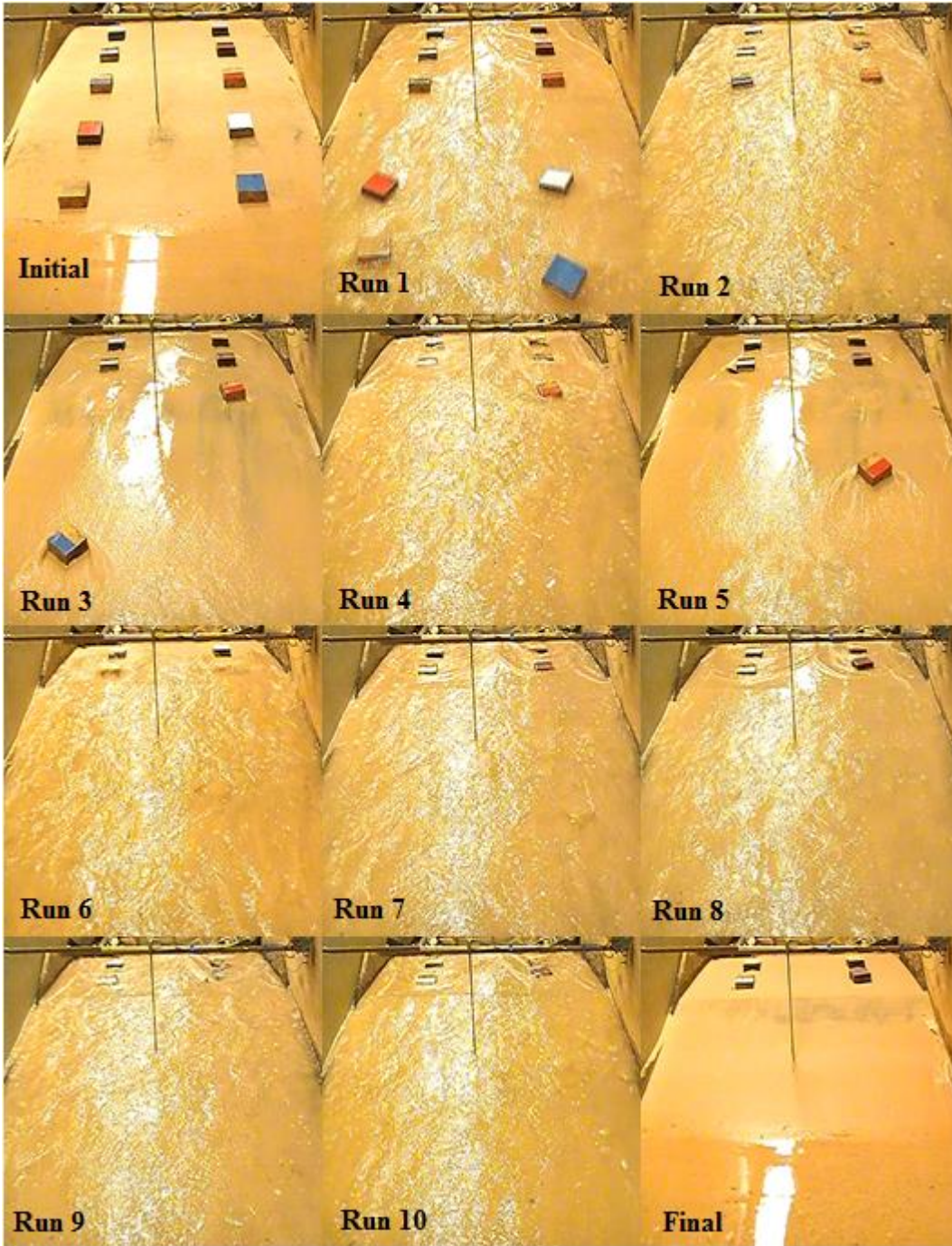


Figure 3.12. Swash and block interactions in each of 10 runs, along with initial and final block photos, MG.

Table 3.27. Block response during each of 10 runs in test MG.

Run	Block number									
	1	2	3	4	5	6	7	8	9	10
MG1	floated	floated	floated	floated	slid	wet	wet	wet	wet	wet
MG2	no	no	no	no	slid	slid	wet	wet	wet	wet
MG3	no	no	no	no	floated	slid	wet	wet	wet	wet
MG4	no	no	no	no	no	wet	wet	wet	wet	wet
MG5	no	no	no	no	no	floated	wet	wet	wet	wet
MG6	no	no	no	no	no	no	slid	wet	wet	wet
MG7	no	no	no	no	no	no	wet	slid	wet	wet
MG8	no	no	no	no	no	no	wet	slid	wet	wet
MG9	no	no	no	no	no	no	wet	wet	wet	wet
MG10	no	no	no	no	no	no	wet	wet	wet	wet

no implies “removed block”.

Table 3.28. Location of 10 blocks during test MG with initial still water shoreline location $x_{SWL} = 18.13$ m.

Block No.	1	2	3	4	5	6	7	8	9	10
Initial location										
x_b (m)	18.28	18.28	18.61	18.61	18.94	18.93	19.26	19.27	19.59	19.60
y_b (m)	0.26	-0.30	0.26	-0.30	0.25	-0.30	0.26	-0.30	0.26	-0.30
Location after run 5										
x_b (m)	-	-	-	-	-	-	19.27	19.28	19.59	19.60
y_b (m)	-	-	-	-	-	-	0.26	-0.30	0.26	-0.30
Final location										
x_b (m)	-	-	-	-	-	-	19.30	19.35	19.59	19.61
y_b (m)	-	-	-	-	-	-	0.26	-0.30	0.26	-0.29

- implies “removed block”.

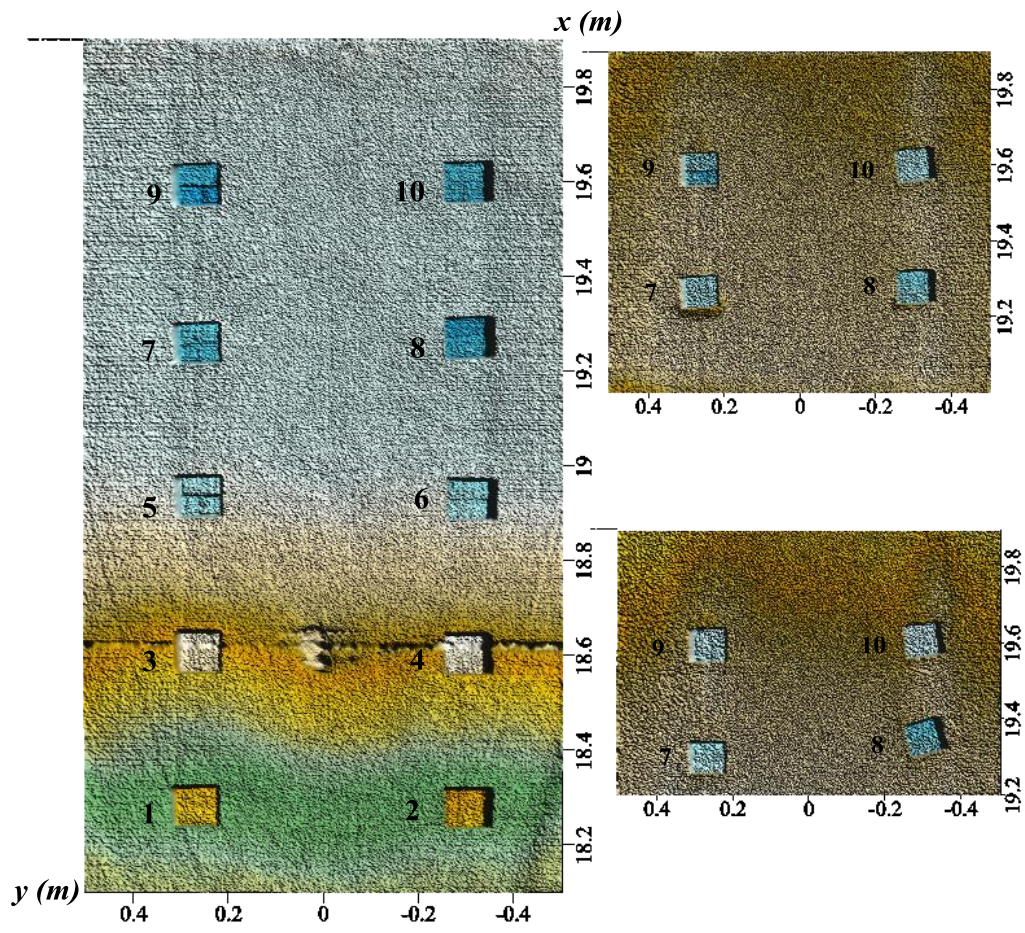


Figure 3.13. Laser line scanner images during test MG: initial (left), after run 5 (right-top), and final (right-bottom).

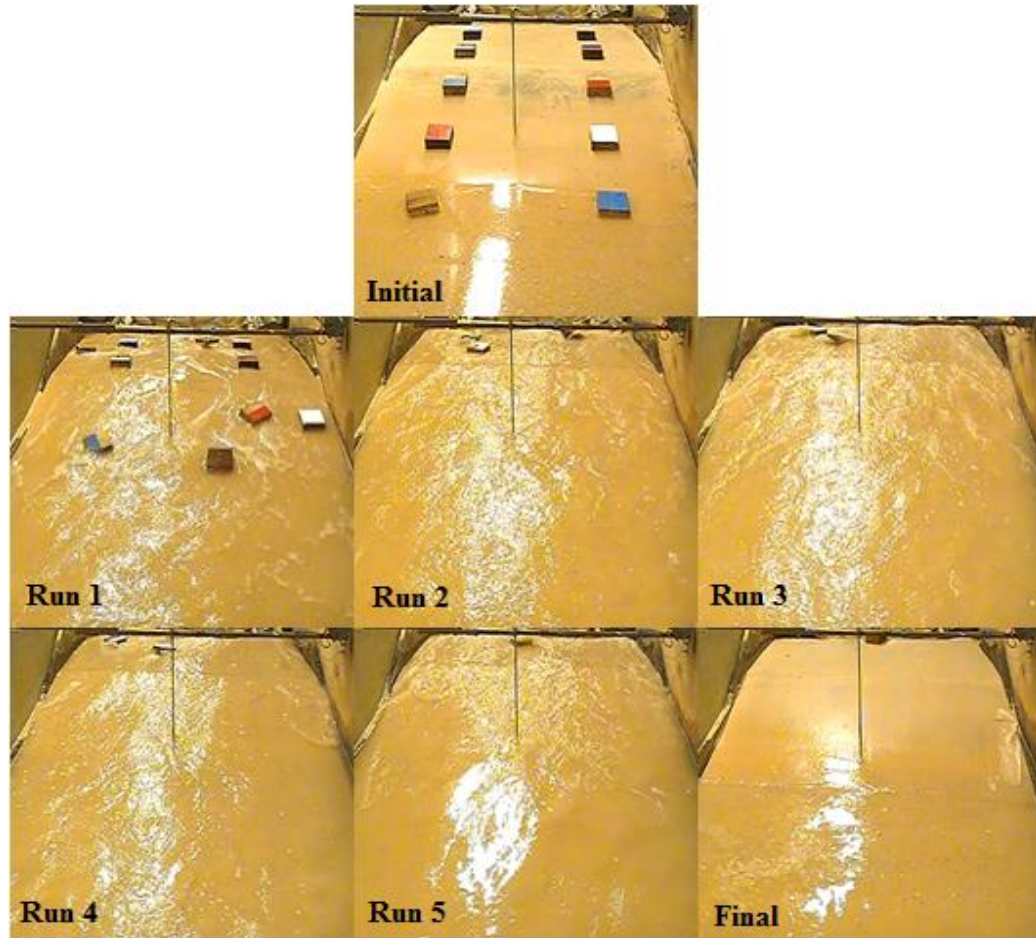


Figure 3.14. Swash and block interactions in each of 5 runs, along with initial and final block photos, HG.

Table 3.29. Block response during each of 5 runs in test HG.

Run	Block number									
	1	2	3	4	5	6	7	8	9	10
HG1	floated	floated	floated	floated	floated	floated	slid	slid	wet	wet
HG2	no	no	no	no	no	no	slid	slid	wet	slid
HG3	no	no	no	no	no	no	slid	no	slid	no
HG4	no	no	no	no	no	no	slid	no	slid	no
HG5	no	no	no	no	no	no	slid	no	no	no

no implies “removed block”.

Table 3.30. Location of 10 blocks during test HG with initial still water shoreline location $x_{SWL} = 18.40$ m.

Block No.	1	2	3	4	5	6	7	8	9	10
Initial location										
x_b (m)	18.29	18.29	18.61	18.61	18.93	18.93	19.26	19.27	19.59	19.59
y_b (m)	0.26	-0.30	0.26	-0.29	0.25	-0.30	0.25	-0.30	0.26	-0.30
Final location after run 5										
x_b (m)	-	-	-	-	-	-	19.84	-	-	-
y_b (m)	-	-	-	-	-	-	-0.02	-	-	-

- implies "removed block".

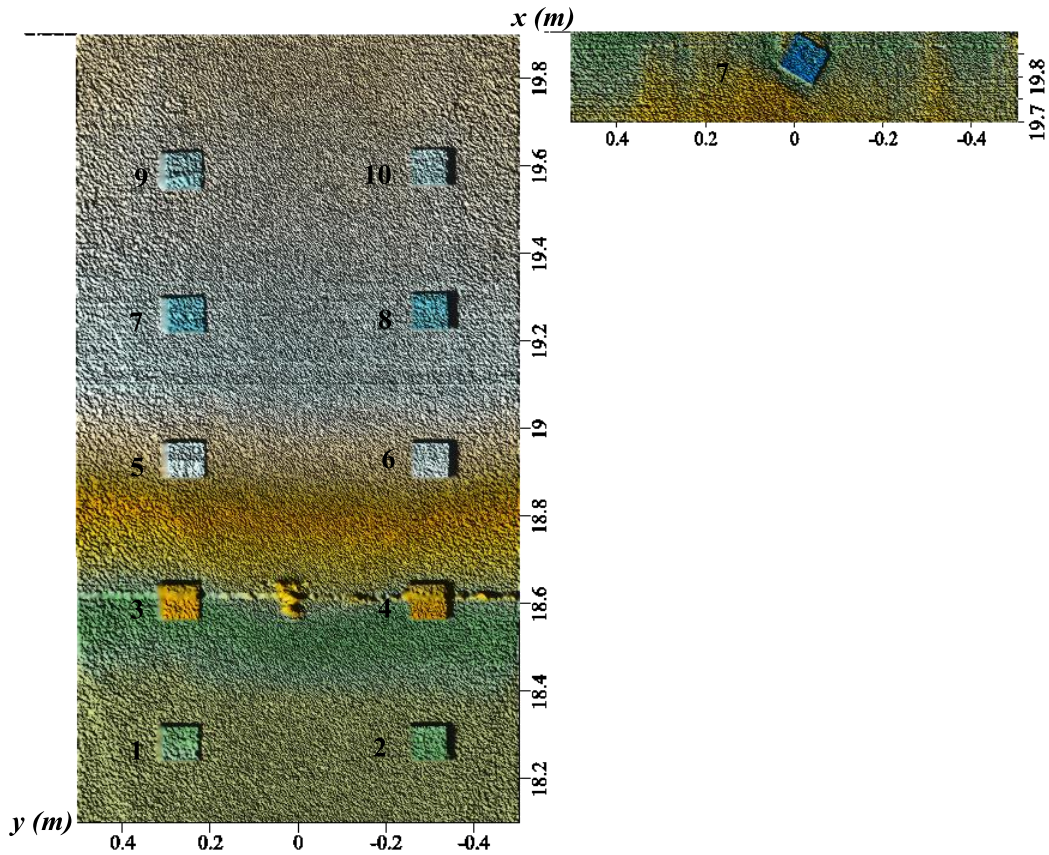


Figure 3.15. Laser line scanner images during test HG: initial (left) and final (right-bottom).

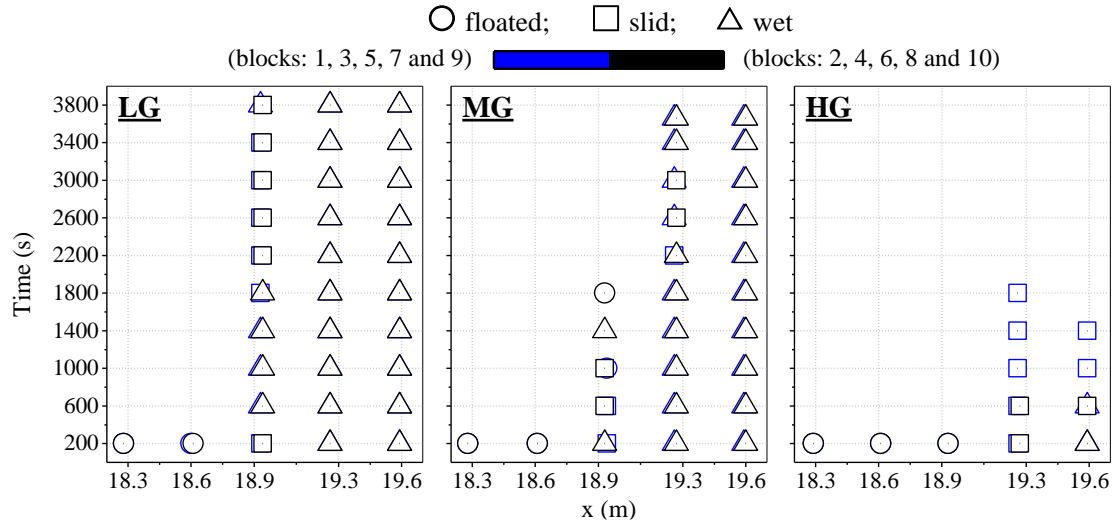


Figure 3.16. Response (floated, slid, and wet) of 10 blocks on ground in each run for tests LG, MG, and HG.

3.2 Blocks on Long Pilings

For the sequence of tests LL, ML, and HL, each of the 10 blocks was placed horizontally on the four dowels with a vertical clearance of 4 cm at the center of the block bottom above the initial beach and berm profile at the start of test LL. The clearance C for all the blocks was 4 cm at time $t = 0$ of test LL. The clearance C varied temporally and spatially as the profile evolved. The profile was not rebuilt at the start of tests ML and HL and the value of C was not equal to 4 cm at time $t = 0$ of tests ML and HL. The elevated blocks were more stable than the blocks with $C = 0$ on the ground in tests LG, MG, and HG.

3.2.1 Hydrodynamics

The incident wave characteristics at the location $x = 0$ m of WG1 for tests LL, ML, and HL (Tables 3.31, 3.32, and 3.33) were similar to those for tests LG, MG, and HG (Tables 3.1, 3.2, and 3.3). The measured values of $\bar{\eta}$, σ_{η} and P_w for all the runs in tests LL, ML, and HL are listed in Tables 3.34 to 3.42 and plotted in Figure 3.17 in the

same way as in Figure 3.1. The values in Figures 3.1 and 3.17 are similar apart from the difference at $x = 18.6$ m in the swash zone between tests HG and HL because test HG was terminated after run 5 as listed in Table 2.5. The measured values of \bar{u} and σ_u in the surf zone listed in Tables 3.43 to 3.45 and plotted in Figures 3.18 are similar to those shown in Figures 3.2. The return current \bar{u} of the order of 4 cm/s is more difficult to measure accurately than the oscillatory velocity standard deviation σ_u of the order of 20 cm/s. The measured hydrodynamics in the surf zone were expected to be similar because the 10 blocks on the ground and long pilings were placed in the swash zone. The 10 blocks on the ground in tests LG, MG, and HG were presumed to affect the swash hydrodynamics more than the 10 blocks on the long pilings in tests LL, ML, and HL. However, the swash hydrodynamics turned out to be fairly similar.

Table 3.31. Incident wave characteristics, LL.

Run	H_{mo} (cm)	H_{rms} (cm)	H_s (cm)	T_p (s)	T_s (s)	R
LL1	17.73	12.54	17.00	2.62	2.05	0.13
LL2	18.23	12.89	17.32	2.62	2.01	0.13
LL3	18.38	13.00	17.52	2.62	2.03	0.13
LL4	18.47	13.06	17.73	2.62	2.03	0.13
LL5	18.54	13.11	17.66	2.62	1.98	0.13
LL6	18.45	13.05	17.64	2.62	2.03	0.14
LL7	18.58	13.14	17.86	2.62	2.01	0.13
LL8	18.68	13.21	17.96	2.62	2.00	0.13
LL9	18.79	13.29	17.99	2.62	2.01	0.13
LL10	18.71	13.23	17.82	2.62	1.99	0.14
Average	18.46	13.05	17.65	2.62	2.01	0.13

Table 3.32. Incident wave characteristics, ML.

Run	H_{mo} (cm)	H_{rms} (cm)	H_s (cm)	T_p (s)	T_s (s)	R
ML1	17.39	12.30	16.88	2.64	2.15	0.18
ML2	17.85	12.62	17.24	2.64	2.13	0.18
ML3	NR	NR	NR	NR	NR	NR
ML4	18.16	12.84	17.50	2.64	2.10	0.20
ML5	18.12	12.82	17.38	2.64	2.10	0.19
ML6	17.18	12.15	16.54	2.64	2.16	0.18
ML7	17.56	12.42	17.02	2.64	2.16	0.17
ML8	17.73	12.54	17.04	2.64	2.14	0.18
ML9	17.86	12.63	17.23	2.64	2.13	0.18
ML10	17.92	12.67	17.34	2.64	2.16	0.17
Average	17.75	12.55	17.13	2.64	2.14	0.18

NR implies "not reliable" data.

Table 3.33. Incident wave characteristics, HL.

Run	H_{mo} (cm)	H_{rms} (cm)	H_s (cm)	T_p (s)	T_s (s)	R
HL1	16.93	11.97	16.19	2.42	2.08	0.16
HL2	17.45	12.34	16.66	2.42	2.11	0.16
HL3	17.75	12.55	17.17	2.42	2.17	0.15
HL4	17.81	12.59	17.18	2.42	2.11	0.15
HL5	17.91	12.66	17.35	2.42	2.11	0.15
HL6	17.27	12.21	16.74	2.42	2.16	0.15
HL7	17.69	12.51	17.00	2.42	2.10	0.14
HL8	17.92	12.67	17.23	2.42	2.11	0.14
HL9	18.02	12.74	17.41	2.42	2.12	0.14
HL10	18.02	12.74	17.47	2.42	2.14	0.14
Average	17.68	12.50	17.04	2.42	2.12	0.15

Table 3.34. Mean free-surface elevation $\bar{\eta}$ (cm) at 7 wave gauge locations, LL.

Run	WG1	WG2	WG3	WG4	WG5	WG6	WG7
LL1	-0.17	-0.20	-0.14	-0.20	0.25	0.38	0.32
LL2	-0.15	-0.18	-0.15	-0.17	0.30	0.42	0.38
LL3	-0.14	-0.16	-0.15	-0.17	0.31	0.42	0.44
LL4	-0.10	-0.14	-0.16	-0.16	0.32	0.42	0.50
LL5	-0.13	-0.16	-0.16	-0.16	0.31	0.42	0.48
LL6	-0.15	-0.19	-0.21	-0.17	0.27	0.40	0.40
LL7	-0.14	-0.17	-0.17	-0.15	0.30	0.41	0.48
LL8	-0.11	-0.12	-0.17	-0.15	0.30	0.41	0.49
LL9	-0.13	-0.15	-0.17	-0.16	0.32	0.45	0.52
LL10	-0.12	-0.14	-0.16	-0.10	0.32	0.42	0.53
Average	-0.13	-0.16	-0.16	-0.16	0.30	0.42	0.45

Table 3.35. Mean free-surface elevation $\bar{\eta}$ (cm) at 7 wave gauge locations, ML.

Run	WG1	WG2	WG3	WG4	WG5	WG6	WG7
ML1	-0.07	-0.16	-0.11	-0.20	0.13	0.16	0.29
ML2	-0.13	-0.12	-0.11	-0.15	0.19	0.32	0.38
ML3	NR	NR	NR	NR	NR	NR	NR
ML4	-0.13	-0.10	-0.13	-0.14	0.24	0.32	NR
ML5	-0.12	-0.08	-0.13	-0.16	0.24	0.32	0.41
ML6	-0.13	-0.20	-0.09	-0.20	0.12	0.29	0.33
ML7	-0.16	-0.17	-0.13	-0.15	0.18	0.30	0.35
ML8	-0.16	-0.12	-0.10	-0.08	0.19	0.33	0.37
ML9	-0.12	-0.11	-0.11	-0.14	0.20	0.34	0.37
ML10	-0.12	-0.13	-0.11	-0.12	0.20	0.34	0.34
Average	-0.13	-0.13	-0.11	-0.15	0.19	0.30	0.36

NR implies "not reliable" data.

Table 3.36. Mean free-surface elevation $\bar{\eta}$ (cm) at 7 wave gauge locations, HL.

Run	WG1	WG2	WG3	WG4	WG5	WG6	WG7
HL1	-0.12	-0.16	-0.12	-0.31	0.01	0.15	0.11
HL2	-0.13	-0.17	-0.13	-0.26	0.08	0.21	0.14
HL3	-0.11	-0.15	-0.11	-0.23	0.13	0.22	0.21
HL4	-0.11	-0.15	-0.12	-0.21	0.13	0.23	0.21
HL5	-0.11	-0.15	-0.11	-0.20	0.13	0.23	0.16
HL6	-0.14	-0.18	-0.11	-0.24	0.11	0.18	0.22
HL7	-0.13	-0.17	-0.13	-0.22	0.08	0.21	0.11
HL8	-0.11	-0.16	-0.13	-0.23	0.11	0.19	0.14
HL9	-0.32	-0.36	-0.33	-0.42	-0.10	0.00	0.01
HL10	-0.12	-0.16	-0.13	-0.21	0.14	0.21	0.24
Average	-0.14	-0.18	-0.14	-0.25	0.08	0.18	0.16

Table 3.37. Free-surface standard deviation σ_{η} (cm) at 7 wave gauge locations, LL.

Run	WG1	WG2	WG3	WG4	WG5	WG6	WG7
LL1	4.37	4.40	4.44	4.09	2.79	2.50	2.33
LL2	4.50	4.53	4.56	4.13	2.82	2.54	2.36
LL3	4.54	4.56	4.59	4.13	2.84	2.56	2.34
LL4	4.57	4.58	4.61	4.14	2.84	2.55	2.35
LL5	4.58	4.61	4.62	4.14	2.85	2.57	2.33
LL6	4.57	4.57	4.61	4.18	2.88	2.60	2.39
LL7	4.61	4.61	4.65	4.21	2.89	2.58	2.39
LL8	4.63	4.64	4.67	4.22	2.92	2.59	2.41
LL9	4.67	4.67	4.68	4.21	2.90	2.60	2.39
LL10	4.64	4.66	4.66	4.20	2.91	2.60	2.39
Average	4.57	4.58	4.61	4.17	2.86	2.57	2.37

Table 3.38. Free-surface standard deviation σ_η (cm) at 7 wave gauge locations, ML.

Run	WG1	WG2	WG3	WG4	WG5	WG6	WG7
ML1	4.41	4.36	4.43	4.18	3.12	2.94	2.68
ML2	4.52	4.47	4.55	4.24	3.12	2.96	2.69
ML3	NR						
ML4	4.69	4.56	4.63	4.27	3.12	2.97	NR
ML5	4.62	4.56	4.65	4.26	3.11	2.96	2.64
ML6	4.31	4.27	4.44	4.10	3.05	2.90	2.61
ML7	4.40	4.38	4.56	4.15	3.03	2.88	2.60
ML8	4.48	4.42	4.60	4.18	3.04	2.88	2.59
ML9	4.52	4.45	4.61	4.19	3.02	2.89	2.58
ML10	4.52	4.48	4.63	4.21	3.03	2.88	2.59
Average	4.50	4.44	4.57	4.20	3.07	2.92	2.62

NR implies "not reliable" data.

Table 3.39. Free-surface standard deviation σ_η (cm) at 7 wave gauge locations, HL.

Run	WG1	WG2	WG3	WG4	WG5	WG6	WG7
HL1	4.14	4.19	4.30	4.07	3.11	2.99	2.59
HL2	4.28	4.31	4.41	4.16	3.11	2.98	2.58
HL3	4.35	4.38	4.48	4.19	3.13	2.97	2.58
HL4	4.36	4.40	4.51	4.23	3.13	2.97	2.57
HL5	4.41	4.43	4.50	4.25	3.15	2.95	2.57
HL6	4.24	4.26	4.35	4.18	3.13	2.92	2.66
HL7	4.37	4.38	4.44	4.23	3.14	2.92	2.59
HL8	4.42	4.44	4.50	4.26	3.14	2.92	2.60
HL9	4.45	4.47	4.52	4.28	3.16	2.94	2.61
HL10	4.45	4.48	4.52	4.30	3.14	2.91	2.59
Average	4.35	4.37	4.45	4.22	3.13	2.95	2.59

Table 3.40. Wet probability P_w , its mean free-surface elevation $\bar{\eta}$ (cm), and free-surface standard deviation σ_η (cm) for WG8, LL.

Run	t (s)	P_w	Z_b (cm)	\bar{h} (cm)	$\bar{\eta}$ (cm)	σ_η (cm)
	0		8.31			
LL1	200	0.33	8.35	0.80	9.15	0.61
LL2	600	0.31	8.41	0.83	9.24	0.68
LL3	1000	0.30	8.48	0.84	9.32	0.71
LL4	1400	0.28	8.54	0.88	9.42	0.72
LL5	1800	0.28	8.61	0.92	9.53	0.72
	2000		8.64			
LL6	2200	0.29	8.64	0.93	9.57	0.73
LL7	2600	0.29	8.64	0.91	9.55	0.73
LL8	3000	0.29	8.64	0.80	9.44	0.78
LL9	3400	0.31	8.64	0.85	9.49	0.8
LL10	3800	0.28	8.65	0.95	9.60	0.83
	4000		8.65			
Average		0.30		0.87	9.43	0.73

Table 3.41. Wet probability P_w , its mean free-surface elevation $\bar{\eta}$ (cm), and free-surface standard deviation σ_η (cm) for WG8, ML.

Run	t (s)	P_w	Z_b (cm)	\bar{h} (cm)	$\bar{\eta}$ (cm)	σ_η (cm)
	0		6.55			
ML1	200	0.49	6.45	1.27	7.72	0.82
ML2	600	0.50	6.26	1.27	7.53	0.87
ML3	1000	NR	6.06	NR	NR	NR
ML4	1400	NR	5.87	NR	NR	NR
ML5	1800	0.53	5.67	1.35	7.02	0.93
	2000		5.58			
ML6	2200	0.52	5.55	1.52	7.07	0.92
ML7	2600	0.55	5.50	1.38	6.88	0.94
ML8	3000	0.53	5.46	1.42	6.88	0.95
ML9	3400	0.56	5.41	1.58	6.99	0.95
ML10	3800	0.57	5.36	1.57	6.93	0.96
	4000		5.33			
Average		0.53		1.42	7.13	0.92

NR implies "not reliable" data.

Table 3.42. Wet probability P_w , its mean free-surface elevation $\bar{\eta}$ (cm), and free-surface standard deviation σ_η (cm) for WG8, HL.

Run	t (s)	P_w	Z_b (cm)	\bar{h} (cm)	$\bar{\eta}$ (cm)	σ_η (cm)
	0		3.42			
HL1	200	0.70	3.14	2.26	5.40	1.36
HL2	600	0.74	2.59	2.22	4.81	1.46
HL3	1000	0.77	2.04	2.41	4.45	1.51
HL4	1400	0.79	1.48	2.53	4.01	1.54
HL5	1800	0.82	0.93	2.54	3.47	1.60
	2000		0.65			
HL6	2200	NR	0.52	NR	NR	NR
HL7	2600	0.86	0.27	2.66	2.93	1.65
HL8	3000	0.87	0.01	2.53	2.54	1.70
HL9	3400	0.88	-0.24	2.35	2.11	1.72
HL10	3800	0.89	-0.50	2.42	1.92	1.73
	4000		-0.62			
Average		0.81		2.44	3.52	1.59

NR implies "not reliable" data.

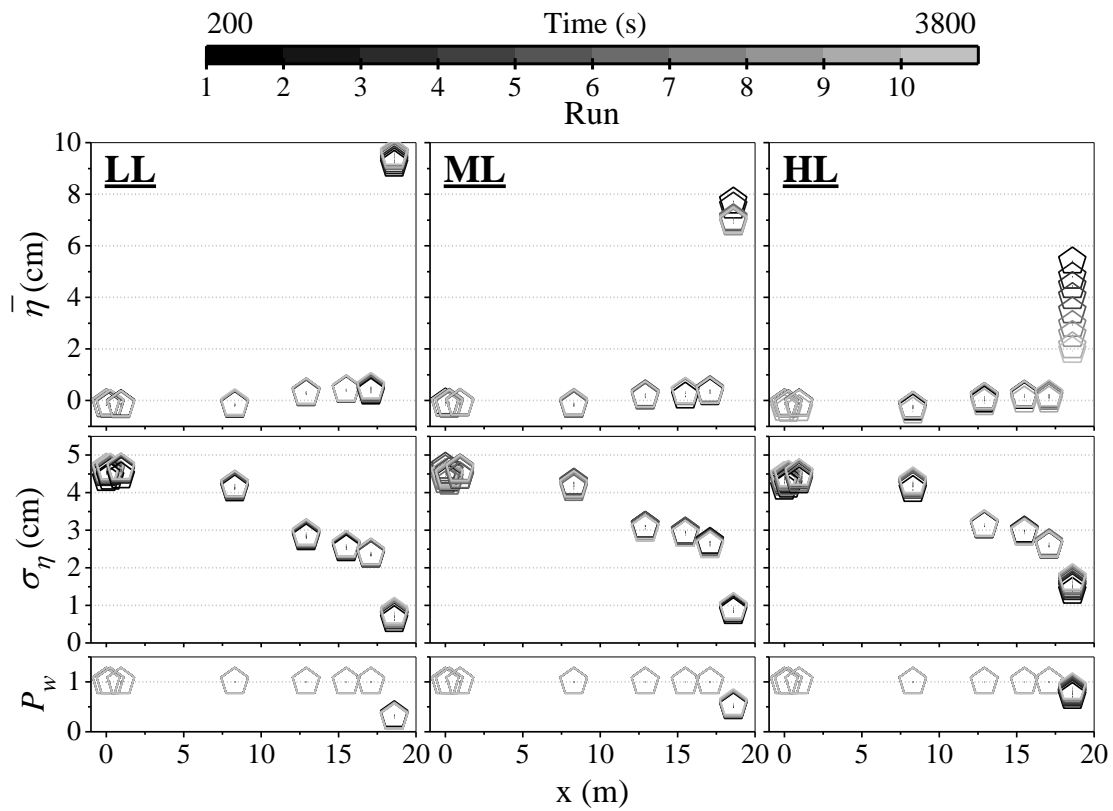


Figure 3.17. Cross-shore variations of mean $\bar{\eta}$ and standard deviation σ_{η} of free surface elevation η above SWL together with wet probability P_w for tests LL, ML, and HL.

Table 3.43. Mean cross-shore \bar{u} and standard deviation σ_u of the 2D ADV co-located with WG4 at $x = 8.30$ m, Red Vectrino co-located with WG5 at $x = 12.90$ m and Blue Vectrino co-located with WG6 at $x = 15.50$ m, LL.

Run	2D ADV at WG4		Red Vectrino at WG5		Blue Vectrino at WG6	
	\bar{u} (cm/s)	σ_u (cm/s)	\bar{u} (cm/s)	σ_u (cm/s)	\bar{u} (cm/s)	σ_u (cm/s)
LL1	-6.48	21.14	-3.70	16.17	-3.94	17.37
LL2	-7.18	21.27	-4.25	15.86	-3.80	17.33
LL3	-6.51	21.40	-4.22	15.88	-3.90	17.25
LL4	-6.45	21.22	NR	NR	-4.44	17.54
LL5	-7.11	21.69	-3.80	16.17	-3.97	17.69
LL6	-7.27	21.44	-3.55	16.12	NR	NR
LL7	-6.67	21.47	NR	NR	-4.09	17.42
LL8	-6.74	21.44	NR	NR	-3.60	17.48
LL9	-7.08	21.69	-3.97	15.94	-3.22	17.42
LL10	-6.86	21.75	-3.47	16.06	-3.16	17.49
Average	-6.84	21.45	-3.85	16.03	-3.79	17.44

NR implies "not reliable" data.

Table 3.44. Mean cross-shore \bar{u} and standard deviation σ_u of the 2D ADV co-located with WG4 at $x = 8.30$ m, Red Vectrino co-located with WG5 at $x = 12.90$ m and Blue Vectrino co-located with WG6 at $x = 15.50$ m, ML.

Run	2D ADV at WG4		Red Vectrino at WG5		Blue Vectrino at WG6	
	\bar{u} (cm/s)	σ_u (cm/s)	\bar{u} (cm/s)	σ_u (cm/s)	\bar{u} (cm/s)	σ_u (cm/s)
ML1	-5.78	20.74	NR	NR	-4.02	17.11
ML2	-6.61	21.08	-3.43	16.92	-3.64	17.40
ML3	NR	NR	NR	NR	NR	NR
ML4	-5.81	21.52	-4.01	17.02	-3.89	17.24
ML5	-7.15	21.30	-3.95	16.86	NR	NR
ML6	-5.61	19.58	-4.20	16.79	-4.51	17.31
ML7	-6.32	21.33	-4.10	16.85	-4.17	17.19
ML8	-6.94	21.49	-3.56	16.82	-4.16	16.90
ML9	-7.13	21.66	-3.49	16.87	-3.91	16.91
ML10	-6.14	21.41	-4.57	16.83	NR	NR
Average	-6.39	21.12	-3.91	16.87	-4.04	17.15

NR implies "not reliable" data.

Table 3.45. Mean cross-shore \bar{u} and standard deviation σ_u of the 2D ADV co-located with WG4 at $x = 8.30$ m, Red Vectrino co-located with WG5 at $x = 12.90$ m and Blue Vectrino co-located with WG6 at $x = 15.50$ m, HL.

Run	2D ADV at WG4		Red Vectrino at WG5		Blue Vectrino at WG6	
	\bar{u} (cm/s)	σ_u (cm/s)	\bar{u} (cm/s)	σ_u (cm/s)	\bar{u} (cm/s)	σ_u (cm/s)
HL1	-5.46	20.99	NR	NR	-4.44	17.55
HL2	-5.53	21.39	NR	NR	-4.14	17.50
HL3	-6.07	21.28	-2.14	17.15	-4.06	17.54
HL4	-5.91	21.35	-2.89	17.08	-3.99	17.54
HL5	-5.57	21.20	NR	NR	-3.73	17.49
HL6	-5.60	19.26	-2.97	16.65	-3.95	17.60
HL7	-6.10	21.13	-4.08	16.37	-3.95	17.70
HL8	-5.52	21.17	-3.57	16.53	-3.77	17.83
HL9	-5.52	21.25	-3.44	16.60	-3.89	17.69
HL10	-5.81	21.30	NR	NR	-3.60	17.68
Average	-5.71	21.03	-3.18	16.73	-3.95	17.61

NR implies "not reliable" data.

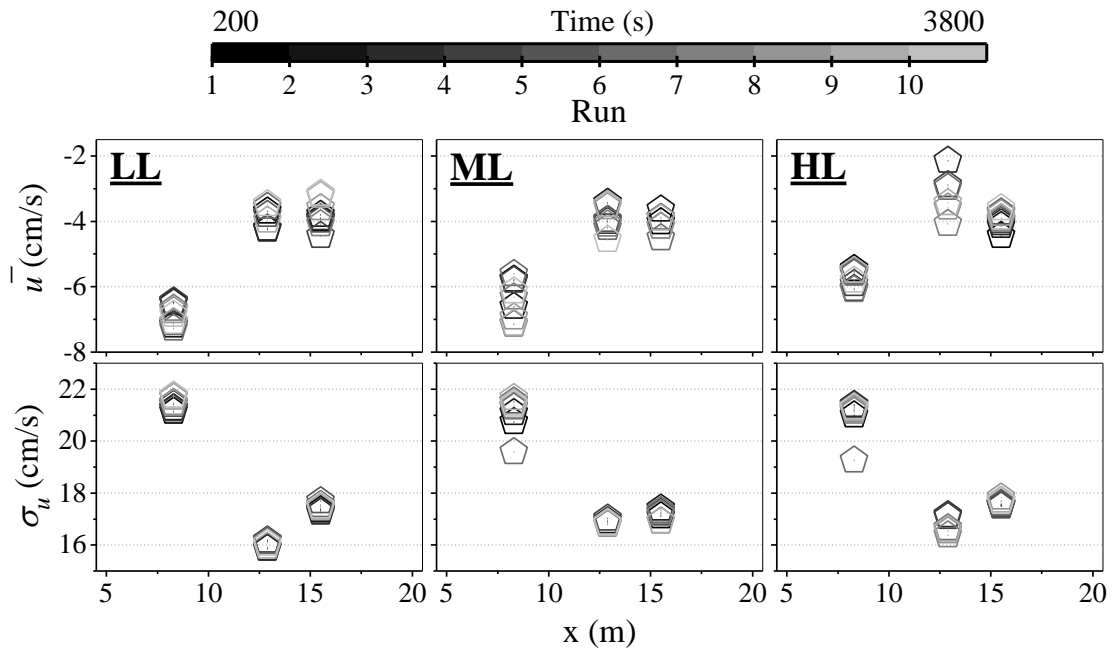


Figure 3.18. Cross-shore variations of mean \bar{u} and standard deviation σ_u of cross-shore velocity u for tests LL, ML, and HL.

3.2.2 Overtopping and Overwash

The wave overtopping rate q_o and sand overwash rate q_{bs} for tests LL, ML, and HL listed in in Tables 3.46 to 3.48 and plotted in Figure 3.19 did not vary much during the 10 runs and are similar to those shown in Figure 3.3.

Table 3.46. Measured sediment overwash rate q_{bs} , water overtopping rate q_o , and their ratio q_{bs}/q_o , LL.

Run	q_{bs} (cm²/s)	q_o (cm²/s)	q_{bs}/q_o
LL1	0.0005	0.090	0.006
LL2	0.0012	0.115	0.010
LL3	0.0009	0.124	0.007
LL4	0.0010	0.121	0.009
LL5	0.0012	0.195	0.006
LL6	0.0012	0.151	0.008
LL7	0.0014	0.135	0.010
LL8	0.0011	0.113	0.010
LL9	0.0008	0.165	0.005
LL10	0.0012	0.119	0.010

Table 3.47. Measured sediment overwash rate q_{bs} , water overtopping rate q_o , and their ratio q_{bs}/q_o , ML.

Run	q_{bs} (cm²/s)	q_o (cm²/s)	q_{bs}/q_o
ML1	0.0091	0.654	0.014
ML2	0.0103	0.599	0.017
ML3	0.0102	0.539	0.019
ML4	0.0095	0.461	0.021
ML5	0.0098	0.427	0.023
ML6	0.0059	0.354	0.017
ML7	0.0096	0.405	0.024
ML8	0.0094	0.379	0.025
ML9	0.0088	0.315	0.028
ML10	0.0091	0.311	0.029

Table 3.48. Measured sediment overwash rate q_{bs} , water overtopping rate q_o , and their ratio q_{bs}/q_o , HL.

Run	q_{bs} (cm ² /s)	q_o (cm ² /s)	q_{bs}/q_o
HL1	0.0641	1.837	0.035
HL2	0.0646	1.868	0.035
HL3	0.0628	1.826	0.034
HL4	0.0629	1.749	0.036
HL5	0.0593	1.649	0.036
HL6	0.0561	1.473	0.038
HL7	0.0570	1.537	0.037
HL8	0.0553	1.552	0.036
HL9	0.0577	1.646	0.035
HL10	0.0541	1.568	0.034

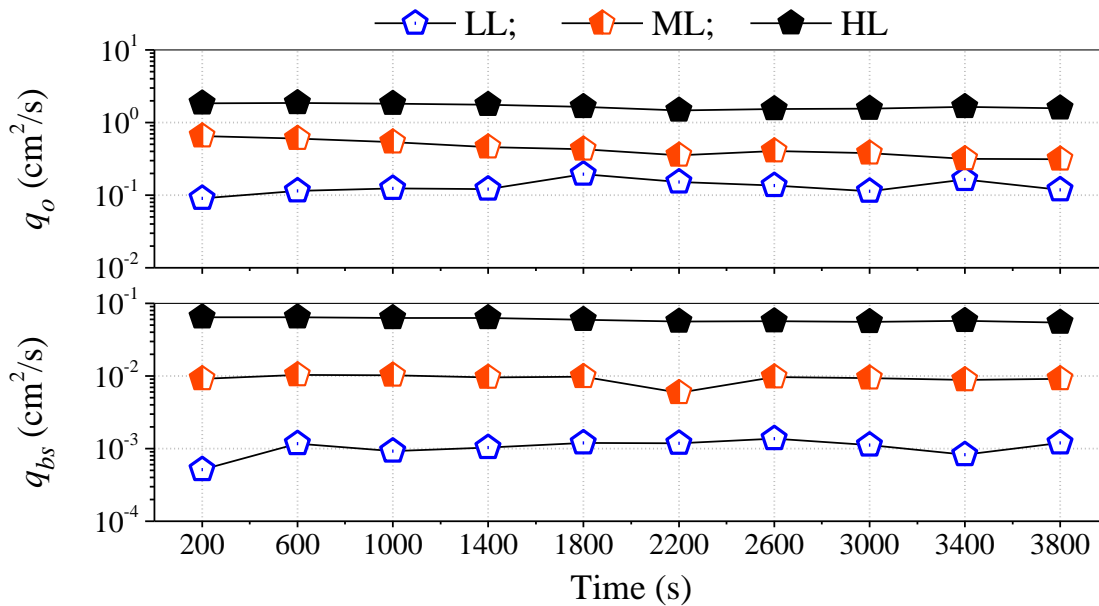


Figure 3.19. Temporal variations of wave overtopping rate q_o and sand overwash rate q_{bs} for tests LL (blue), ML (red), and HL (black).

3.2.3 Profile Evolution

Figure 3.20 shows the measured profile evolutions for tests LL, ML, and HL in the same way as in Figure 3.4. The overall profile evolution looks very similar to the profile evolution of the tests for the blocks on the ground apart from a hole created by sand leakage through a gap of the dividing wall ($x = 10.3$ m) during test HL. The gap and hole were repaired after test HL.

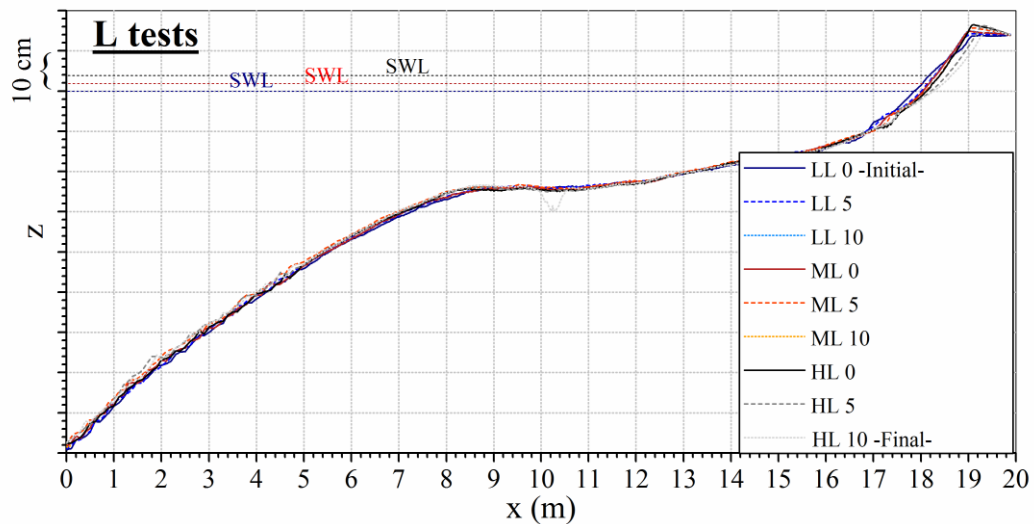


Figure 3.20. Profile evolution during tests LL, ML, and HL.

3.2.4 Foreshore and Berm Accretion or Erosion

The accretional profile evolution of the berm is similar for tests LG and LL as well as for tests MG and ML. The sediment budget is analyzed for tests LL (Table 3.49) and ML (Table 3.51). The maximum erosion and deposition are listed in Tables 3.50 and 3.52 for tests LL and ML, respectively, along with the foreshore and berm profile changes in Figures 3.21 and 3.22. On the other hand, the erosional berm evolutions during runs 1 to 5 in tests HG and HL are similar. The sediment budget is presented in Tables 3.53. The foreshore and berm profile changes are summarized in Table 3.54, and

Figure 3.23. The measured profile after run 10 in test HL indicates the continuing erosion of the berm at its seaward edge and the corresponding decrease of the foreshore slope. The beach profile evolutions during tests LL, ML, and HL are shown in Figures 3.24 and 3.25.

Table 3.49. Cumulative volume changes (cm^3/cm): eroded V_e , and deposited V_d sand volumes, net volume change V_c , cumulative sand overwash volume V_o , offshore sand loss volume V_l as well as the ratios $V_l/|V_c|$ and $V_o/|V_c|$ for the zone $x = 16$ to 19.9 m, LL.

Run	V_e	V_d	V_c	V_o	V_l	$V_l/ V_c $	$V_o/ V_c $
LL5	-200.74	367.01	166.27	3.23	163.04	0.98	0.02
LL10	-386.76	379.97	-6.79	7.04	-0.25	-0.04	1.04

Table 3.50. Maximum erosion depth and deposition height at cross-shore location x , and bottom elevation change Δz_b at WG7 and WG8 locations, LL.

RUN	max erosion		max deposition		WG7	WG8
	depth (cm)	x (m)	height (cm)	x (m)	Δz_b (cm)	Δz_b (cm)
LL5	-1.69	18.08	1.94	18.86	-0.46	0.32
LL10	-2.14	17.84	2.69	18.94	-1.61	0.33

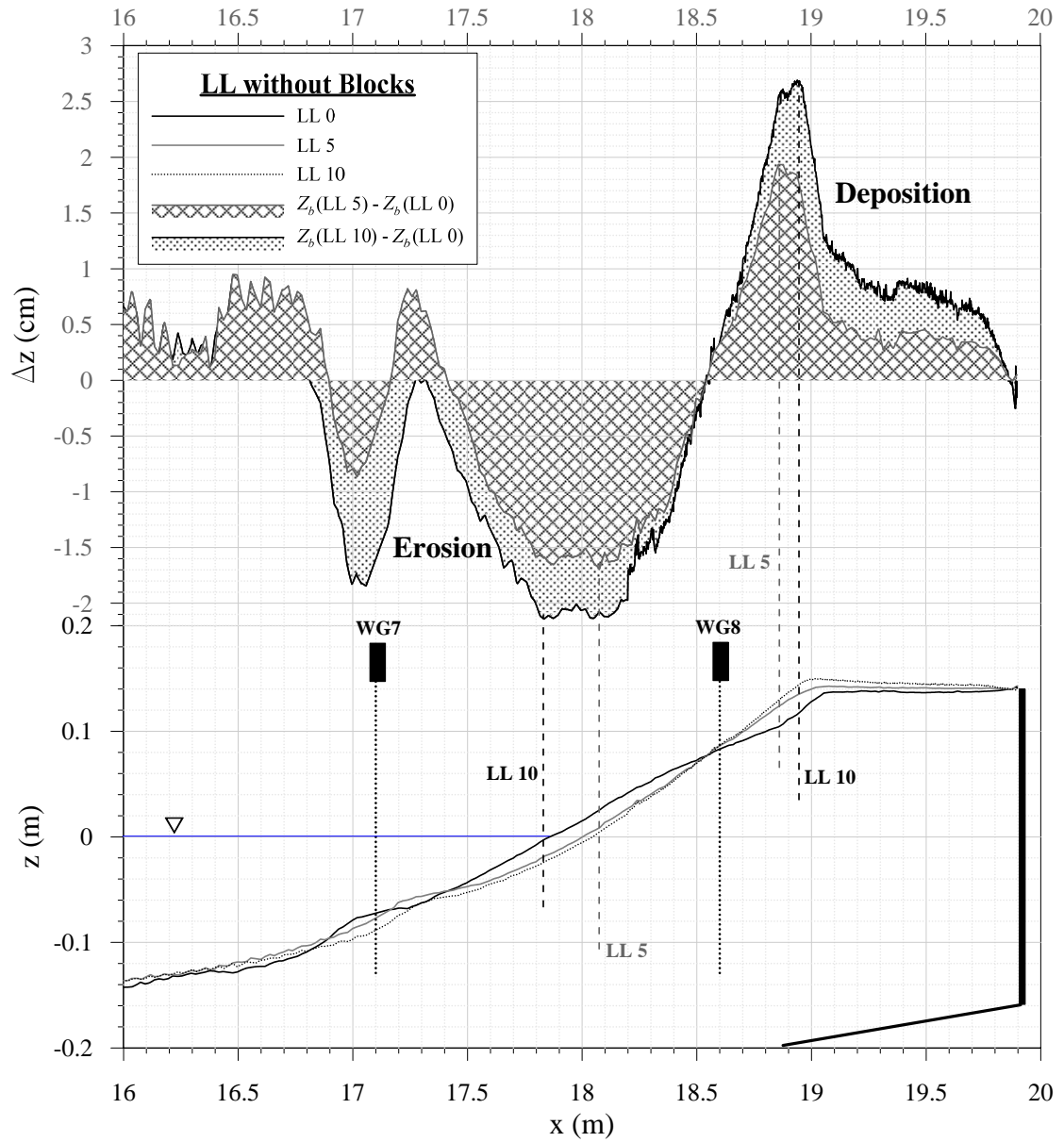


Figure 3.21. Bottom elevation difference between initial profile and profile measured after run 5 and 10 in test LL.

Table 3.51. Cumulative volume changes (cm^3/cm): eroded V_e , and deposited V_d sand volumes, net volume change V_c , cumulative sand overwash volume V_o , offshore sand loss volume V_l as well as the ratios $V_l/|V_c|$ and $V_o/|V_c|$ for the zone $x = 16$ to 19.9 m, ML.

Run	V_e	V_d	V_c	V_o	V_l	$V_l/ V_c $	$V_o/ V_c $
ML5	-240.40	201.21	-39.19	32.65	6.54	0.17	0.83
ML10	-463.79	181.30	-282.49	61.22	221.26	0.78	0.22

Table 3.52. Maximum erosion depth and deposition height at cross-shore location x , and bottom elevation change Δz_b at WG7 and WG8 locations, ML.

RUN	max erosion		max deposition		WG7	WG8
	depth (cm)	x (m)	height (cm)	x (m)	Δz_b (cm)	Δz_b (cm)
ML5	-1.43	18.23	1.05	19.08	-0.21	-0.97
ML10	-2.61	17.30	1.80	19.11	-0.35	-1.21

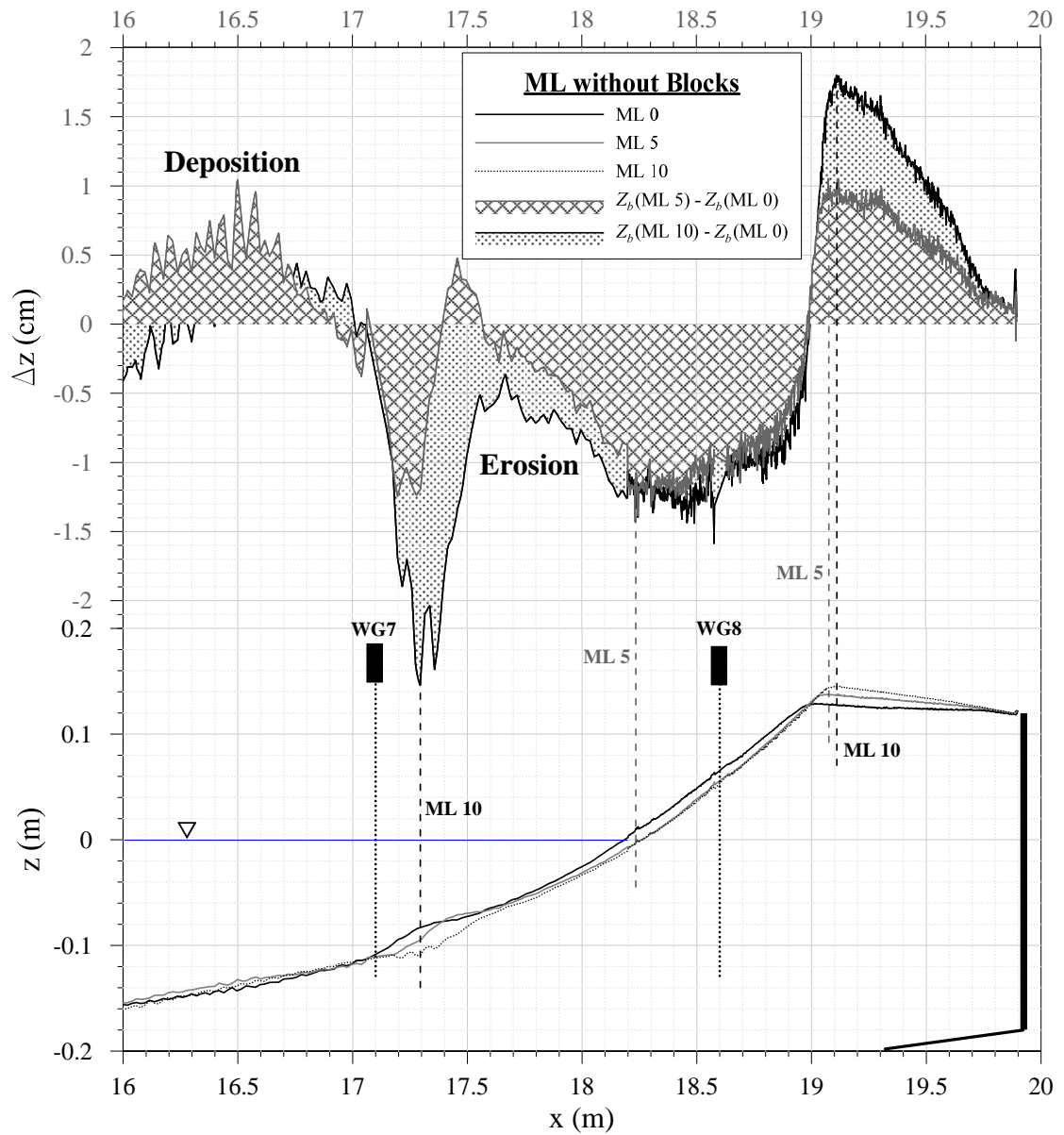


Figure 3.22. Bottom elevation difference between initial profile and profile measured after run 5 and 10 in test ML.

Table 3.53. Cumulative volume changes (cm^3/cm): eroded V_e , and deposited V_d sand volumes, net volume change V_c , cumulative sand overwash volume V_o , offshore sand loss volume V_l as well as the ratios $V_l/|V_c|$ and $V_o/|V_c|$ for the zone $x = 16$ to 19.9 m, HL.

Run	V_e	V_d	V_c	V_o	V_l	$V_l/ V_c $	$V_o/ V_c $
HL5	-620.45	109.88	-510.57	209.22	301.34	0.59	0.41
HL10	-1691.96	19.20	-1672.77	396.03	1276.74	0.76	0.24

Table 3.54. Maximum erosion depth and deposition height at cross-shore location x , and bottom elevation change Δz_b at WG7 and WG8 locations, HL.

RUN	max erosion		max deposition		WG7	WG8
	depth (cm)	x (m)	height (cm)	x (m)	Δz_b (cm)	Δz_b (cm)
HL5	-4.15	19.04	1.02	17.57	0.21	-2.77
HL10	-6.57	19.07	0.84	17.30	0.22	-4.04

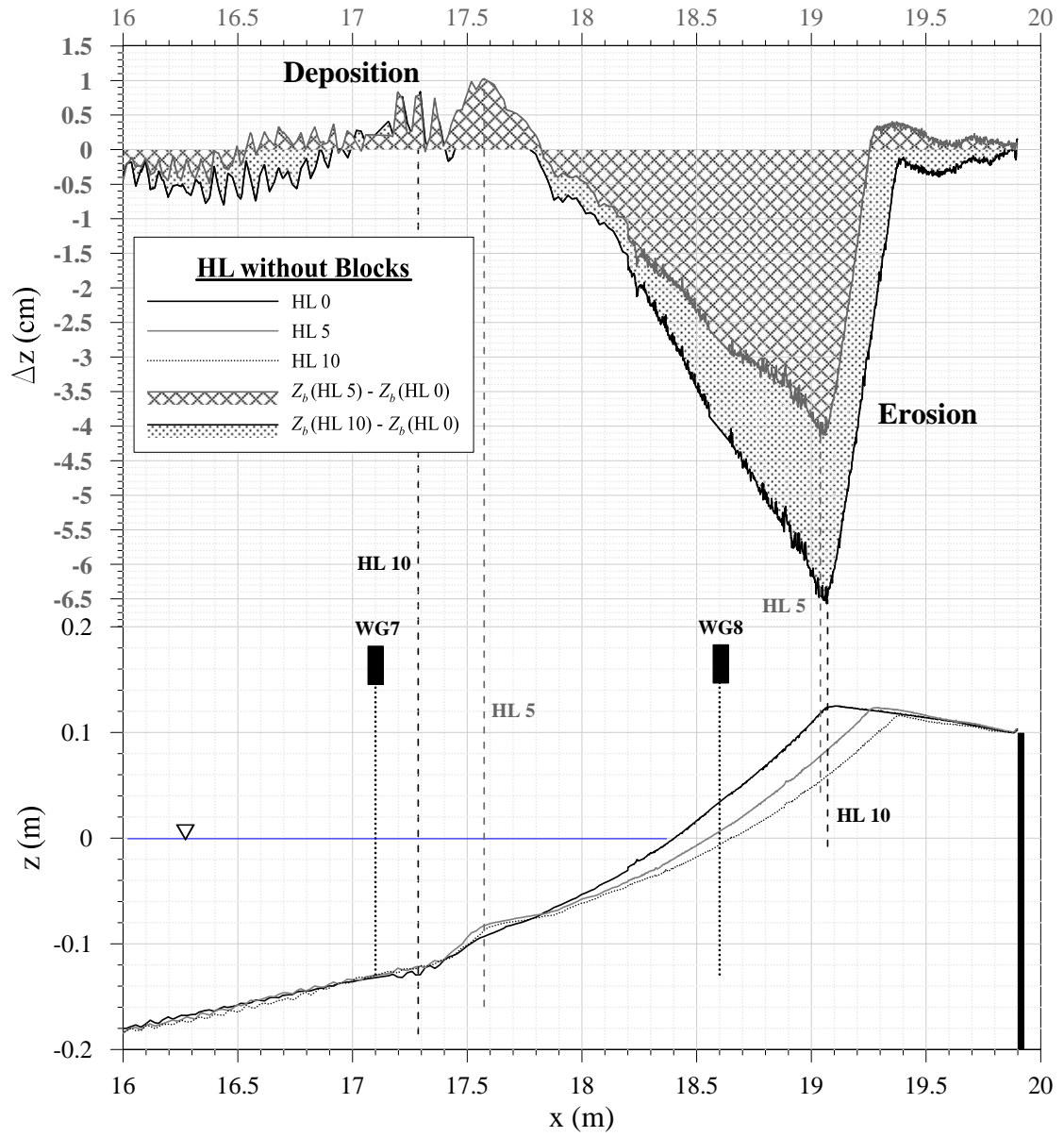


Figure 3.23. Bottom elevation difference between initial profile and profile measured after run 5 and 10 in test HL.

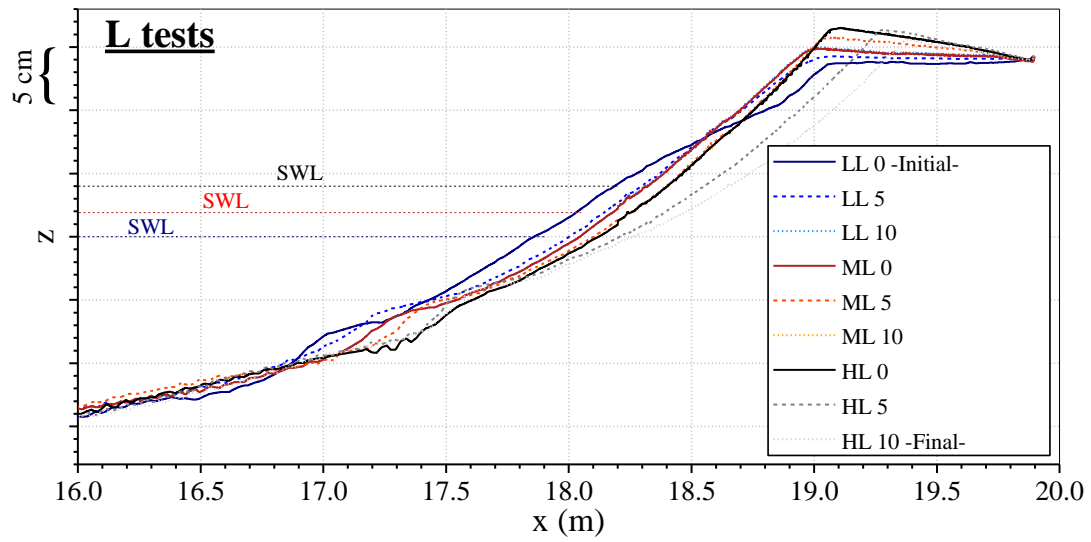


Figure 3.24. Beach profile evolution for series of tests LL, ML, and HL.

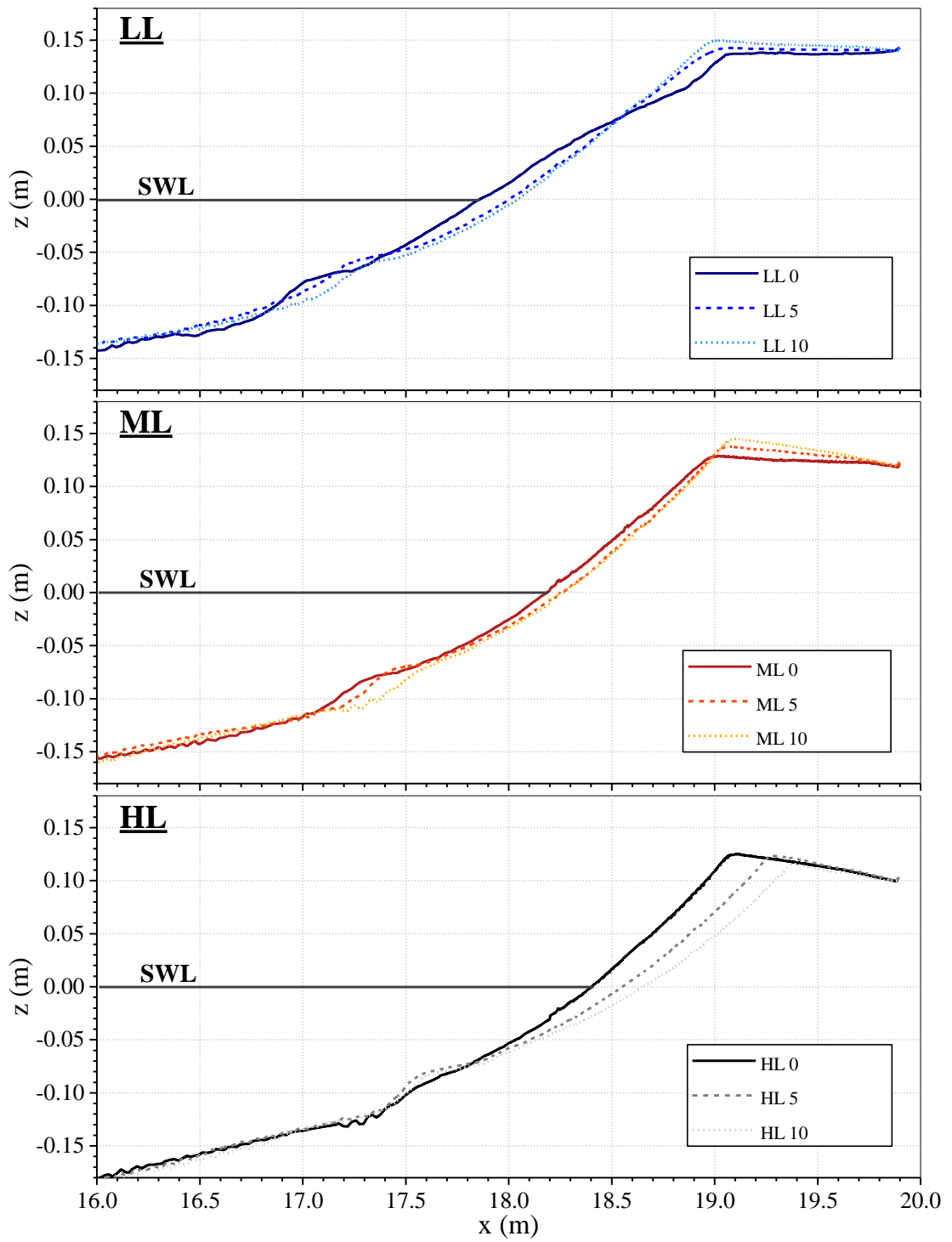


Figure 3.25. Comparison of beach profile evolution for tests LL, ML, and HL.

3.2.5 Block Movement

Figures 3.26, 3.28 and 3.30 depict the photos of the blocks before, during, and after tests LL, ML, and HL. Tables 3.55, 3.58 and 3.61 list the block response during the tests. The coordinates of the center of the bottom for each of the 10 blocks are given in Tables 3.56, 3.59, and 3.62. The laser line scanner images used to obtain the block coordinates are shown in Figures 3.27, 3.29, and 3.31. The clearance of each block during each run is listed in Tables 3.57, 3.60, and 3.63. This clearance was calculated by averaging the measured clearance before and after each run. The initial clearance of 4 cm for the 10 blocks in test LL varied with time (run 1 to 10) and spatially (block number) through the sequence of the three tests.

Figure 3.32 summarizes the reaction (fell, wet, and dry) of the 10 blocks in runs 1 to 10 of tests LL, ML, and HL performed in sequence without rebuilding the beach and berm. Blocks 1 and 2 fell from the pilings and floated in uprushing and downrushing water during run 1 of test LL. Block 1 floating in uprushing water collided against block 3 which fell from its pilings. This was the sole occurrence of collision-induced block falling in this experiment and this block is excluded from the block reaction analysis. The three fallen blocks were removed after run 1. During runs 1 to 10 of test LL, block 4 was wet always, blocks 5 and 6 were dry initially and became wet, and blocks 7 to 10 were dry always. During run 1 of test ML, blocks 1, 2, 5 and 6 fell, blocks 3 and 4 were wet, and blocks 7 to 10 were dry. The clearance of blocks 5 and 6 was reduced noticeably at the end of test LL and wave uprush impacted blocks 5 and 6 strongly unlike blocks 3 and 4 with a sufficient clearance. During runs 2 to 10 of test ML, blocks 3 and 4 were wet initially and became dry, whereas blocks 7 and 8 were dry initially and became wet. Blocks 9 and 10 were dry always. As for test HL, blocks 1 to 4 fell during run 1, blocks 5 to 8 were wet initially and became dry, and blocks 9 and 10 were

dry always. Comparison of Figures 3.16 and 3.32 indicates the effectiveness of raising the block elevation in reducing block damage (floating, sliding, and falling). The block reaction was sensitive to the block clearance which varied with the beach and berm profile change of the order of 4 cm in Figure 3.25.

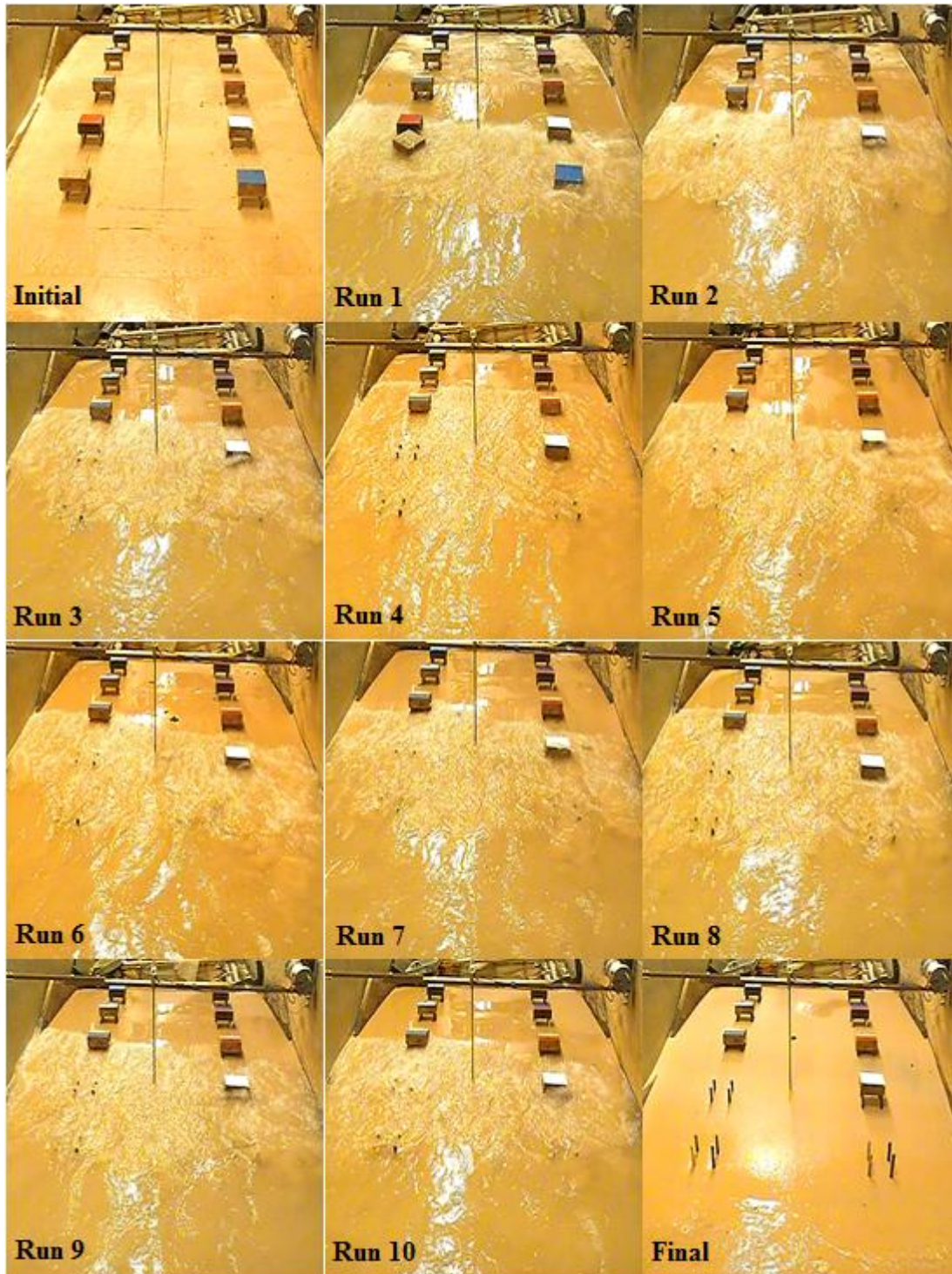


Figure 3.26. Swash and block interactions in each of 10 runs, along with initial and final block photos, LL.

Table 3.55. Block response during each of 10 runs in test LL.

Run	Block number									
	1	2	3	4	5	6	7	8	9	10
LL1	fell	fell	fell *	wet	dry	dry	dry	dry	dry	dry
LL2	no	no	no	wet	dry	dry	dry	dry	dry	dry
LL3	no	no	no	wet	dry	dry	dry	dry	dry	dry
LL4	no	no	no	wet	dry	dry	dry	dry	dry	dry
LL5	no	no	no	wet	wet	wet	dry	dry	dry	dry
LL6	no	no	no	wet	wet	wet	dry	dry	dry	dry
LL7	no	no	no	wet	wet	wet	dry	dry	dry	dry
LL8	no	no	no	wet	wet	wet	dry	dry	dry	dry
LL9	no	no	no	wet	wet	wet	dry	dry	dry	dry
LL10	no	no	no	wet	wet	wet	dry	dry	dry	dry

no implies “removed block”.

* implies “removed block after collision between blocks”.

Table 3.56. Location of 10 blocks during test LL with initial still water shoreline location $x_{SWL} = 17.86$ m.

Block No.	1	2	3	4	5	6	7	8	9	10
Initial location										
x_b (m)	18.28	18.27	18.61	18.60	18.94	18.93	19.28	19.26	19.60	19.59
y_b (m)	0.26	-0.30	0.26	-0.29	0.26	-0.30	0.26	-0.29	0.26	-0.29
Location after run 5										
x_b (m)	-	-	-	18.60	18.94	18.92	19.27	19.25	19.59	19.59
y_b (m)	-	-	-	-0.29	0.26	-0.29	0.26	-0.29	0.26	-0.29
Final location										
x_b (m)	-	-	-	18.60	18.93	18.92	19.27	19.25	19.59	19.59
y_b (m)	-	-	-	-0.29	0.26	-0.30	0.26	-0.29	0.26	-0.29

- implies “removed block”.

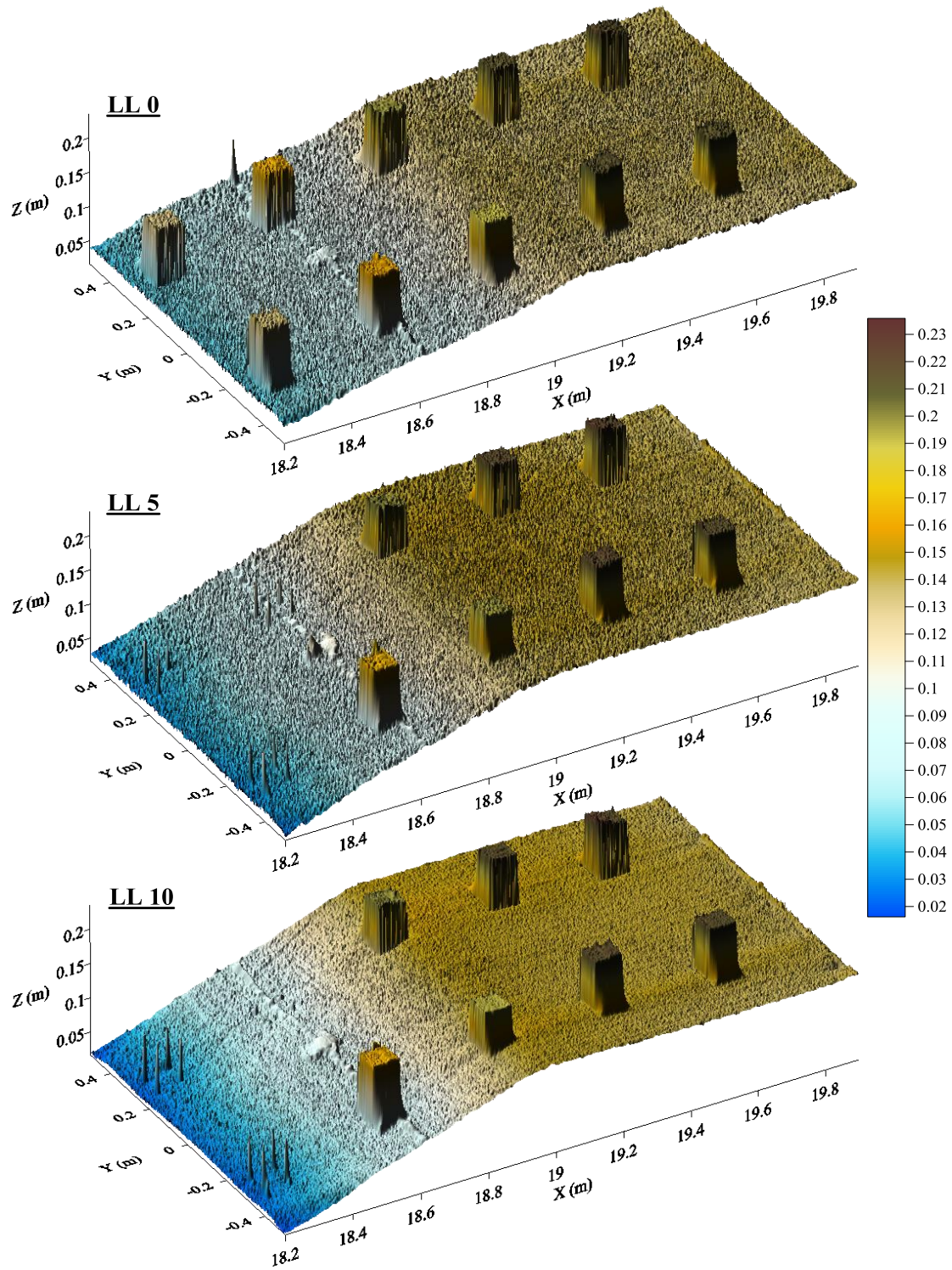


Figure 3.27. Laser line scanner images during test LL: initial (top), after run 5 (middle), and final (bottom).

Table 3.57. Clearance C (cm) during each run, LL.

Run	Block number									
	1	2	3	4	5	6	7	8	9	10
LL1	4.63	4.65	4.08	4.15	3.78	3.75	4.00	4.00	4.00	4.00
LL2	5.38	5.40	4.33	4.40	3.25	3.30	3.90	3.90	3.90	3.90
LL3	5.65	5.65	4.50	4.50	2.80	2.90	3.78	3.80	3.78	3.80
LL4	5.90	5.90	4.50	4.55	2.53	2.60	3.68	3.75	3.73	3.80
LL5	5.95	5.95	4.46	4.53	2.30	2.43	3.55	3.65	3.65	3.75
LL6	5.90	5.90	4.36	4.40	2.10	2.23	3.48	3.58	3.53	3.65
LL7	6.00	6.00	4.30	4.33	1.94	2.03	3.38	3.53	3.43	3.55
LL8	6.30	6.30	4.40	4.30	1.86	1.85	3.23	3.46	3.35	3.48
LL9	6.45	6.45	4.50	4.30	1.83	1.65	3.10	3.40	3.26	3.45
LL10	6.40	6.40	4.55	4.30	1.73	1.53	2.98	3.29	3.19	3.43

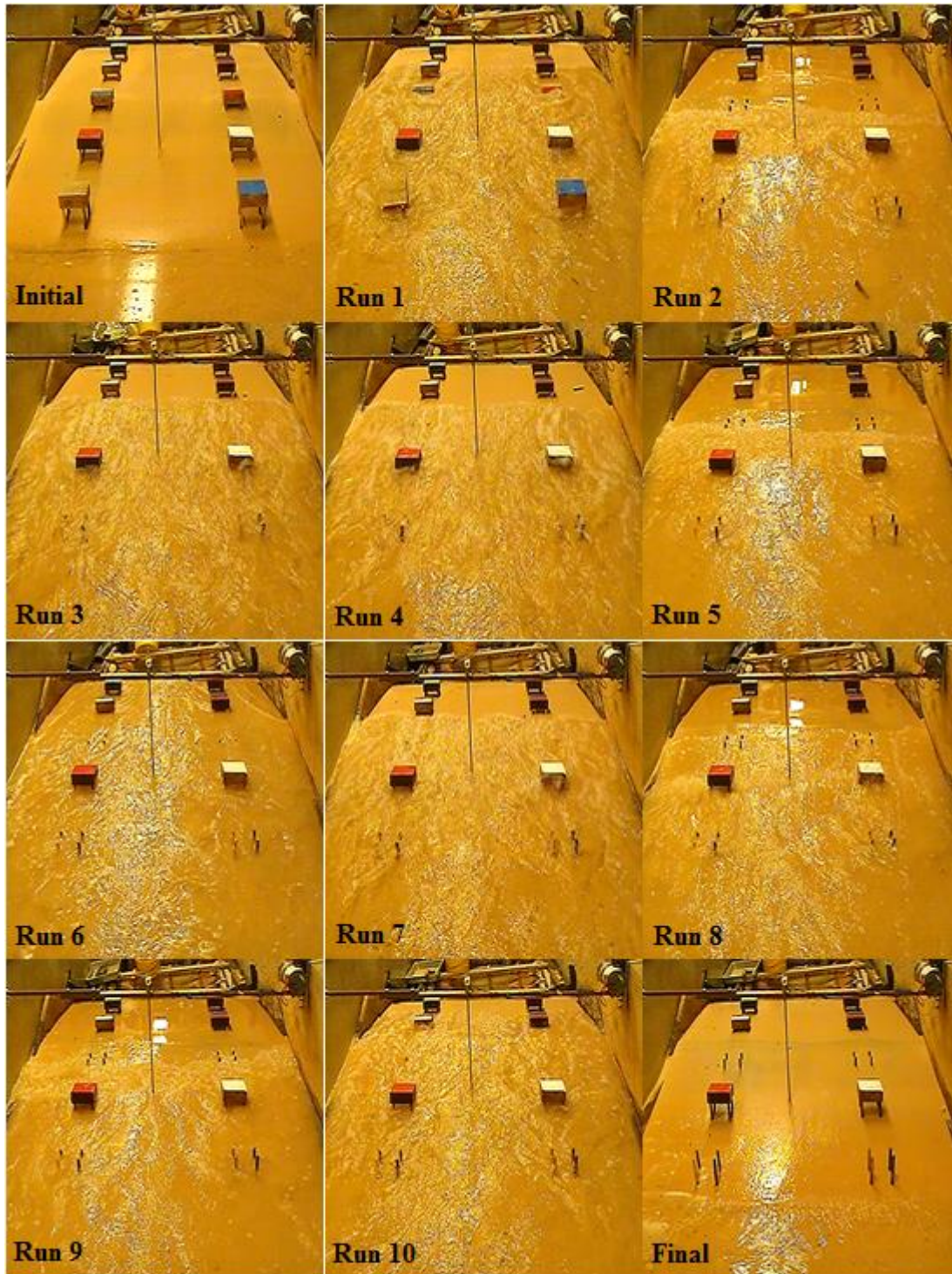


Figure 3.28. Swash and block interactions in each of 10 runs, along with initial and final block photos, ML.

Table 3.58. Block response during each of 10 runs in test ML.

Run	Block number									
	1	2	3	4	5	6	7	8	9	10
ML1	fell	fell	wet	wet	fell	fell	dry	dry	dry	dry
ML2	no	no	wet	wet	no	no	dry	dry	dry	dry
ML3	no	no	wet	wet	no	no	dry	dry	dry	dry
ML4	no	no	wet	wet	no	no	dry	dry	dry	dry
ML5	no	no	wet	wet	no	no	dry	dry	dry	dry
ML6	no	no	wet	wet	no	no	dry	dry	dry	dry
ML7	no	no	dry	wet	no	no	wet	wet	dry	dry
ML8	no	no	dry	dry	no	no	wet	wet	dry	dry
ML9	no	no	dry	dry	no	no	wet	wet	dry	dry
ML10	no	no	dry	dry	no	no	wet	wet	dry	dry

no implies “removed block”.

Table 3.59. Location of 10 blocks during test ML with initial still water shoreline location $x_{SWL} = 18.19$ m.

Block No.	1	2	3	4	5	6	7	8	9	10
Initial location										
x_b (m)	18.27	18.27	18.60	18.60	18.93	18.92	19.27	19.26	19.59	19.59
y_b (m)	0.26	-0.29	0.26	-0.29	0.26	-0.30	0.26	-0.29	0.26	-0.29
Location after run 5										
x_b (m)	-	-	18.60	18.60	-	-	19.28	19.26	19.60	19.60
y_b (m)	-	-	0.26	-0.29	-	-	0.26	-0.29	0.26	-0.29
Final location										
x_b (m)	-	-	18.60	18.59	-	-	19.27	19.25	19.59	19.59
y_b (m)	-	-	0.26	-0.29	-	-	0.26	-0.29	0.26	-0.29

- implies “removed block”.

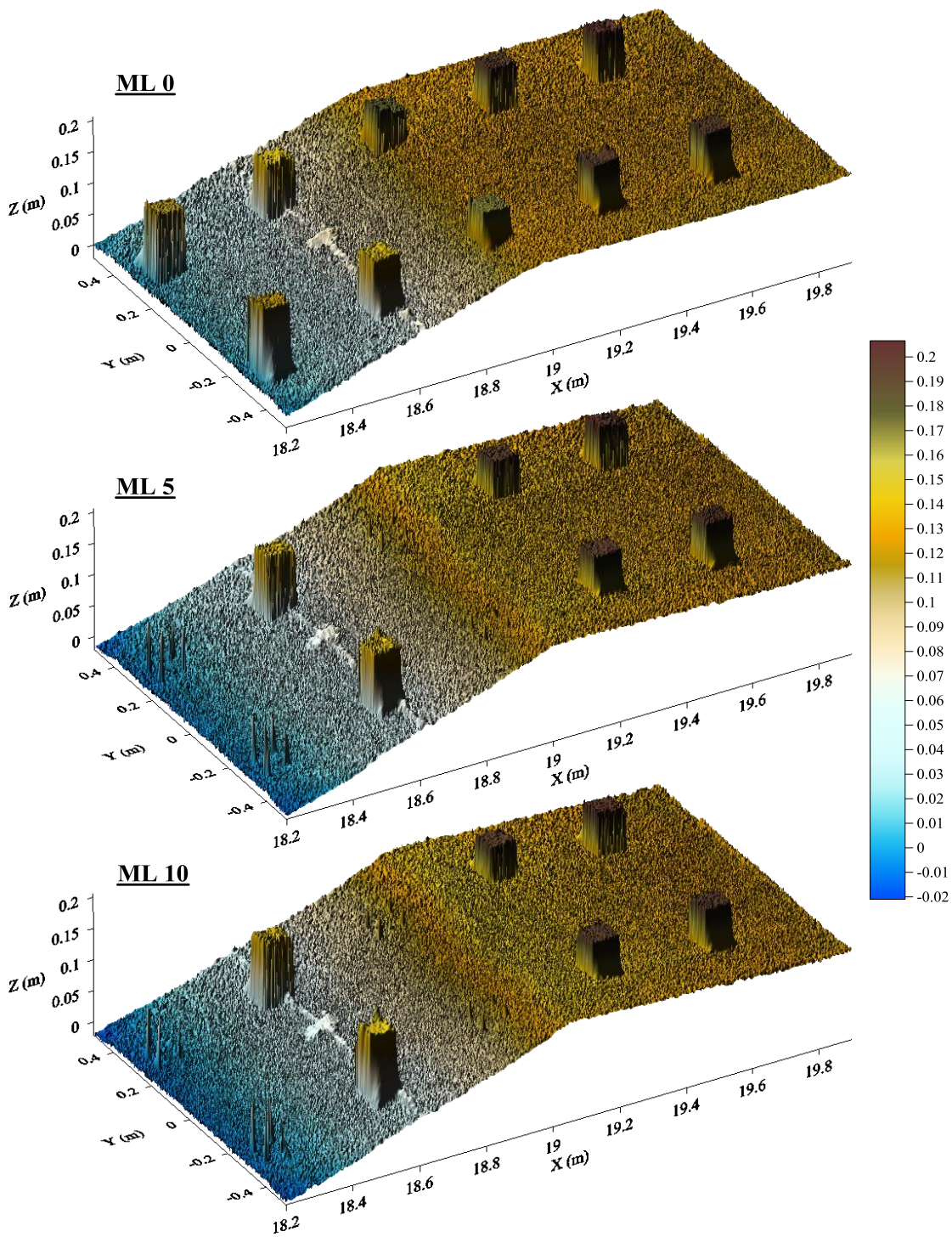


Figure 3.29. Laser line scanner images during test ML: initial (top), after run 5 (middle), and final (bottom).

Table 3.60. Clearance C (cm) during each run, ML.

Run	Block number									
	1	2	3	4	5	6	7	8	9	10
ML1	6.50	6.50	4.53	4.30	1.68	1.45	2.83	3.08	3.08	3.30
ML2	6.83	6.83	4.58	4.45	1.73	1.36	2.63	2.78	2.95	3.10
ML3	7.10	7.10	4.80	4.73	1.95	1.39	2.43	2.55	2.90	2.98
ML4	7.15	7.15	5.05	4.88	2.20	1.61	2.28	2.45	2.88	2.93
ML5	7.33	7.33	5.28	5.08	2.35	1.89	2.15	2.30	2.83	2.85
ML6	7.40	7.40	5.30	5.13	2.40	1.95	2.00	2.05	2.75	2.75
ML7	7.30	7.30	5.30	5.10	2.48	1.95	1.85	1.85	2.65	2.65
ML8	7.40	7.40	5.45	5.25	2.70	2.06	1.75	1.75	2.60	2.60
ML9	7.55	7.55	5.58	5.50	2.80	2.21	1.65	1.65	2.58	2.55
ML10	7.63	7.63	5.68	5.70	2.90	2.34	1.55	1.55	2.58	2.50

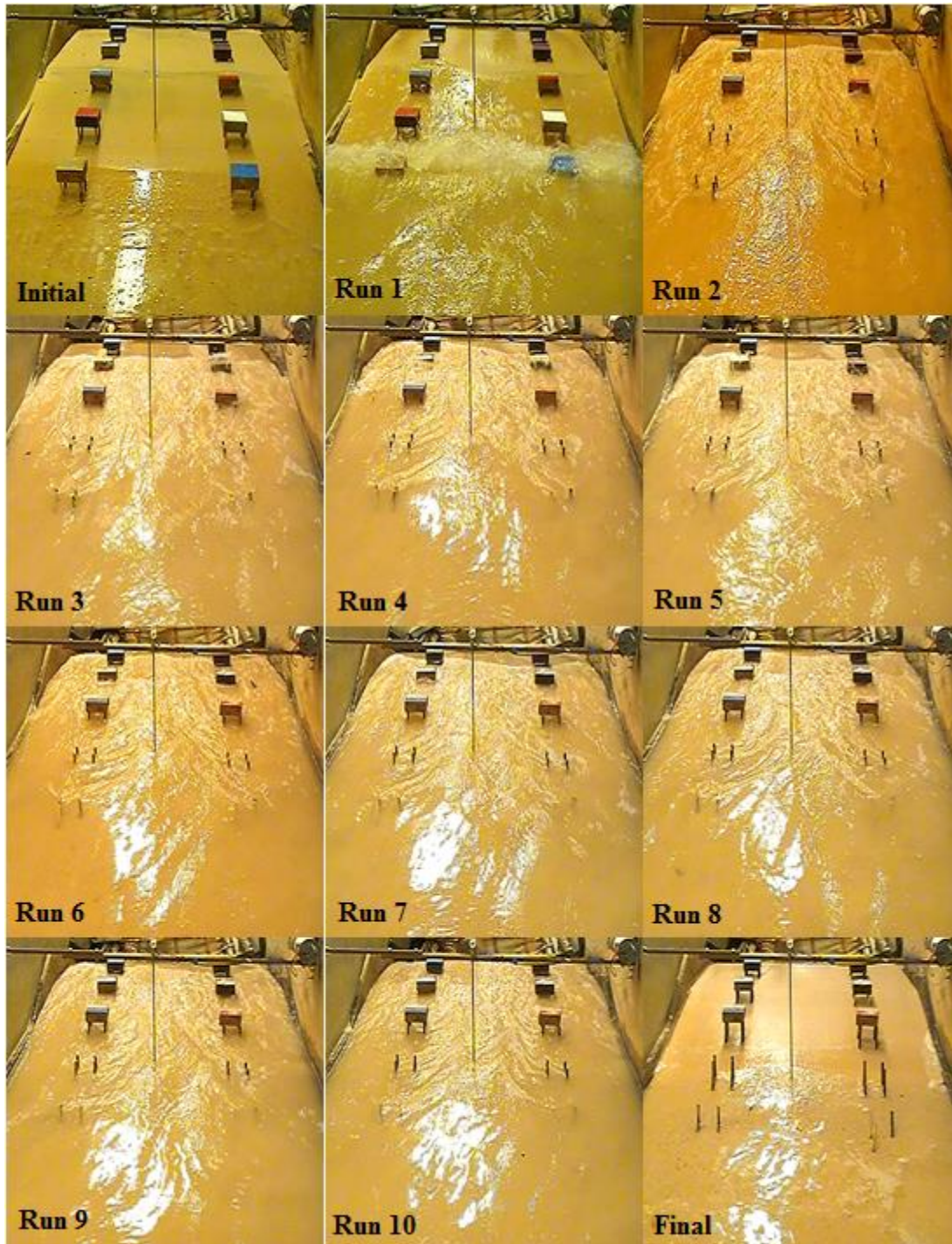


Figure 3.30. Swash and block interactions in each of 10 runs, along with initial and final block photos, HL.

Table 3.61. Block response during each of 10 runs in test HL.

Run	Block number									
	1	2	3	4	5	6	7	8	9	10
HL1	fell	fell	fell	fell	wet	wet	wet	wet	dry	dry
HL2	no	no	no	no	wet	wet	wet	wet	dry	dry
HL3	no	no	no	no	wet	wet	wet	wet	dry	dry
HL4	no	no	no	no	dry	dry	wet	wet	dry	dry
HL5	no	no	no	no	dry	dry	wet	wet	dry	dry
HL6	no	no	no	no	dry	dry	wet	wet	dry	dry
HL7	no	no	no	no	dry	dry	wet	wet	dry	dry
HL8	no	no	no	no	dry	dry	wet	dry	dry	dry
HL9	no	no	no	no	dry	dry	dry	dry	dry	dry
HL10	no	no	no	no	dry	dry	dry	dry	dry	dry

no implies "removed block".

Table 3.62. Location of 10 blocks during test HL with initial still water shoreline location $x_{SWL} = 18.40$ m.

Block No.	1	2	3	4	5	6	7	8	9	10
Initial location										
x_b (m)	18.28	18.27	18.60	18.60	18.94	18.93	19.27	19.26	19.60	19.60
y_b (m)	0.26	-0.29	0.26	-0.29	0.26	-0.29	0.26	-0.29	0.26	-0.29
Location after run 5										
x_b (m)	-	-	-	-	18.94	18.94	19.27	19.26	19.60	19.60
y_b (m)	-	-	-	-	0.26	-0.29	0.26	-0.29	0.26	-0.29
Final location										
x_b (m)	-	-	-	-	18.93	18.94	19.27	19.26	19.60	19.59
y_b (m)	-	-	-	-	0.26	-0.29	0.26	-0.29	0.26	-0.29

- implies "removed block".

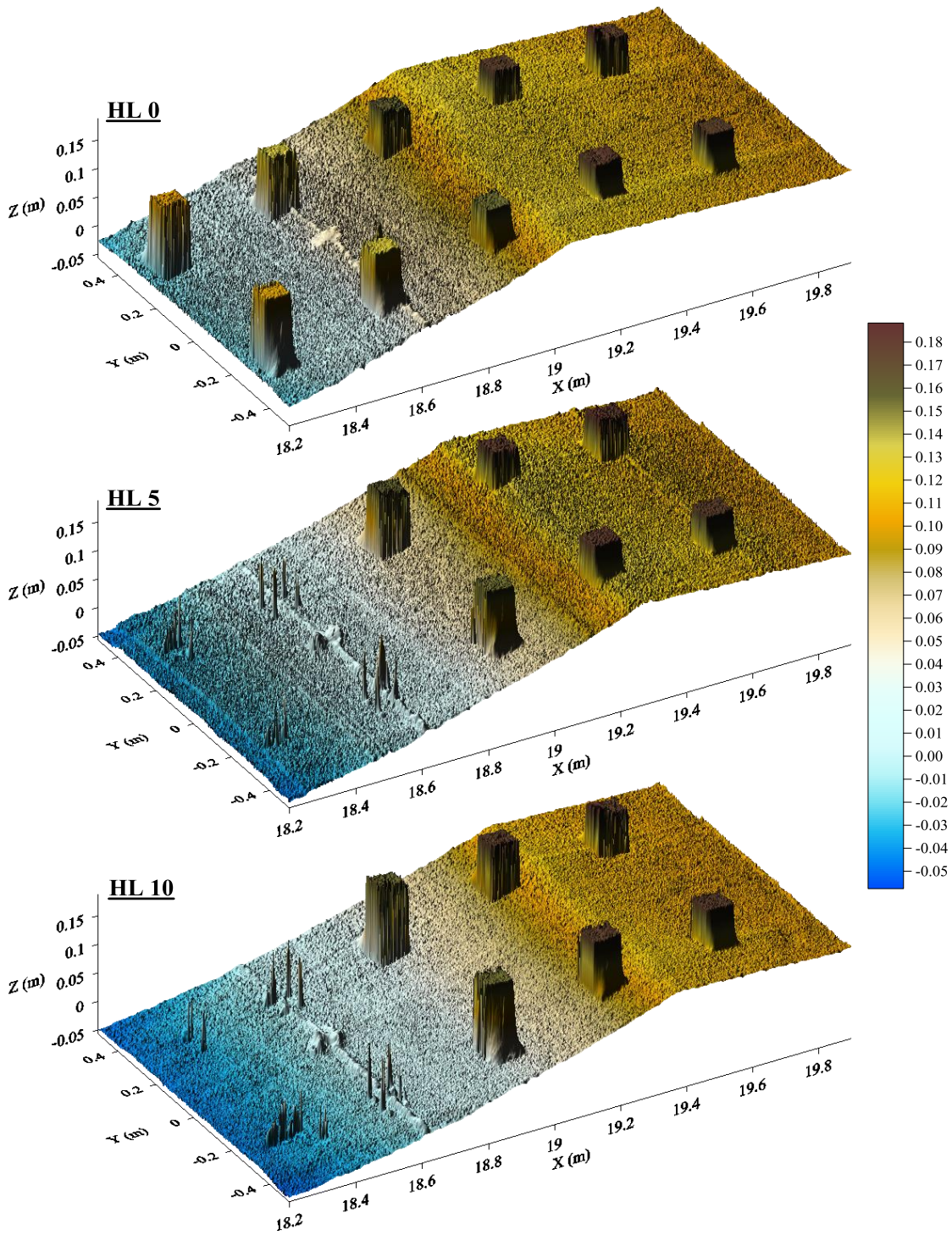


Figure 3.31. Laser line scanner images during test HL: initial (top), after run 5 (middle), and final (bottom).

Table 3.63. Clearance C (cm) during each run, HL.

Run	Block number									
	1	2	3	4	5	6	7	8	9	10
HL1	8.08	8.08	6.00	5.95	3.23	2.59	1.50	1.48	2.50	2.35
HL2	8.58	8.58	6.55	6.53	3.75	3.25	1.50	1.33	2.35	2.10
HL3	8.78	8.78	7.18	6.98	4.55	4.08	1.53	1.18	2.28	2.00
HL4	9.00	9.00	7.65	7.30	5.33	4.90	1.55	1.25	2.35	2.03
HL5	9.28	9.28	7.95	7.80	5.98	5.75	1.83	1.60	2.50	2.08
HL6	9.60	9.60	8.38	8.30	6.65	6.28	2.30	2.18	2.53	2.23
HL7	NR	NR	8.83	8.48	7.05	6.58	2.74	2.73	2.55	2.38
HL8	NR	NR	9.03	8.73	7.45	6.98	3.26	3.25	2.68	2.43
HL9	NR	NR	9.20	9.10	7.93	7.35	3.93	3.73	2.80	2.48
HL10	NR	NR	9.40	9.30	8.30	7.75	4.55	4.18	2.93	2.65

NR implies “not reliable” data.

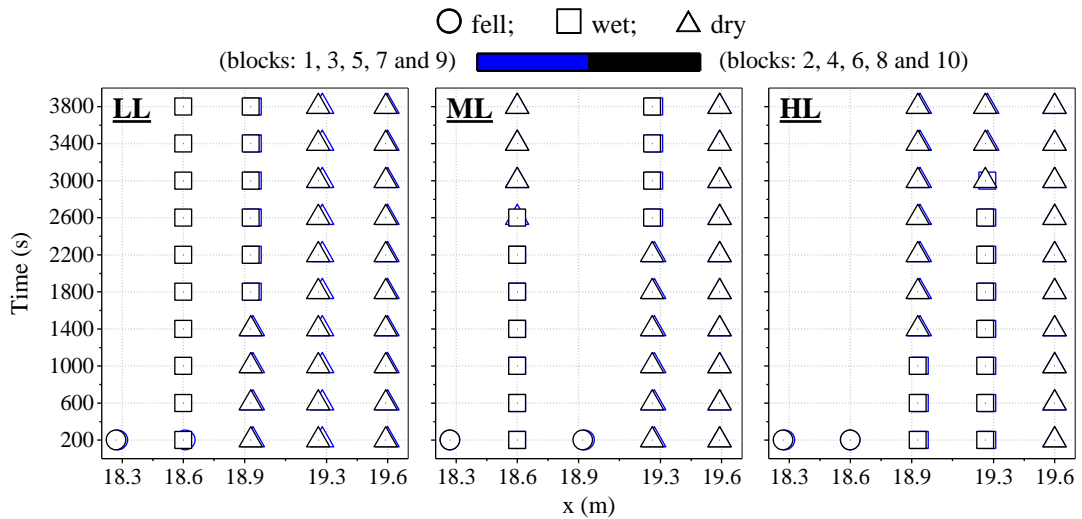


Figure 3.32. Response (fell, wet, and dry) of 10 blocks on long pilings in each run for tests LL, ML, and HL.

3.3 Blocks on Short Pilings

The clearance of the 10 blocks on short pilings above the rebuilt beach and berm profile was reduced to 2 cm at the start of test LS to examine the block clearance effect further.

3.3.1 Hydrodynamics

The incident wave characteristics at the location $x = 0$ of WG1 (Tables 3.64 and 3.65) remained similar to those in the tests for the blocks on the ground (Tables 3.1, 3.2, and 3.3) and on the long piling (Tables 3.31, 3.32, and 3.33).

The mean $\bar{\eta}$ and standard deviation σ_{η} of the free surface elevation η and wet probability P_w for tests LS and MS listed in Tables 3.66 to 3.71 and shown in Figure 3.33 are similar to those for tests LL and ML in Figure 3.17. The mean \bar{u} and standard deviation σ_u of the cross-shore velocity u for tests LS and MS listed in Tables 3.72 and 3.73 and plotted in Figure 3.34 are also similar to those for tests LL and ML in Figure 3.18.

Table 3.64. Incident wave characteristics, LS.

Run	H_{mo} (cm)	H_{rms} (cm)	H_s (cm)	T_p (s)	T_s (s)	R
LS1	17.63	12.47	17.02	2.62	2.07	0.13
LS2	18.16	12.84	17.47	2.62	2.04	0.13
LS3	18.46	13.05	17.67	2.62	2.04	0.14
LS4	18.51	13.09	17.70	2.62	2.00	0.13
LS5	18.56	13.12	17.88	2.62	2.01	0.13
LS6	17.17	12.14	16.42	2.62	2.02	0.14
LS7	17.69	12.51	16.87	2.62	2.02	0.13
LS8	17.89	12.65	17.10	2.62	2.02	0.14
LS9	18.06	12.77	17.33	2.62	2.00	0.14
LS10	18.08	12.78	17.30	2.62	2.02	0.14
Average	18.02	12.74	17.28	2.62	2.02	0.13

Table 3.65. Incident wave characteristics, MS.

Run	H_{mo} (cm)	H_{rms} (cm)	H_s (cm)	T_p (s)	T_s (s)	R
MS1	17.20	12.16	16.64	2.64	2.17	0.18
MS2	17.63	12.47	17.08	2.64	2.15	0.19
MS3	17.81	12.59	17.20	2.64	2.16	0.19
MS4	17.90	12.66	17.19	2.64	2.14	0.19
MS5	17.91	12.66	17.27	2.64	2.15	0.19
MS6	17.29	12.23	16.65	2.64	2.15	0.18
MS7	NR	NR	NR	NR	NR	NR
Average	17.62	12.46	17.00	2.64	2.15	0.19

NR implies "not reliable" data.

Table 3.66. Mean free-surface elevation $\bar{\eta}$ (cm) at 7 wave gauge locations, LS.

Run	WG1	WG2	WG3	WG4	WG5	WG6	WG7
LS1	-0.14	-0.19	-0.14	-0.18	0.23	0.39	0.24
LS2	-0.13	-0.15	-0.14	-0.15	0.28	0.37	0.31
LS3	-0.13	-0.16	-0.14	-0.14	0.31	0.41	0.31
LS4	-0.12	-0.14	-0.15	-0.15	0.31	0.41	0.39
LS5	-0.12	-0.16	-0.14	-0.13	0.32	0.41	0.44
LS6	-0.16	-0.19	-0.12	-0.16	0.25	0.35	0.36
LS7	-0.14	-0.14	-0.13	-0.16	0.30	0.36	0.40
LS8	-0.11	-0.13	-0.14	-0.15	0.32	0.37	0.43
LS9	-0.12	-0.08	-0.14	-0.14	0.32	0.40	0.73
LS10	-0.13	-0.16	-0.14	-0.11	0.32	0.42	0.43
Average	-0.13	-0.15	-0.14	-0.15	0.30	0.39	0.40

Table 3.67. Mean free-surface elevation $\bar{\eta}$ (cm) at 7 wave gauge locations, MS.

Run	WG1	WG2	WG3	WG4	WG5	WG6	WG7
MS1	-0.15	-0.27	-0.11	-0.20	0.14	0.22	0.10
MS2	-0.14	-0.16	-0.10	-0.14	0.17	0.29	0.36
MS3	-0.16	-0.12	-0.12	-0.14	0.20	0.33	0.36
MS4	-0.16	-0.13	-0.12	-0.13	0.21	0.33	0.32
MS5	-0.12	-0.11	-0.12	-0.15	0.17	0.32	0.38
MS6	-0.13	-0.18	-0.13	-0.19	0.15	0.31	0.35
MS7	NR	NR	NR	NR	NR	NR	NR
Average	-0.14	-0.16	-0.12	-0.16	0.17	0.30	0.31

NR implies "not reliable" data.

Table 3.68. Free-surface standard deviation σ_η (cm) at 7 wave gauge locations, LS.

Run	WG1	WG2	WG3	WG4	WG5	WG6	WG7
LS1	4.36	4.38	4.41	4.06	2.85	2.51	2.36
LS2	4.50	4.52	4.54	4.08	2.87	2.54	2.40
LS3	4.57	4.59	4.60	4.13	2.88	2.55	2.40
LS4	4.59	4.61	4.63	4.10	2.87	2.57	2.40
LS5	4.60	4.63	4.64	4.13	2.89	2.56	2.37
LS6	4.24	4.21	4.35	3.89	2.78	2.50	1.76
LS7	4.38	4.34	4.47	3.96	2.80	2.51	1.76
LS8	4.42	4.40	4.53	3.95	2.83	2.51	1.73
LS9	4.47	4.43	4.57	3.96	2.83	2.52	1.79
LS10	4.48	4.44	4.58	4.00	2.85	2.53	1.81
Average	4.46	4.46	4.53	4.03	2.85	2.53	2.08

Table 3.69. Free-surface standard deviation σ_η (cm) at 7 wave gauge locations, MS.

Run	WG1	WG2	WG3	WG4	WG5	WG6	WG7
MS1	4.30	4.30	4.43	4.12	3.07	2.94	2.35
MS2	4.45	4.42	4.57	4.17	3.06	2.91	2.33
MS3	4.51	4.47	4.61	4.18	3.05	2.91	2.32
MS4	4.56	4.50	4.63	4.20	3.06	2.92	2.26
MS5	4.51	4.47	4.63	4.18	3.06	2.92	2.26
MS6	4.34	4.31	4.45	4.15	3.09	2.96	3.09
MS7	NR						
Average	4.45	4.41	4.55	4.17	3.07	2.93	2.44

NR implies "not reliable" data.

Table 3.70. Wet probability P_w , its mean free-surface elevation $\bar{\eta}$ (cm), and free-surface standard deviation σ_η (cm) for WG8, LS.

Run	t (s)	P_w	Z_b (cm)	\bar{h} (cm)	$\bar{\eta}$ (cm)	σ_η (cm)
	0		8.38			
LS1	200	0.38	8.37	0.82	9.19	0.62
LS2	600	0.32	8.34	0.83	9.17	0.7
LS3	1000	0.32	8.32	0.96	9.28	0.75
LS4	1400	0.31	8.30	0.91	9.21	0.74
LS5	1800	0.30	8.27	0.90	9.17	0.78
	2000		8.26			
LS6	2200	0.30	8.26	1.04	9.30	0.78
LS7	2600	0.31	8.26	1.06	9.32	0.81
LS8	3000	0.34	8.26	0.97	9.23	0.83
LS9	3400	0.31	8.25	1.04	9.29	0.83
LS10	3800	0.31	8.25	1.08	9.33	0.84
	4000		8.25			
Average		0.32		0.96	9.25	0.77

Table 3.71. Wet probability P_w , its mean free-surface elevation $\bar{\eta}$ (cm), and free-surface standard deviation σ_η (cm) for WG8, MS.

Run	t (s)	P_w	Z_b (cm)	\bar{h} (cm)	$\bar{\eta}$ (cm)	σ_η (cm)
	0		6.39			
MS1	200	0.55	6.23	1.28	7.51	0.88
MS2	600	0.53	5.93	1.47	7.40	0.93
MS3	1000	0.53	5.63	1.36	6.99	0.96
MS4	1400	0.55	5.32	1.50	6.82	0.99
MS5	1800	0.56	5.02	1.52	6.54	0.99
	2000		4.87			
MS6	2200	0.58	4.87	1.51	6.38	1.02
MS7	2600	NR	4.87	NR	NR	NR
	2800		4.87			
Average		0.55		1.44	6.94	0.96

NR implies "not reliable" data.

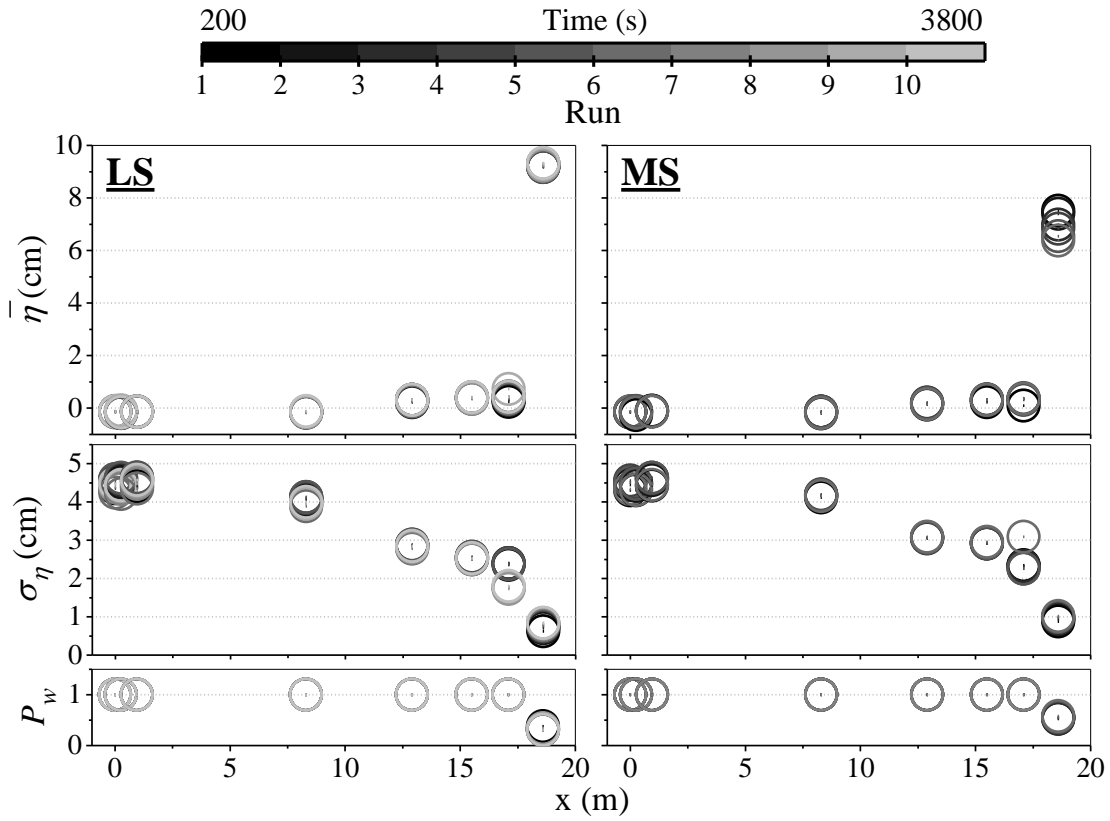


Figure 3.33. Cross-shore variations of mean $\bar{\eta}$ and standard deviation σ_{η} of free surface elevation η above SWL together with wet probability P_w for tests LS and MS.

Table 3.72. Mean cross-shore \bar{u} and standard deviation σ_u of the 2D ADV co-located with WG4 at $x = 8.30$ m, Red Vectrino co-located with WG5 at $x = 12.90$ m and Blue Vectrino co-located with WG6 at $x = 15.50$ m, LS.

Run	2D ADV at WG4		Red Vectrino at WG5		Blue Vectrino at WG6	
	\bar{u} (cm/s)	σ_u (cm/s)	\bar{u} (cm/s)	σ_u (cm/s)	\bar{u} (cm/s)	σ_u (cm/s)
LS1	-6.85	21.33	NR	NR	-4.14	17.15
LS2	-6.59	21.36	NR	NR	NR	NR
LS3	-7.11	21.59	NR	NR	-3.59	17.17
LS4	-6.33	21.74	NR	NR	-3.90	17.18
LS5	-6.85	21.50	NR	NR	NR	NR
LS6	-6.14	21.17	-3.37	15.98	-3.88	16.91
LS7	-5.76	21.91	-3.52	16.10	-3.71	17.23
LS8	-6.18	21.84	-3.59	16.32	-3.61	17.25
LS9	-6.95	22.08	-3.21	16.45	-3.27	17.08
LS10	-6.16	21.86	-3.47	16.20	-3.16	17.03
Average	-6.49	21.64	-3.43	16.21	-3.66	17.13

NR implies "not reliable" data.

Table 3.73. Mean cross-shore \bar{u} and standard deviation σ_u of the 2D ADV co-located with WG4 at $x = 8.30$ m, Red Vectrino co-located with WG5 at $x = 12.90$ m and Blue Vectrino co-located with WG6 at $x = 15.50$ m, MS.

Run	2D ADV at WG4		Red Vectrino at WG5		Blue Vectrino at WG6	
	\bar{u} (cm/s)	σ_u (cm/s)	\bar{u} (cm/s)	σ_u (cm/s)	\bar{u} (cm/s)	σ_u (cm/s)
MS1	-6.94	21.28	-3.31	17.13	-4.18	17.21
MS2	-6.62	21.27	-3.19	17.16	-3.60	17.31
MS3	-6.74	21.32	-3.47	17.15	NR	NR
MS4	-6.97	21.42	-3.68	17.28	NR	NR
MS5	-7.03	21.26	-2.60	17.25	-3.60	17.19
MS6	-5.92	21.15	-3.26	17.24	-3.95	17.23
MS7	NR	NR	NR	NR	NR	NR
Average	-6.70	21.28	-3.25	17.20	-3.83	17.24

NR implies "not reliable" data.

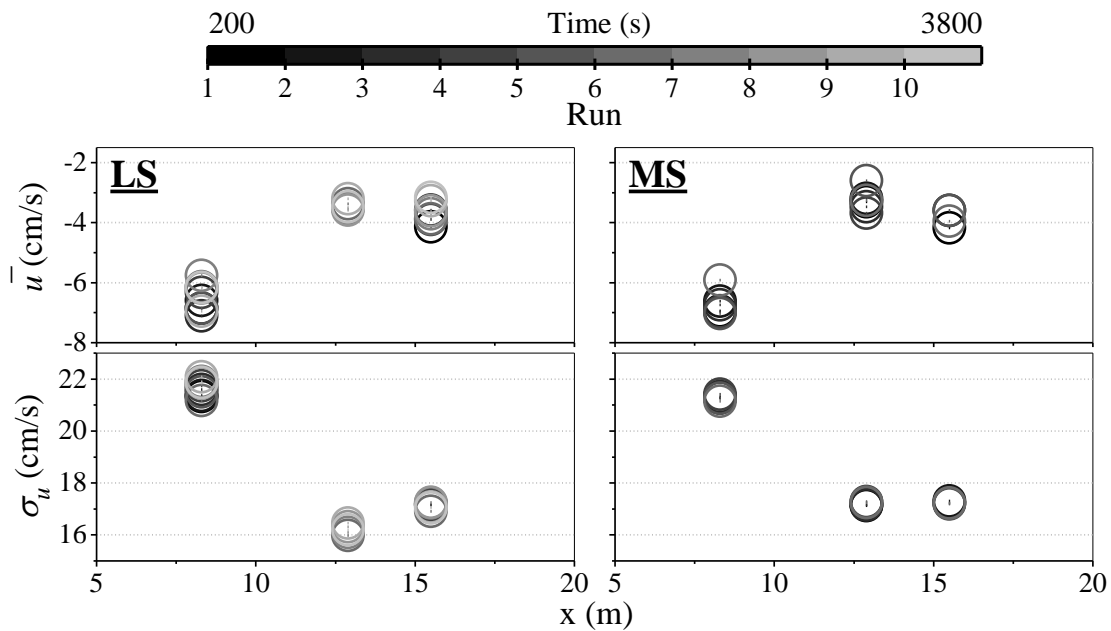


Figure 3.34. Cross-shore variations of mean \bar{u} and standard deviation σ_u of cross-shore velocity u for tests LS, and MS.

3.3.2 Overtopping and Overwash

The temporal variations of the wave overtopping rate q_o and sand overwash rate q_{bs} in Tables 3.74 and 3.75 for tests LS and MS are shown in Figure 3.35 where only 6 runs are plotted for test MS because of the wave maker malfunction during run 7. Comparing Figure 3.19 and 3.35, the reduction of the initial clearance of the 10 blocks from 4 cm to 2 cm did not change q_o and q_{bs} noticeably.

Table 3.74. Measured sediment overwash rate q_{bs} , water overtopping rate q_o , and their ratio q_{bs}/q_o , LS.

Run	q_{bs} (cm²/s)	q_o (cm²/s)	q_{bs}/q_o
LS1	0.0009	0.098	0.009
LS2	0.0019	0.117	0.016
LS3	0.0023	0.126	0.018
LS4	0.0023	0.124	0.019
LS5	0.0020	0.160	0.013
LS6	0.0018	0.130	0.014
LS7	0.0025	0.139	0.018
LS8	0.0021	0.143	0.015
LS9	0.0020	0.146	0.014
LS10	0.0023	0.152	0.015

Table 3.75. Measured sediment overwash rate q_{bs} , water overtopping rate q_o , and their ratio q_{bs}/q_o , MS.

Run	q_{bs} (cm ² /s)	q_o (cm ² /s)	q_{bs}/q_o
MS1	0.0122	0.774	0.016
MS2	0.0120	0.654	0.018
MS3	0.0118	0.573	0.021
MS4	0.0133	0.632	0.021
MS5	0.0115	0.532	0.022
MS6	0.0107	0.466	0.023

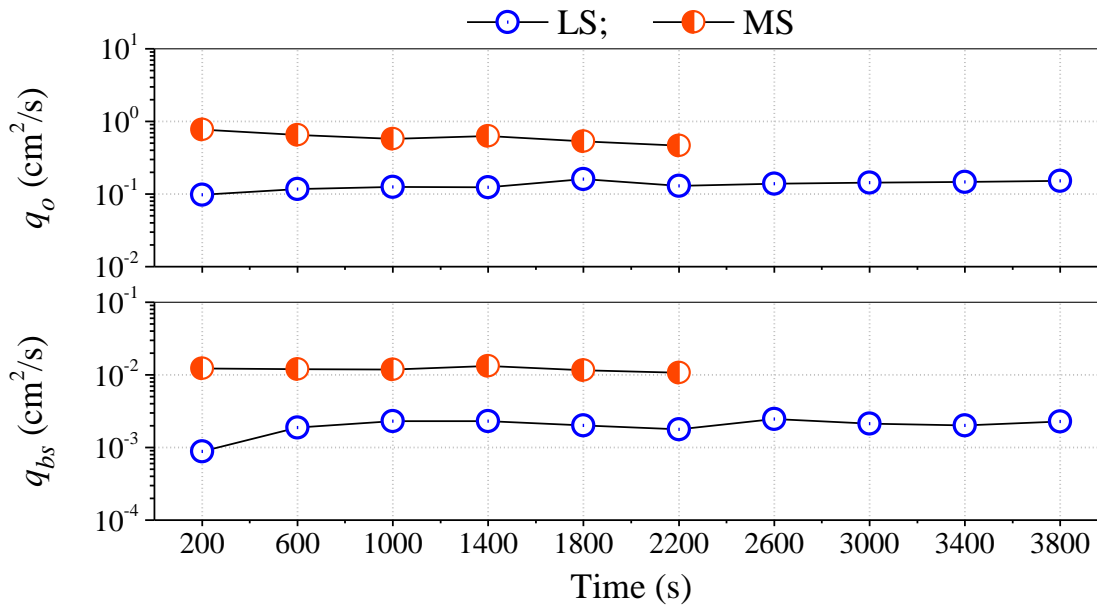


Figure 3.35. Temporal variations of wave overtopping rate q_o and sand overwash rate q_{bs} for tests LS (blue), and MS (red).

3.3.3 Profile Evolution

Figure 3.36 shows the measured profile evolutions for tests LS and MS. The measured profiles after runs 5 and 7 in test MS were almost the same in spite of the generation of a large wave during run 7 due to wave maker malfunction. The profile

evolutions in Figure 3.20 and Figure 3.36 are similar between tests LL and LS as well as between tests ML and MS.

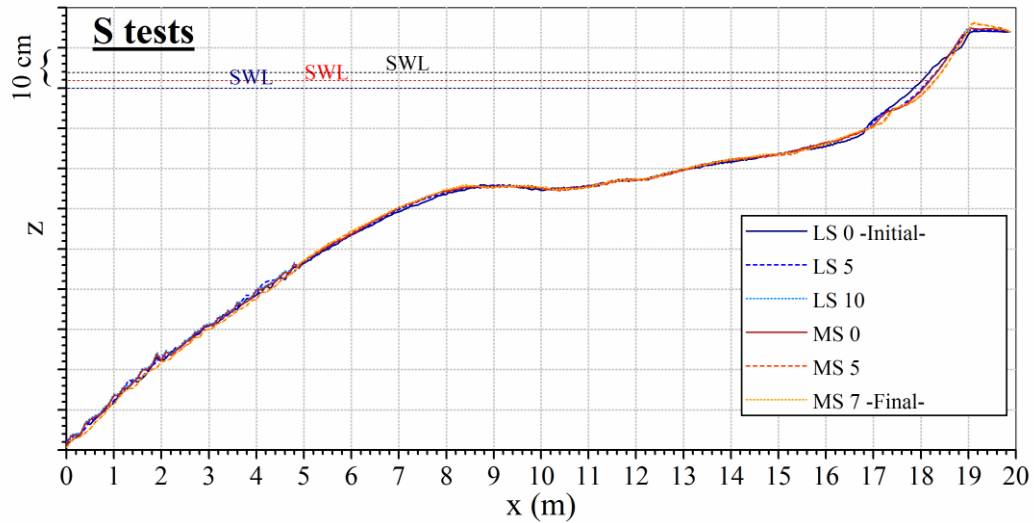


Figure 3.36. Profile evolution during tests LS and MS.

3.3.4 Foreshore and Berm Accretion or Erosion

The sediment budget is analyzed for tests LS and MS (Tables 3.76 and 3.78). The foreshore and berm profile changes for tests LS and MS are shown in Figures 3.37 and 3.38, respectively, and the corresponding maximum erosion and deposition are listed in Tables 3.77 and 3.79. The accretional profile evolutions plotted in Figures 3.39 and 3.40 for tests LS and MS are clearly similar to those of tests LL and ML in Figure 3.25, respectively. The reduction of the initial clearance of the 10 blocks from 4 cm to 2 cm did not change the profile evolution noticeably.

Table 3.76. Cumulative volume changes (cm^3/cm): eroded V_e , and deposited V_d sand volumes, net volume change V_c , cumulative sand overwash volume V_o , offshore sand loss volume V_l as well as the ratios $V_l/|V_c|$ and $V_o/|V_c|$ for the zone $x = 16$ to 19.9 m, LS.

Run	V_e	V_d	V_c	V_o	V_l	$V_l/ V_c $	$V_o/ V_c $
LS5	-351.21	303.73	-47.48	6.26	41.22	0.87	0.13
LS10	-506.16	367.92	-138.24	13.37	124.87	0.90	0.10

Table 3.77. Maximum erosion depth and deposition height at cross-shore location x , and bottom elevation change Δz_b at WG7 and WG8 locations, LS.

RUN	max erosion		max deposition		WG7	WG8
	depth (cm)	x (m)	height (cm)	x (m)	Δz_b (cm)	Δz_b (cm)
LS5	-2.19	18.24	1.86	18.85	-0.27	-0.12
LS10	-2.51	17.88	2.63	18.90	-0.95	-0.13

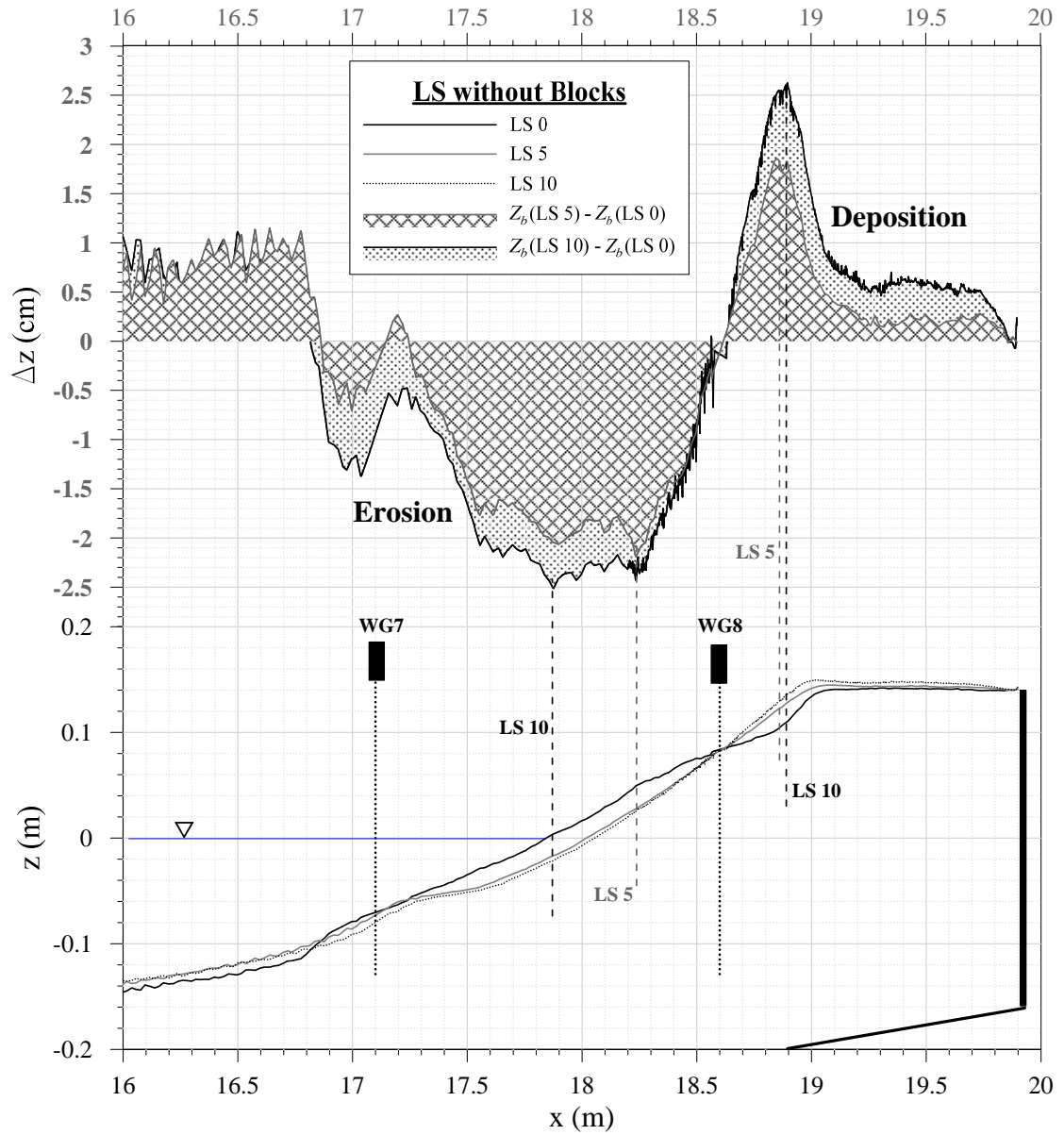


Figure 3.37. Bottom elevation difference between initial profile and profile measured after run 5 and 10 in test LS.

Table 3.78. Cumulative volume changes (cm^3/cm): eroded V_e , and deposited V_d sand volumes, net volume change V_c , cumulative sand overwash volume V_o , offshore sand loss volume V_l as well as the ratios $V_l/|V_c|$ and $V_o/|V_c|$ for the zone $x = 16$ to 19.9 m, MS.

Run	V_e	V_d	V_c	V_o	V_l	$V_l/ V_c $	$V_o/ V_c $
MS5	-424.28	128.18	-296.10	40.61	255.49	0.86	0.14
MS7	-423.29	161.89	-261.40	98.27	163.13	0.62	0.38

Table 3.79. Maximum erosion depth and deposition height at cross-shore location x , and bottom elevation change Δz_b at WG7 and WG8 locations, MS.

RUN	max erosion		max deposition		WG7	WG8
	depth (cm)	x (m)	height (cm)	x (m)	Δz_b (cm)	Δz_b (cm)
MS5	-1.77	18.44	1.30	19.13	-1.07	-1.52
MS7	-1.90	17.24	1.59	19.12	-0.92	-1.52

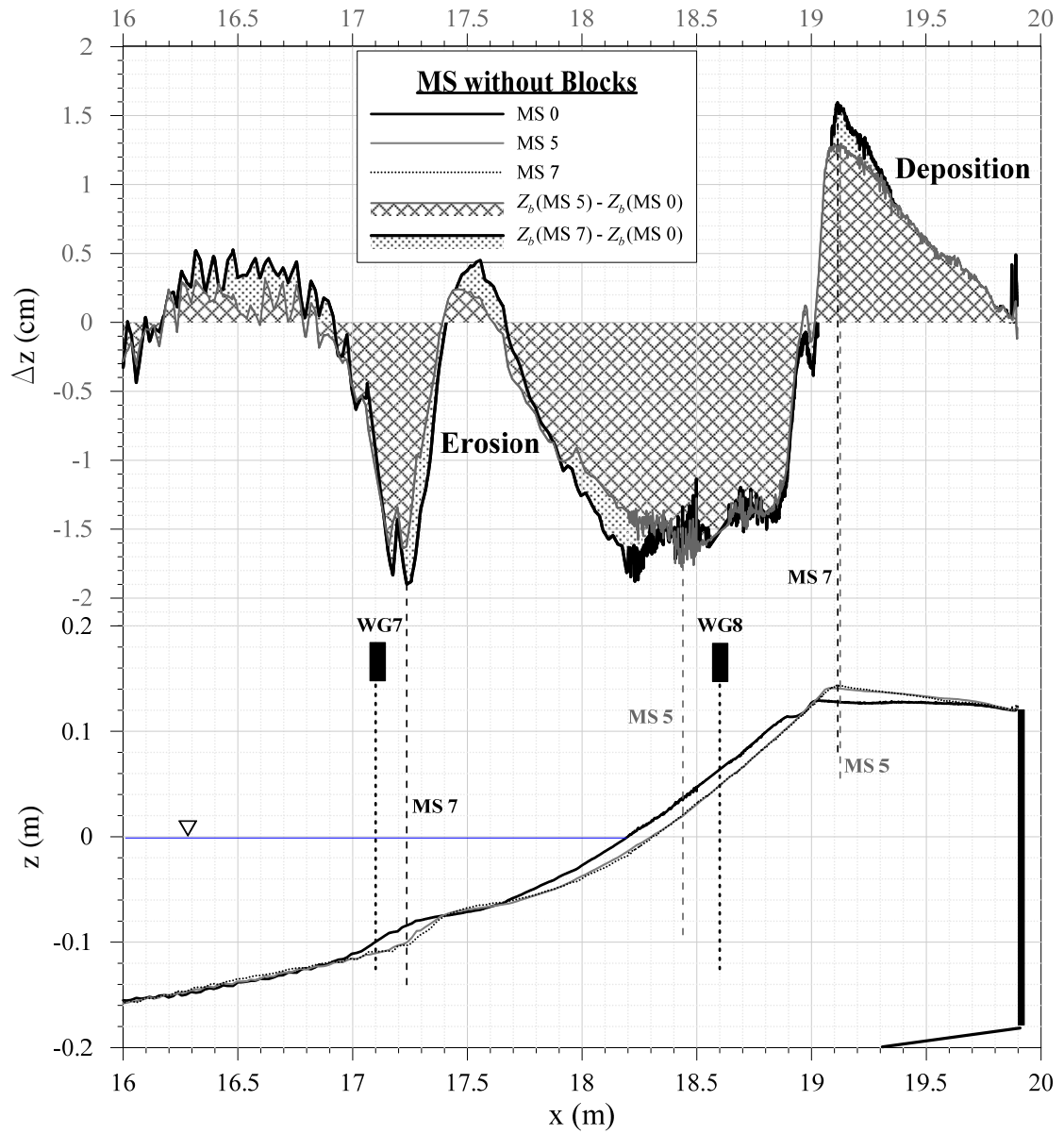


Figure 3.38. Bottom elevation difference between initial profile and profile measured after run 5 and 7 in test MS.

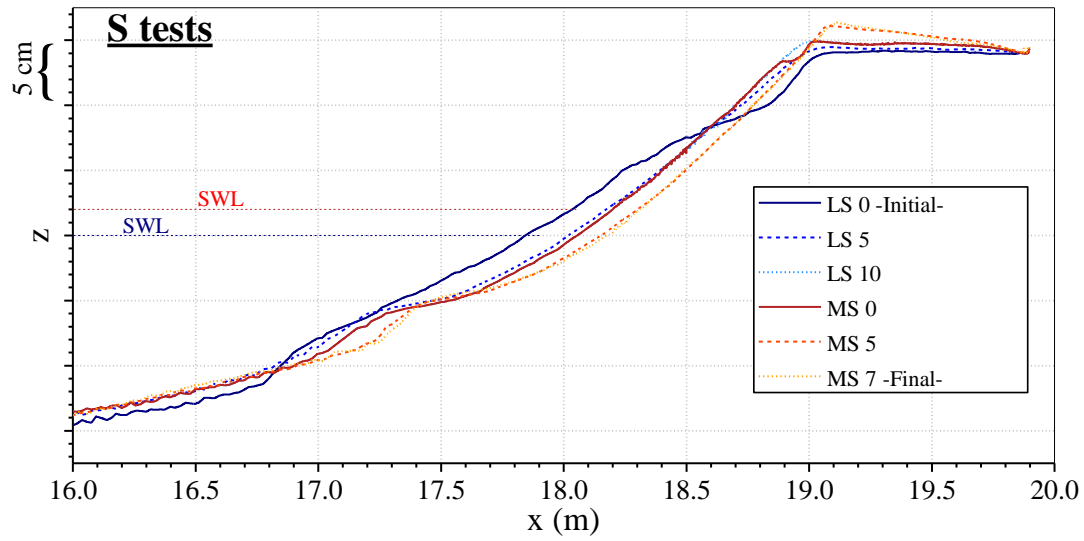


Figure 3.39. Beach profile evolution for series of tests LS and MS.

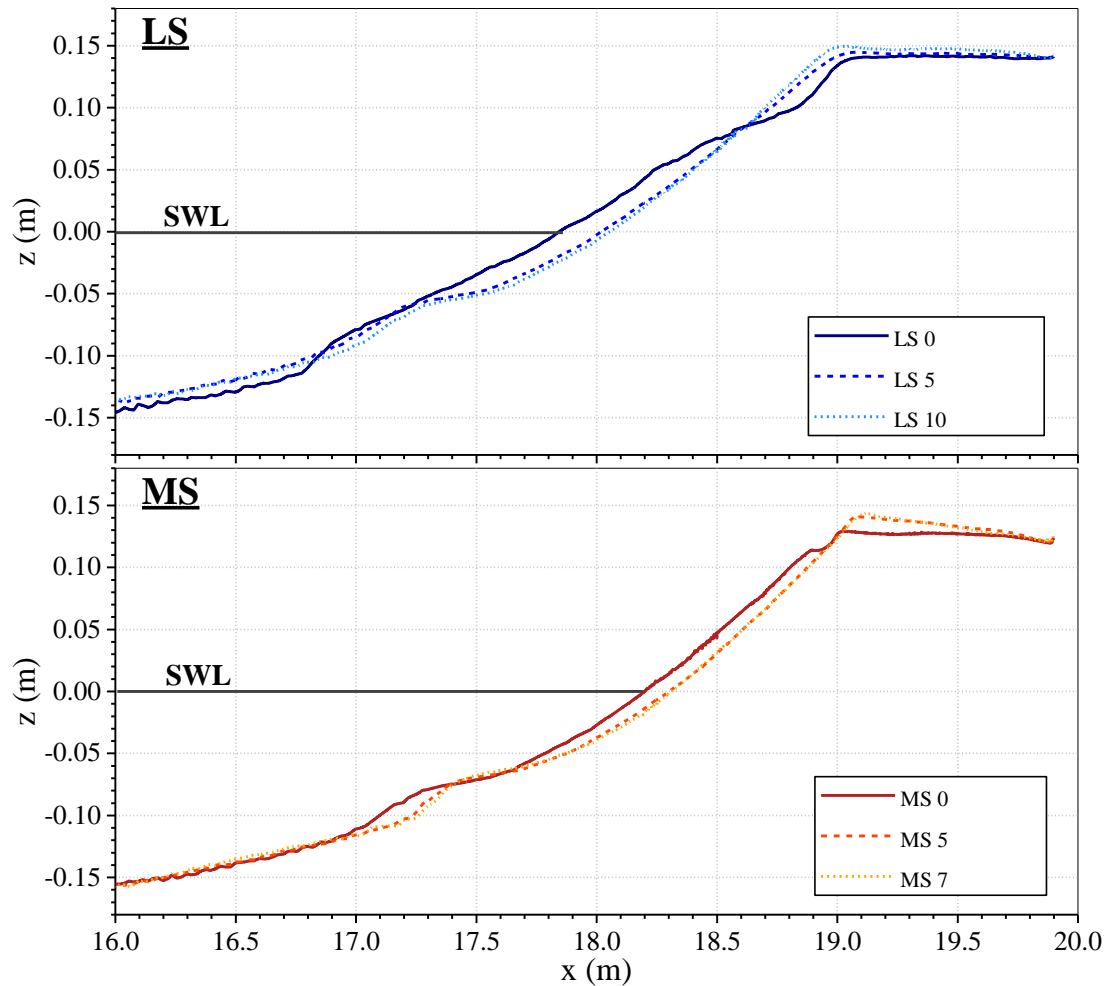


Figure 3.40. Comparison of beach profile evolution for tests LS and MS.

3.3.5 Block Movement

Figures 3.41 and 3.43 present the photos of the blocks before and after tests LS and MS, along with during each of their 10 runs. The large wave during run 7 in test MS is included in Figure 3.43 to show the consequence of the wave maker malfunction. The block responses during tests LS and MS were described in Tables 3.80 and 3.83, respectively. The block coordinates and laser scanner images are presented in Table 3.81 and Figure 3.42 for test LS and Table 3.84 and Figure 3.44 for test MS. Tables 3.82

and 3.85 list the clearance of each block during each run where the initial clearance was 2 cm at the beginning of the series of tests LS and MS.

Figure 3.45 summarizes the reaction of the blocks in tests LS and MS. For test LS during run 1, blocks 1 to 4 fell, blocks 5 and 6 were wet, and blocks 7 to 10 were dry. Block 5 fell during run 4 and block 6 fell during run 2. Blocks 7 and 8 became wet during runs 5 to 7. Blocks 9 and 10 remained dry throughout test LS. On the other hand, for test MS, blocks 1 to 6 fell during run 1. Blocks 7 to 10 were wet during run 1 and fell in the subsequent runs. The effect of the initial block clearance of 2 or 4 cm on the block reaction can be assessed by comparing tests LS and MS in Figure 3.45 with tests LL and ML in Figure 3.32, respectively. The zone of block falling extended farther landward with the 2-cm reduction of clearance.

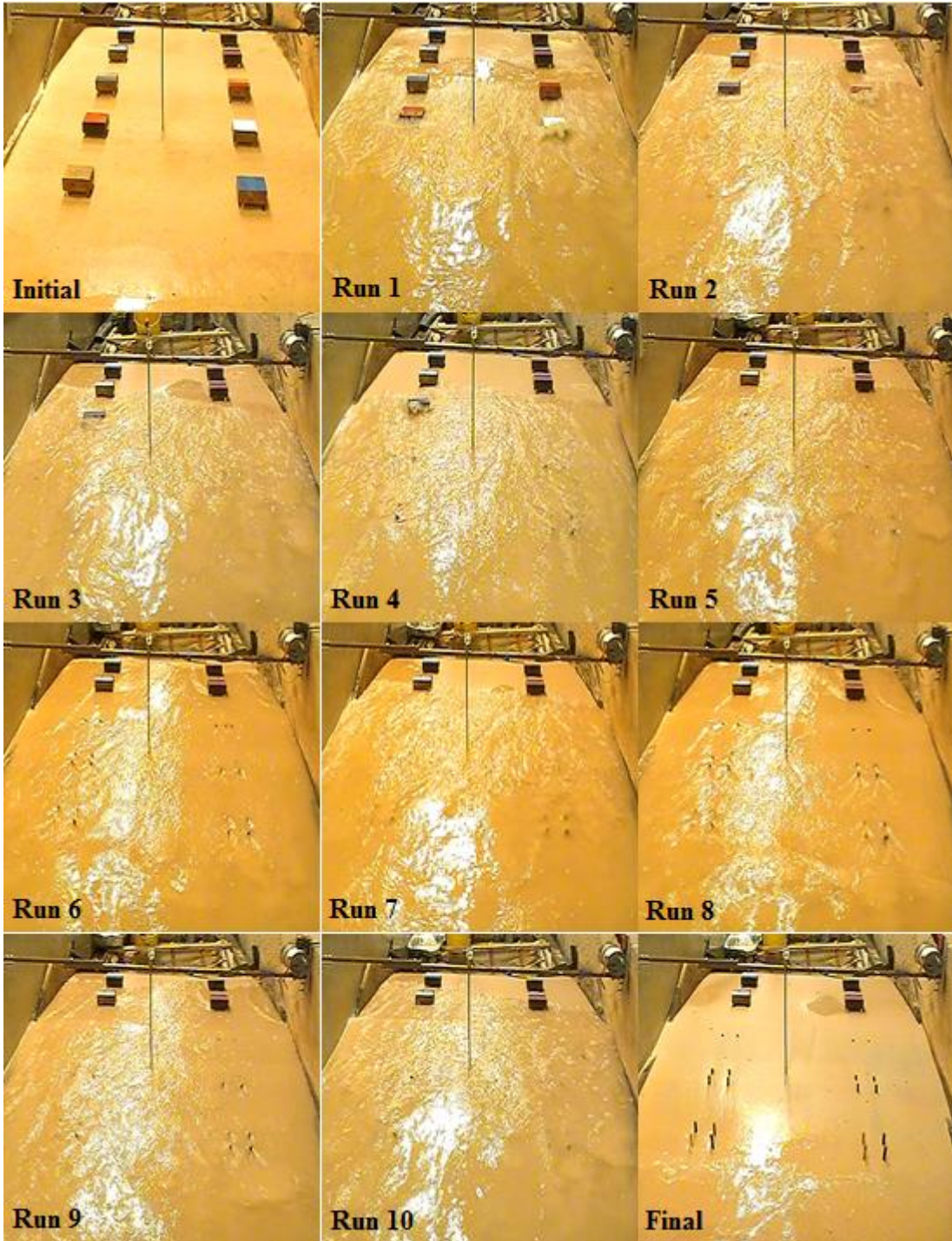


Figure 3.41. Swash and block interactions in each of 10 runs, along with initial and final block photos, LS.

Table 3.80. Block response during each of 10 runs in test LS.

Run	Block number									
	1	2	3	4	5	6	7	8	9	10
LS1	fell	fell	fell	fell	wet	wet	dry	dry	dry	dry
LS2	no	no	no	no	wet	fell	dry	dry	dry	dry
LS3	no	no	no	no	wet	no	dry	dry	dry	dry
LS4	no	no	no	no	fell	no	dry	dry	dry	dry
LS5	no	no	no	no	no	no	wet	wet	dry	dry
LS6	no	no	no	no	no	no	wet	wet	dry	dry
LS7	no	no	no	no	no	no	wet	wet	dry	dry
LS8	no	no	no	no	no	no	dry	dry	dry	dry
LS9	no	no	no	no	no	no	dry	dry	dry	dry
LS10	no	no	no	no	no	no	dry	dry	dry	dry

no implies "removed block".

Table 3.81. Location of 10 blocks during test LS with initial still water shoreline location $x_{SWL} = 17.84$ m.

Block No.	1	2	3	4	5	6	7	8	9	10
Initial location										
x_b (m)	18.28	18.27	18.61	18.61	18.93	18.92	19.27	19.26	19.60	19.59
y_b (m)	0.25	-0.30	0.26	-0.30	0.26	-0.30	0.26	-0.29	0.25	-0.29
Location after run 5										
x_b (m)	-	-	-	-	-	-	19.27	19.26	19.59	19.59
y_b (m)	-	-	-	-	-	-	0.26	-0.29	0.26	-0.29
Final location										
x_b (m)	-	-	-	-	-	-	19.27	19.26	19.60	19.59
y_b (m)	-	-	-	-	-	-	0.26	-0.29	0.26	-0.30

- implies "removed block".

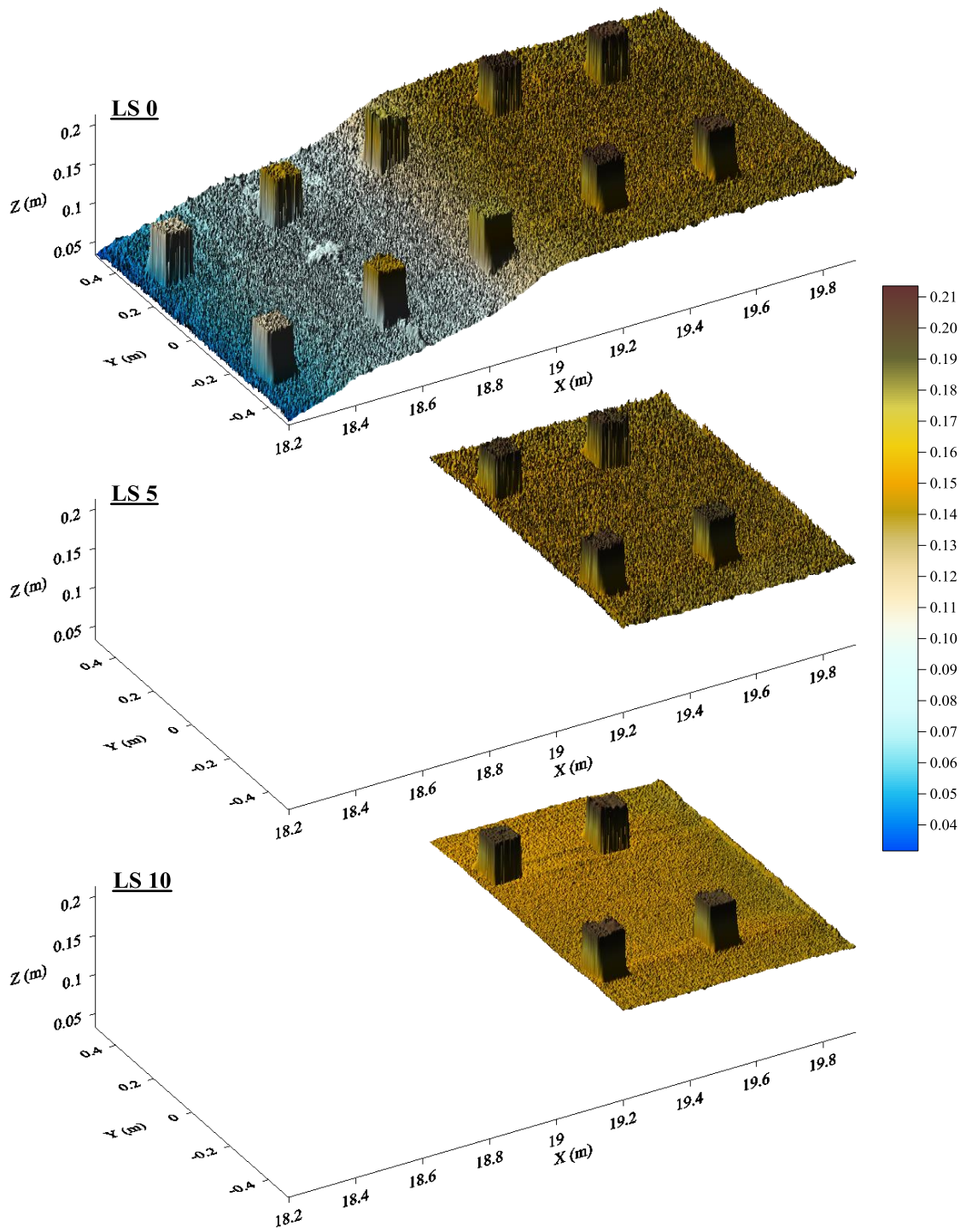


Figure 3.42. Laser line scanner images during test LS: initial (top), after run 5 (middle), and final (bottom).

Table 3.82. Clearance C (cm) during each run, LS.

Run	Block number									
	1	2	3	4	5	6	7	8	9	10
LS1	2.65	2.70	2.08	2.05	1.85	1.75	1.95	1.93	1.95	1.90
LS2	3.45	3.50	2.20	2.18	1.48	1.35	1.83	1.80	1.80	1.78
LS3	3.60	3.78	2.28	2.20	1.10	1.06	1.68	1.73	1.65	1.68
LS4	3.73	3.98	2.35	2.18	0.98	0.83	1.56	1.65	1.55	1.55
LS5	3.93	4.00	2.45	2.28	0.78	0.64	1.49	1.55	1.48	1.48
LS6	4.00	3.93	2.30	2.20	0.40	0.40	1.43	1.50	1.43	1.43
LS7	4.05	3.93	2.10	2.03	0.20	0.15	1.38	1.48	1.38	1.38
LS8	4.10	4.00	2.15	2.03	0.05	-0.06	1.28	1.40	1.28	1.33
LS9	4.10	4.05	2.24	2.10	-0.11	-0.23	1.16	1.40	1.15	1.28
LS10	4.30	4.25	2.39	2.15	-0.23	-0.13	1.08	1.43	1.08	1.20

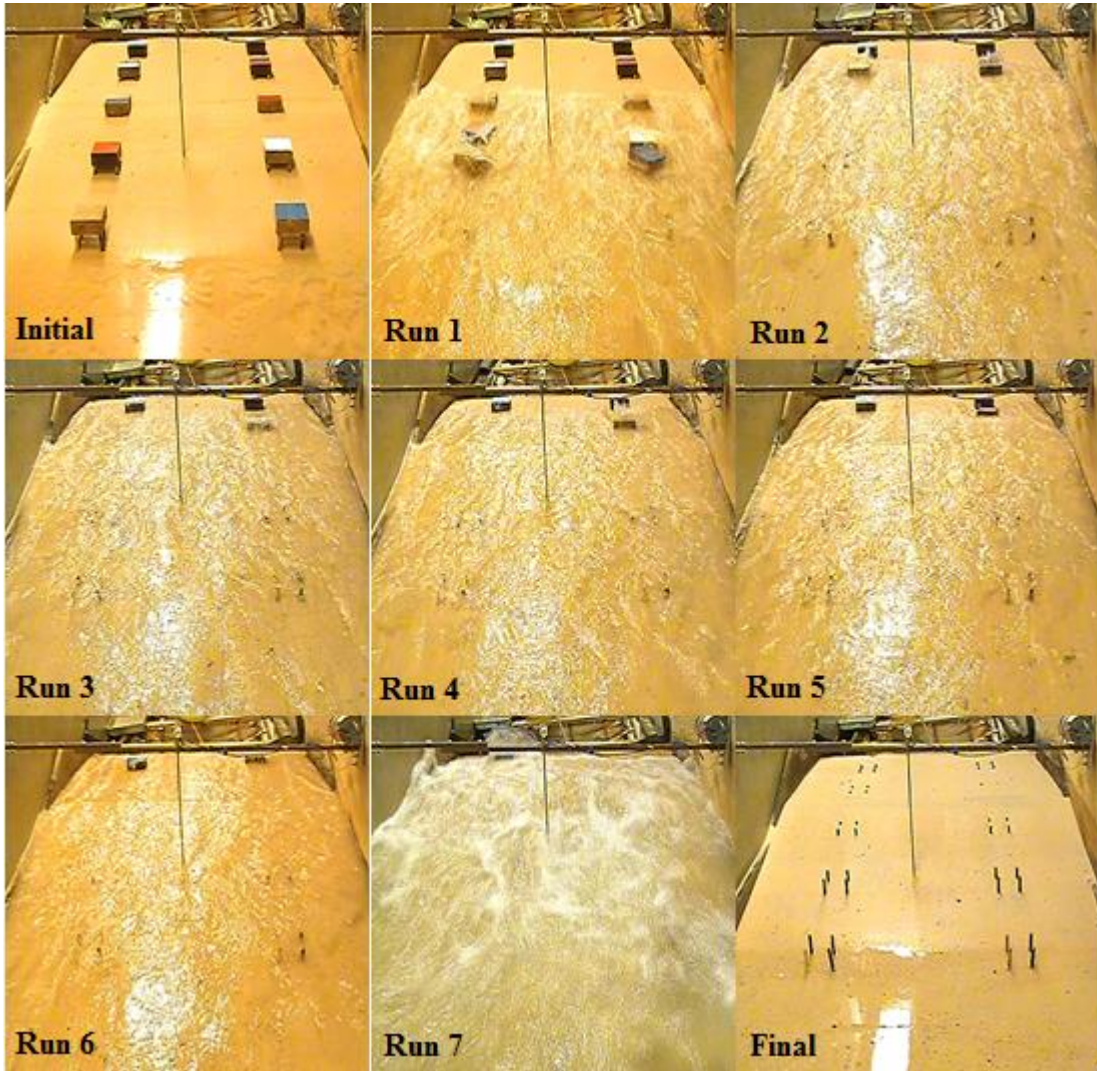


Figure 3.43. Swash and block interactions in each of 7 runs, along with initial and final block photos, MS.

Table 3.83. Block response during each of 7 runs in test MS.

Run	Block number									
	1	2	3	4	5	6	7	8	9	10
MS1	fell	fell	fell	fell	fell	fell	wet	wet	wet	wet
MS2	no	no	no	no	no	no	fell	wet	wet	wet
MS3	no	no	no	no	no	no	no	wet	wet	wet
MS4	no	no	no	no	no	no	no	wet	wet	wet
MS5	no	no	no	no	no	no	no	fell	wet	wet
MS6	no	no	no	no	no	no	no	no	wet	fell
MS7	no	no	no	no	no	no	no	no	fell	no

no implies "removed block".

Table 3.84. Location of 10 blocks during test MS with initial still water shoreline location $x_{SWL} = 18.20$ m.

Block No.	1	2	3	4	5	6	7	8	9	10
Initial location										
x_b (m)	18.28	18.27	18.61	18.60	18.93	18.92	19.27	19.26	19.59	19.59
y_b (m)	0.26	-0.30	0.26	-0.30	0.26	-0.30	0.26	-0.29	0.26	-0.30
Location after run 5										
x_b (m)	-	-	-	-	-	-	-	-	19.60	19.60
y_b (m)	-	-	-	-	-	-	-	-	0.26	-0.30

- implies "removed block".

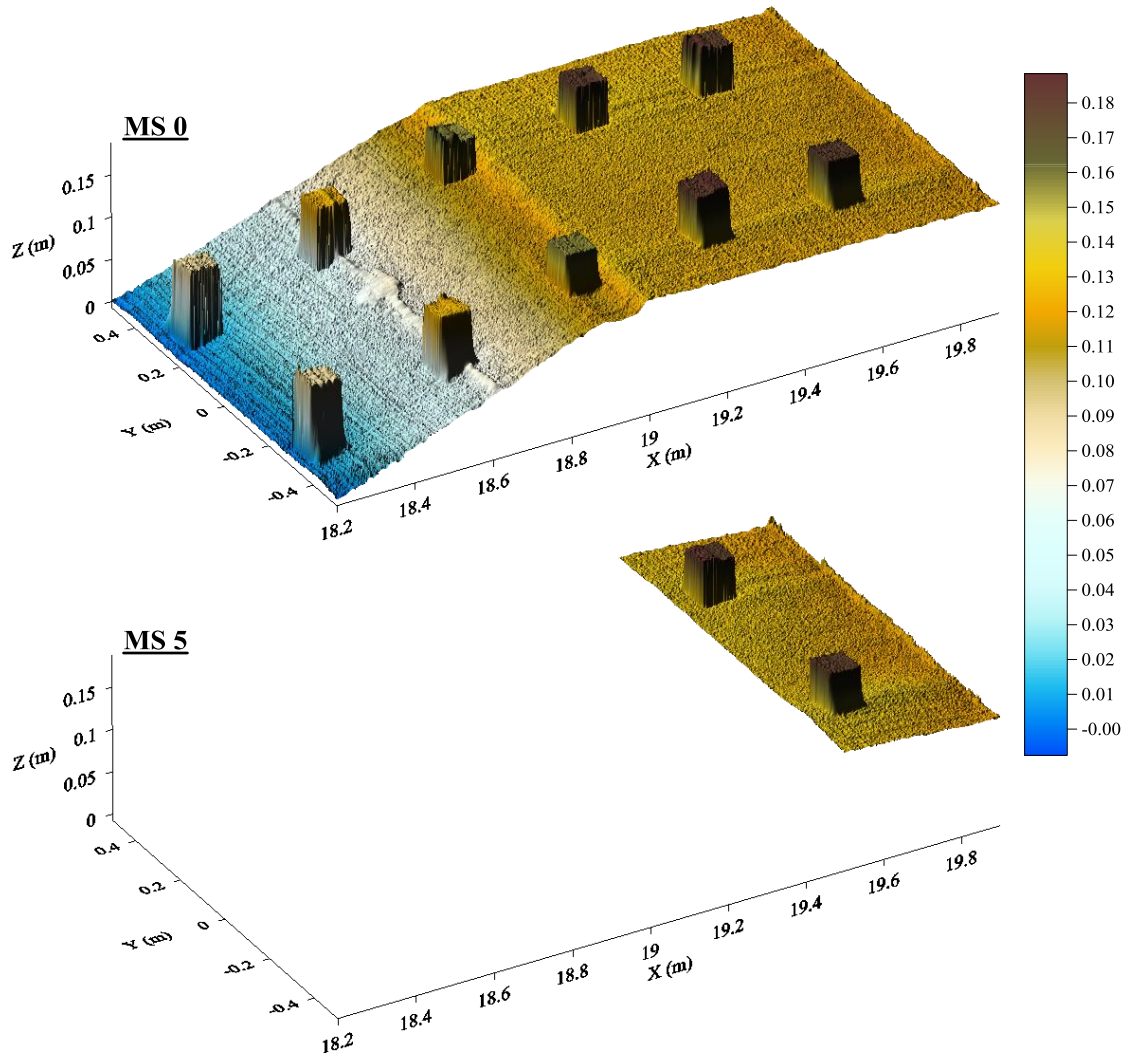


Figure 3.44. Laser line scanner images during test MS: initial (top), and after run 5 (bottom).

Table 3.85. Clearance C (cm) during each run, MS.

Run	Block number									
	1	2	3	4	5	6	7	8	9	10
MS1	4.73	4.65	2.75	2.45	-0.14	0.04	0.84	1.10	0.98	1.03
MS2	4.98	5.00	3.05	2.80	0.13	0.15	0.63	0.73	0.83	0.83
MS3	5.25	5.25	3.25	2.93	0.43	0.35	0.58	0.63	0.75	0.73
MS4	5.50	5.45	3.45	3.13	0.68	0.55	0.48	0.53	0.78	0.60
MS5	5.60	5.53	3.55	3.33	0.80	0.75	0.30	0.33	0.78	0.40
MS6	5.75	5.68	3.75	3.48	1.05	0.93	0.15	0.10	0.70	0.38
MS7	6.15	5.90	3.98	3.73	1.43	1.20	0.25	0.03	1.00	0.83

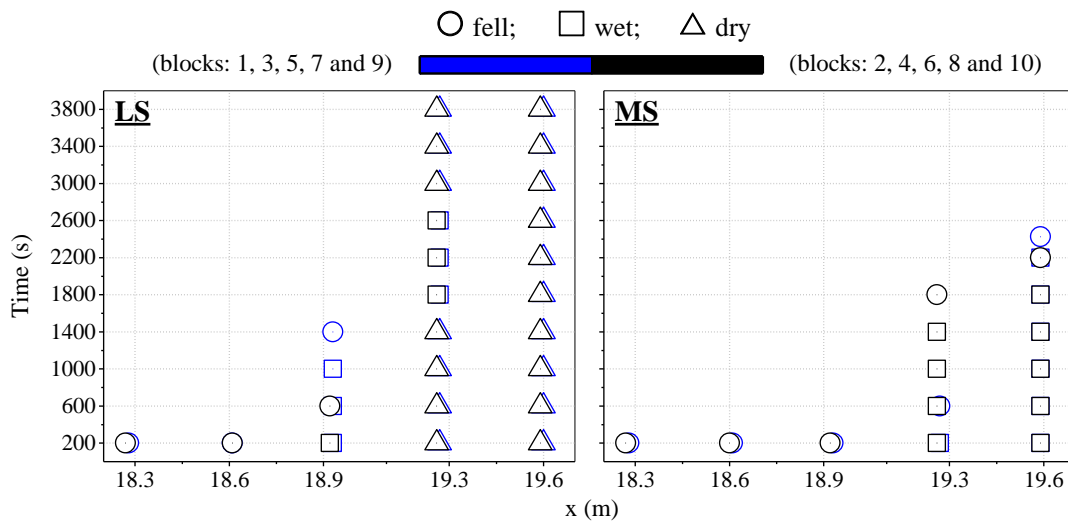


Figure 3.45. Response (fell, wet, and dry) of 10 blocks on short pilings in each run for tests LS and MS.

3.4 Block Effects on Hydrodynamics

The still water level (SWL) was increased by 2 and 4 cm for the medium (M) and high (H) water levels above the low (L) water level in the 8 tests. The 10 blocks were placed on the ground (G) as well as the long (L) and short (S) pilings with the initial clearance of 2 and 4 cm above the same initial beach and berm profile at the start of tests LG, LL, and LS. The figures plotted above for the sequence of the three or two tests indicate the significant effect of SWL on the swash dynamics and profile evolution. The block elevation effect is examined below in more detail.

The wave overtopping rate q_o and the sand overwash rate q_{bs} plotted in Figures 3.3, 3.19, and 3.35, are compared for the three different block elevations of G, L, and S for the given L, M, and H water levels in Figure 3.46. The difference of the three measured values for the given SWL and time t (run number in each test) is within a factor of 2 and much smaller than the order-of-magnitude difference caused by the SWL difference. The temporal variations of q_o and q_{bs} in each test are also within a factor of 2. The beach profile evolutions in Figures 3.8, 3.24, and 3.39 are plotted again in Figure 3.47 for their comparisons. Figure 3.48 shows the profiles in Figures 3.9, 3.25, and 3.40 for the three or two tests with the same SWL. The measured profiles are almost the same for the give SWL and run number. The still water shoreline locations before run 1, after run 5 and after run 10 for tests L, M and H are almost the same as listed in Table A. 1 in Appendix. The profile changes of the foreshore and berm are discernible but relatively small in comparison to the dune profile changes measured by Figlus et al. (2011) in this wave flume. The block elevation effect on the swash dynamics and profile evolution was not detectable in these 8 tests. Figure 3.49 compares the free surface elevation and velocity statistics of the 8 tests. The hydrodynamics were similar for the 8 tests except for the swash hydrodynamics at WG8 affected by the SWL.

The present experiment was limited to the two blocks with the combined width of $2B = 17.8$ cm placed in the 115-cm wide flume. The width ratio was $1/6.5$ and relatively small. Large wave uprush overflowed on the 3.8-cm high block on the ground as depicted in Figure 3.10. The blocks modified the local flow pattern but their effect on the width-averaged flow and sediment transport turned out to be very small. Ayat and Kobayashi (2015) used the dowels used in this experiment to examine the effect of the dowel spacing on dune erosion and overwash in the same flume. The effectiveness of the dowels in reducing dune erosion and overwash diminished when the ratio between the dowel diameter and spacing became less than $1/6.7$. The effectiveness of the dowels was apparent for the ratio exceeding $1/4.7$. The block effect may become more discernible if the number of cross-shore block columns is increased from 2 to 3 but additional tests are required to confirm this conjecture.

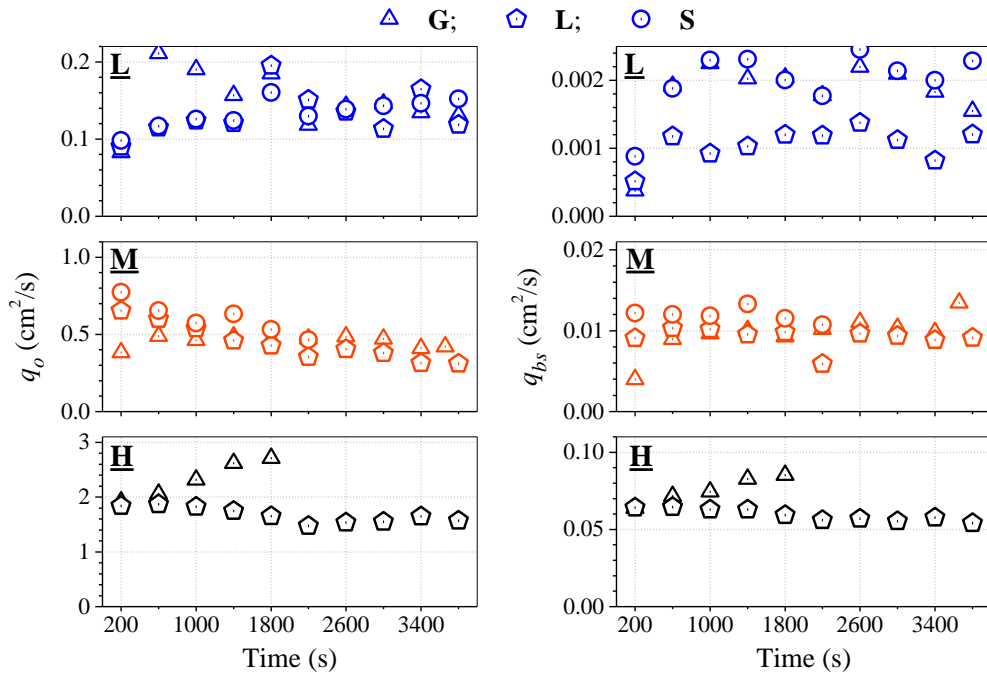


Figure 3.46. Comparisons of q_o and q_{bs} for tests with low (L), medium (M), and high (H) water levels.

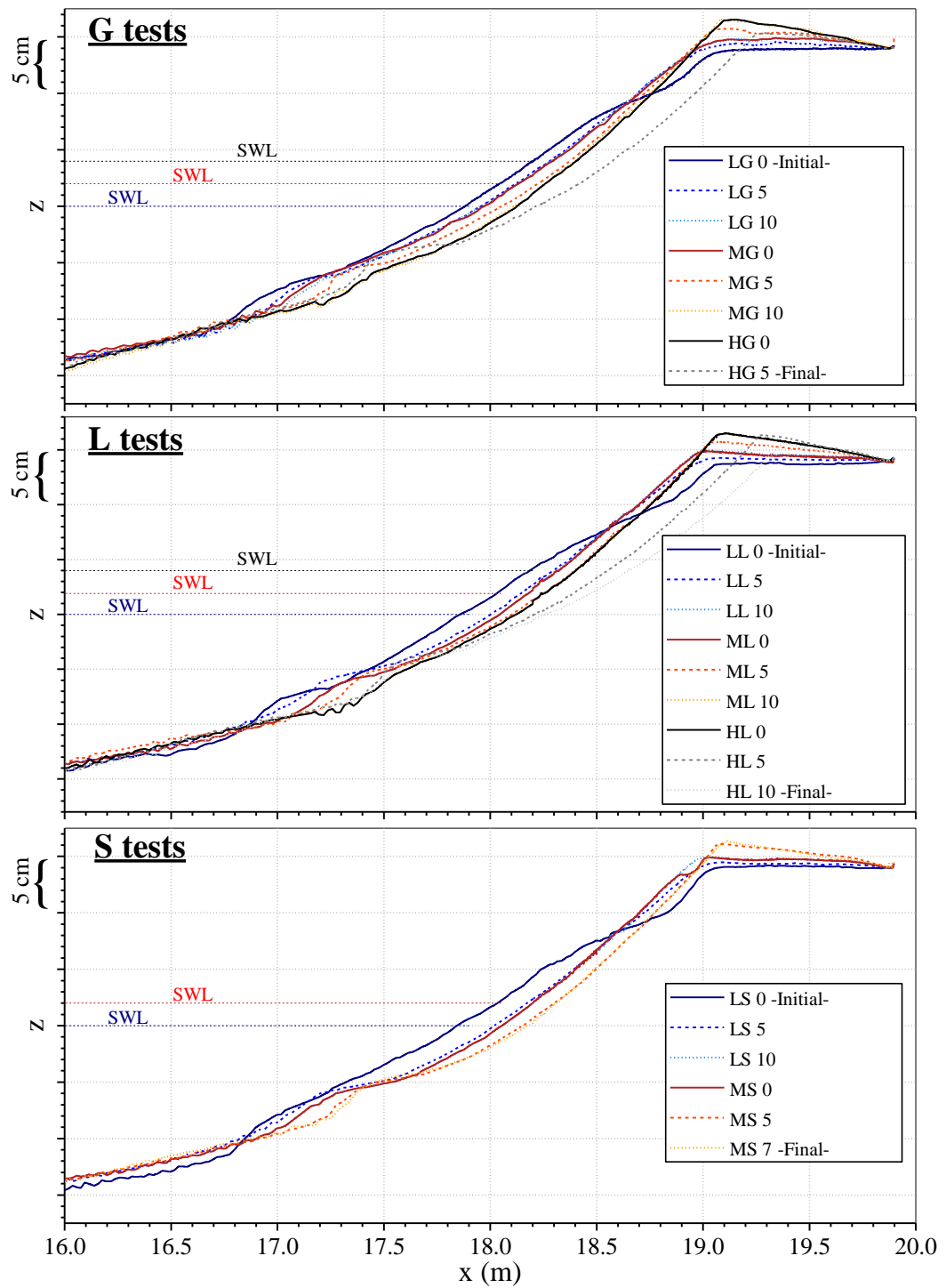


Figure 3.47. Beach profile evolution for 8 tests: tests G (LG, MG, and HG), tests L (LL, ML, and HL), and tests S (LS, and MS).

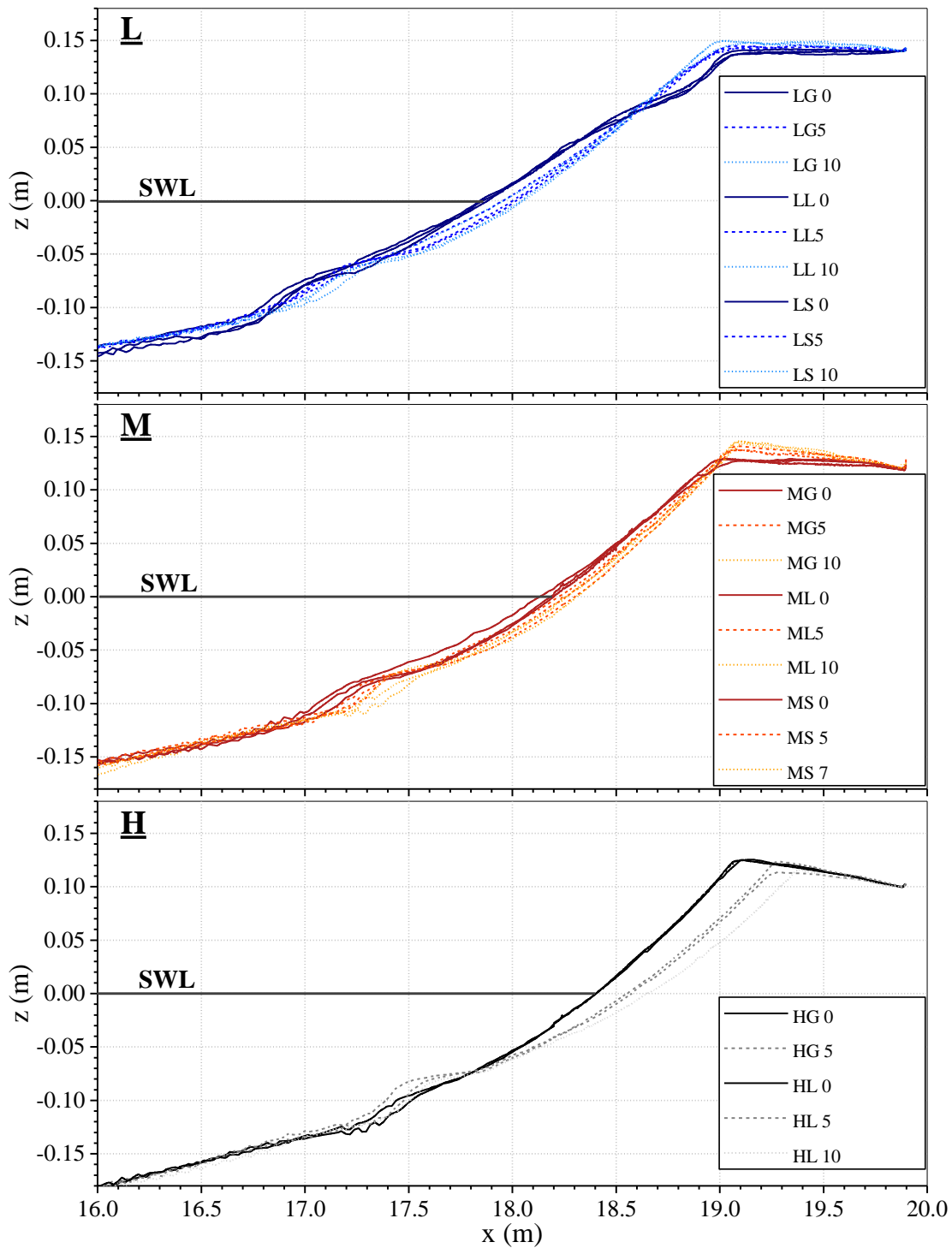


Figure 3.48. Beach profile evolution for 8 tests: tests L (LG, LL, and LS), tests M (MG, ML, and MS), and tests H (HG, and HL).

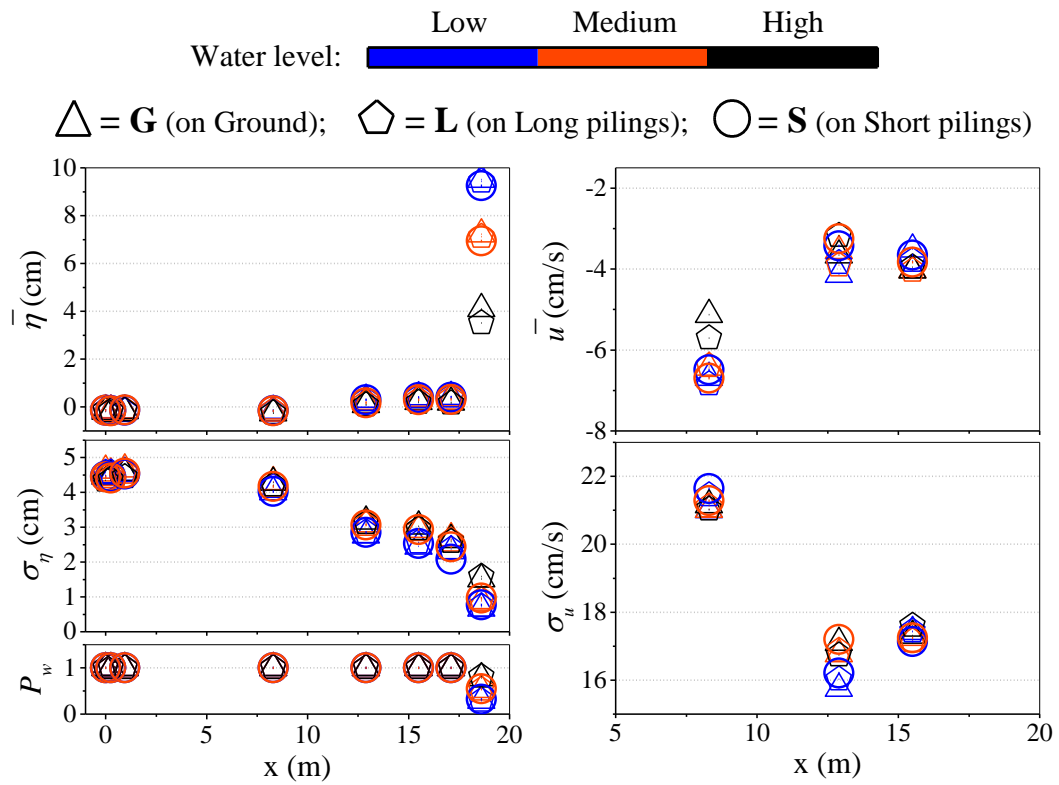


Figure 3.49. Cross-shore variations of the mean (left top) and standard deviation (left middle) of free surface elevation η , wet probability P_w (left bottom), and cross-shore variations of the mean (right top) and standard deviation (right bottom) of the cross-shore velocity u at the three velocimeters for the 8 tests using the average values of each test.

Chapter 4

BLOCK MOVEMENT ANALYSIS

The block movement data presented in Chapter 3 are analyzed in this Chapter in order to synthesize the data for the 8 tests. A simple method is also proposed to estimate probabilities of block sliding and floating.

4.1 Block Elevation Above Still Water Level

The reaction (or response) of the 10 blocks was sensitive to the SWL difference as shown in Figures 3.16, 3.32, and 3.45. The elevation E of the bottom center of each of the 10 blocks above the SWL of each test (Table 4.3) is the sum of the initial bottom elevation z_b above SWL (Table 4.1) and the initial block clearance C (Table 4.2) in the test if the block is not displaced. The cross-shore block location x of each block used in Figures 3.16, 3.32, and 3.45 is replaced by the normalized block elevation (E/H_{m0}) where the value of the significant wave height H_{m0} of each test is used to account for the slight variation of H_{m0} among the 8 tests. Figures 4.1 and 4.2 show the block reaction in terms of (E/H_{m0}). The former plots the 8 tests together, whereas the latter separates the three or two tests with the same SWL (L, M, and H). The damaged blocks in both figures include the floated and slid blocks in the G tests and the fallen blocks in the S and L tests. The block reaction for each test is plotted in Appendix (Figures A. 1 to A. 8) for clarity. The blocks were damaged for (E/H_{m0}) < 0.6 and remained dry for (E/H_{m0}) > 0.9 . The transition zone of (E/H_{m0}) = 0.6 to 0.9 is different for the L, M, and H water levels with the different profile evolutions as shown in Figures 3.48. The initial block elevation $E = (z_b + C)$ at time $t = 0$ does not account for the temporal variations of z_b and C during each test. The block movement is caused by the water

depth and velocity above the bottom which impact on the block located at $z = (z_b + C)$.

Table 4.1. Bottom elevation z_b (cm) above SWL at $t = 0$.

Test	Block Number									
	1	2	3	4	5	6	7	8	9	10
LG	4.9	4.9	8.8	8.9	11.8	11.9	13.9	13.9	14.0	14.0
MG	1.9	1.9	6.7	6.6	11.5	11.4	12.8	12.8	12.7	12.7
HG	-1.6	-1.6	3.4	3.5	9.3	9.4	12.2	12.2	11.2	11.1
LL	5.0	4.9	8.4	8.3	11.6	11.4	13.8	13.8	13.7	13.7
ML	1.4	1.3	6.6	6.5	12.1	12.0	12.5	12.5	12.3	12.3
HL	-1.8	-2.0	3.5	3.4	9.6	9.2	12.1	12.1	11.1	11.1
LS	5.4	5.3	8.5	8.4	11.9	11.6	14.1	14.2	14.1	14.1
MS	1.2	1.1	6.5	6.4	11.4	11.4	12.7	12.7	12.7	12.6

Table 4.2. Clearance C (cm) at $t = 0$.

Test	Block Number									
	1	2	3	4	5	6	7	8	9	10
LG	0.0	0.0	0.0	0.0	0.0	0.0	0.0	0.0	0.0	0.0
MG	0.0	0.0	0.0	0.0	0.0	0.0	0.0	0.0	0.0	0.0
HG	0.0	0.0	0.0	0.0	0.0	0.0	0.0	0.0	0.0	0.0
LL	4.0	4.0	4.0	4.0	4.0	4.0	4.0	4.0	4.0	4.0
ML	6.4	6.4	4.6	4.3	1.7	1.5	2.9	3.2	3.2	3.4
HL	7.7	7.7	5.8	5.7	3.0	2.4	1.5	1.5	2.6	2.5
LS	2.0	2.0	2.0	2.0	2.0	2.0	2.0	2.0	2.0	2.0
MS	4.5	4.4	2.5	2.2	-0.3	0.0	1.0	1.4	1.1	1.2

Table 4.3. Block bottom elevation E (cm) above SWL at $t = 0$.

Test	Block Number									
	1	2	3	4	5	6	7	8	9	10
LG	4.9	4.9	8.8	8.9	11.8	11.9	13.9	13.9	14.0	14.0
MG	1.9	1.9	6.7	6.6	11.5	11.4	12.8	12.8	12.7	12.7
HG	-1.6	-1.6	3.4	3.5	9.3	9.4	12.2	12.2	11.2	11.1
LL	9.0	8.9	12.4	12.3	15.6	15.4	17.8	17.8	17.7	17.7
ML	7.8	7.7	11.2	10.8	13.8	13.5	15.4	15.7	15.4	15.7
HL	5.8	5.7	9.2	9.1	12.6	11.6	13.6	13.6	13.7	13.6
LS	7.4	7.3	10.5	10.4	13.9	13.6	16.1	16.2	16.1	16.1
MS	5.7	5.5	9.0	8.6	11.1	11.4	13.7	14.1	13.7	13.8

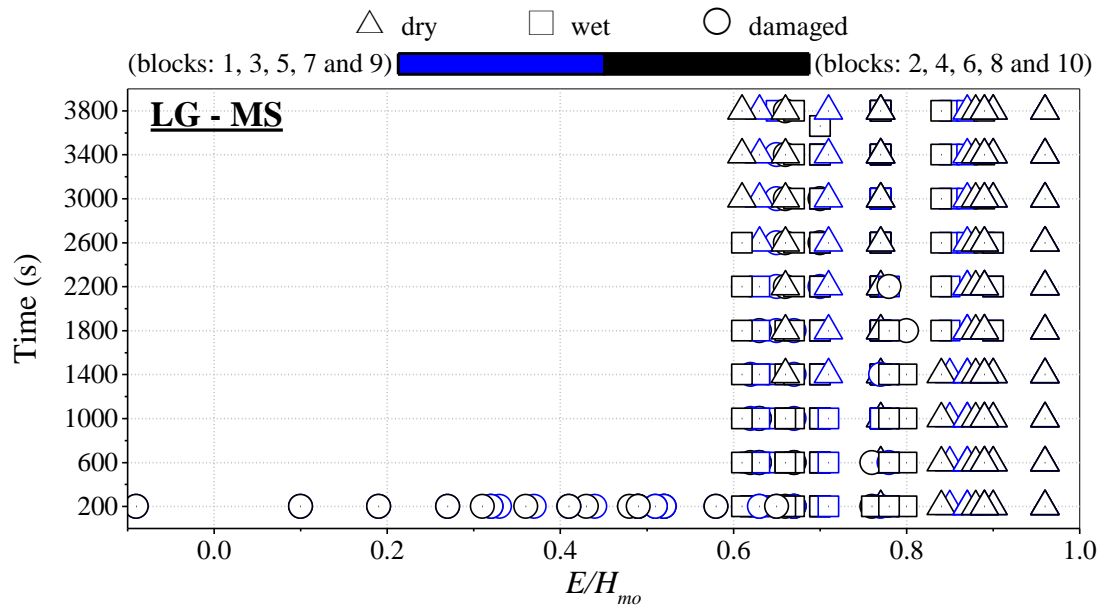


Figure 4.1. Comparisons of response (damaged, wet, and dry) of 10 blocks in each run for the 8 tests together using block elevation E above SWL normalized by incident wave height H_{m0} .

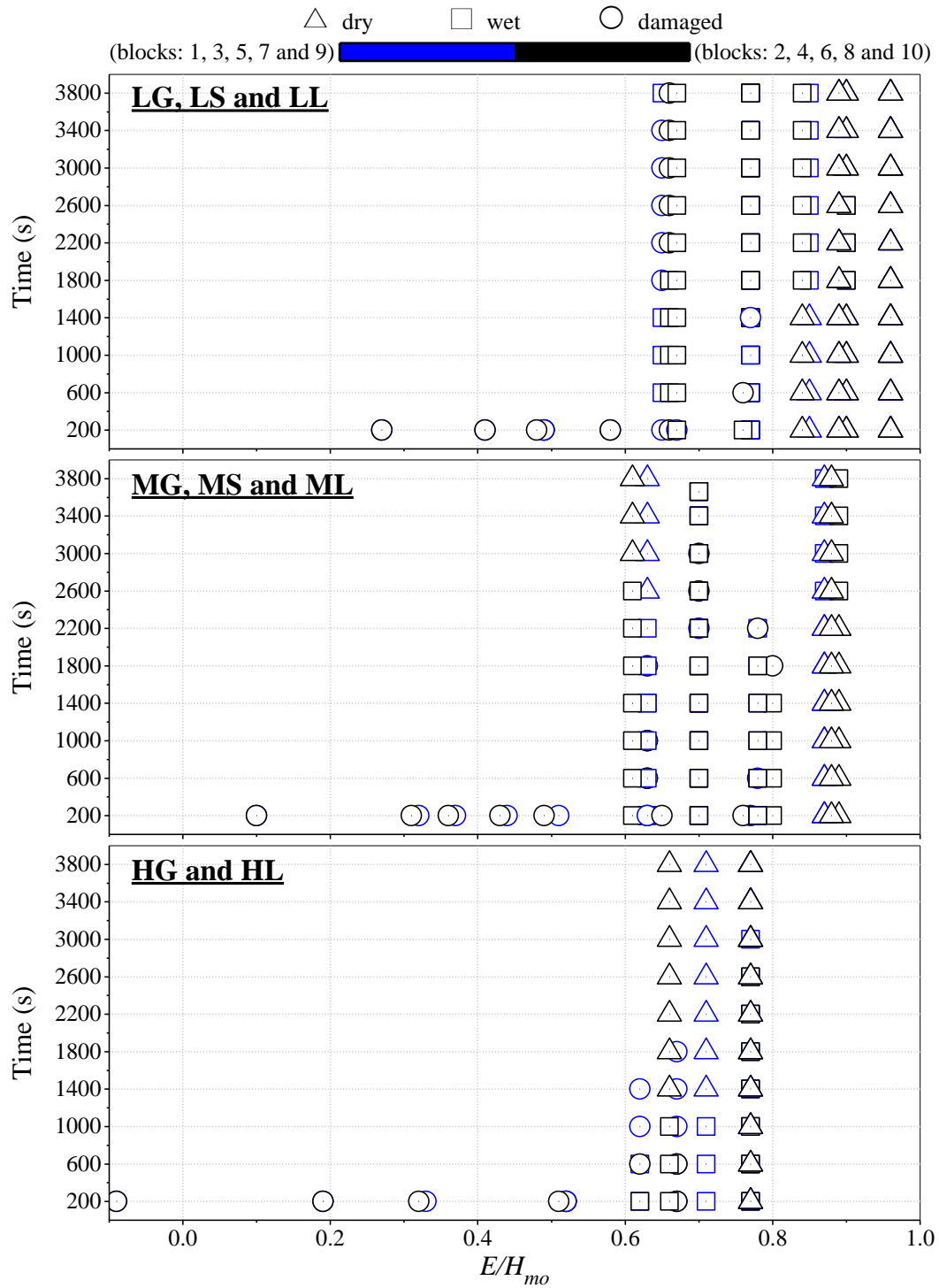


Figure 4.2. Comparisons of response (damaged, wet, and dry) of 10 blocks in each run for tests with low, medium, and high water levels using block elevation E above SWL normalized by incident wave height H_{m0} .

4.2 Block Sliding and Floating Probabilities

Blocks 3 and 4 were located at $x = 18.6$ m in Figure 2.1 where WG8 was also located at $x = 18.6$ m between blocks 3 and 4. The water depth h measured at WG8 is used to analyze the movement of blocks 3 and 4. The block characteristics used for block floating and sliding are listed in Table 4.4 for all the blocks. The free surface elevation η above SWL is given by $\eta = (h + z_b)$ where the bottom elevation z_b did not vary much during each 400-s run and is assumed constant during each run. The value of z_b for each run is obtained by interpolating the initial, intermediate, and final profiles measured for each test shown in Figure 3.48. The mean free surface elevation $\bar{\eta} = (\bar{h} + z_b)$ is related to the mean water depth \bar{h} and the standard deviations σ_η and σ_h for η and h are the same. The wet probability P_w is the probability of $h > 0$ and the dry probability $(1 - P_w)$ is the probability of $h = 0$. The measured values of \bar{h} and P_w at WG8 for each run are used in the following analysis.

The measured values of the width B , length L , thickness T , and wet mass M_w of blocks 3 and 4 are used for the block floating and sliding analysis where these blocks with $C = 0$ float in water depth exceeding approximately 2.1 cm. The block becomes wet when the instantaneous water depth h exceeds the block clearance C measured during the progression of each test where $C = 0$ for the blocks on the ground and $C > 0$ for the blocks on the pilings. The block floats if h exceeds the floating depth h_f given by

$$h_f = C + M_w/(\rho BL) \quad (1)$$

which is based on the vertical force balance between the block weight and buoyancy force. Table 4.4 lists the values of h_f for each block on the ground ($C = 0$).

When $C < h < h_f$, the block may slide on the wet sand surface or on the pilings. The sliding water depth h_s is estimated using the balance between the drag force and the frictional force between the block and the wet sand or pilings

$$\frac{1}{2}\rho C_D B(h_s - C)U^2 = C_f [gM_w - \rho g(h_s - C)BL] \quad (2)$$

which neglects the inertia and lift forces and the effect of bottom slope of the order of 0.1 (*e.g.*, Kobayashi and Otta, 1987). Both sides of Equation (2) with g = gravitational acceleration are positive for $C < h_s < h_f$. The drag coefficient C_D is taken as $C_D = 1.9$ calibrated for an object in the swash zone (Ayat and Kobayashi 2015). The wave uprush velocity U is estimated as $U = \alpha\sqrt{gh_s}$ with $\alpha = 1.6$ on the sand foreshore (Figlus *et al.* 2012). The measured friction coefficient was $C_f = 0.78$ and 0.96 for the block on the wet sand and pilings, respectively. Equation (2) yield

$$h_s = \frac{\sqrt{b^2 + 4ah_f} - b}{2a}; \quad a = \frac{\alpha^2 C_D}{2LC_f}; \quad b = (1 - aC) \quad (3)$$

which can be shown to satisfy $C < h_s < h_f$. Table 4.5 lists the calculated values of h_s and h_f for $C = 0$ to 4 cm. The values of h_s and h_f for the 10 blocks on the ground ($C = 0$) correspond to those for tests LG, MG, and HG. The values of h_s and h_f for tests LL, ML, HL, LS, and MS are calculated using the measured clearance C for each run in each test and listed in Tables 4.6 to 4.15.

The probability density function of the water depth h in the swash zone is assumed to be exponential (Kobayashi *et al.*, 2010). The corresponding exceedance probability $P(h)$ is given by

$$P(h) = P_w \exp\left(-P_w \frac{h}{\bar{h}}\right) \quad \text{for } h > 0 \quad (4)$$

The wetting probability P_c , floating probability P_f , and sliding probability P_s of the block are estimated as

$$P_c = P(h = C); \quad P_f = P(h = h_f); \quad P_s = P(h = h_s) \quad (5)$$

by substituting C , h_f , and h_s into h in Equation (4). Since $C < h_s < h_f$, $P_c > P_s > P_f$ and the upper limit of P_c corresponding to $C=0$ is the wet probability P_w on the sand surface.

The estimated values of P_f , P_s and P_c for blocks 3 and 4 for the 8 tests are listed in Appendix (Tables A. 2 to A. 9) and shown in Figures 4.3 to 4.10. The foreshore slope change during each test is included to examine a possible correlation between the slope change and the probability change in each test. There is no clear correlation in these figures. Figure 4.1 summarizes the response for blocks 3 and 4 for the 8 tests. For tests LG, MG, and HG, blocks 3 and 4 floated during run 1 (middle time $t = 200$ s) and the floating probability P_f is denoted by a filled circle. For tests LS, MS, and HL, blocks 3 and 4 fell from the pilings during run 1 and the sliding probability is denoted by a filled square, assuming that the block sliding on the pilings caused the block falling. For tests

LL and ML, blocks 3 and 4 at $x = 18.6$ m were wet or dry but did not fall from the pilings during runs 1 – 10.

The floating probabilities for the three G tests and the sliding probabilities for the five S and L tests in Figure 4.11 are plotted together with the corresponding values of (E/H_{m0}) for blocks 3 and 4 in Figure 4.12. Blocks 3 and 4 on the ground (G) floated when P_f exceeded 8%. Blocks 3 and 4 on the short (S) and long (L) pilings fell when P_s exceeded 8% but did not fall (no damage) when P_s was less than 8%. The damage threshold probability of 8% corresponds to the damage threshold value of $(E/H_{m0}) = 0.6$ for blocks 3 and 4. The damage data for the 10 blocks in Figure 4.2 indicate damage up to $(E/H_{m0}) = 0.8$. As a result, the damage threshold probability of 8% for blocks 3 and 4 may not be applicable to the other blocks. Additional tests are necessary to establish the damage threshold probability.

Table 4.4. Blocks characteristics used for block floating and sliding.

Block No.	Block Geometry (wet block)			Wet Block M_w (g)	h_f [C=0] (cm)	Friction coefficient C_f	
	T (cm)	B (cm)	L (cm)			Wet sand	Dowels
1	3.9	8.9	8.2	150.8	2.07	0.78	1.05
2	3.9	8.9	8.1	149.4	2.07	0.79	0.99
3	3.8	8.8	8.3	148.6	2.03	0.78	1.06
4	3.8	8.8	8.2	170.9	2.37	0.79	0.92
5	3.9	9.0	8.3	155.8	2.09	0.77	0.96
6	3.9	8.9	8.2	154.1	2.11	0.78	0.93
7	3.9	8.9	8.1	173.3	2.40	0.80	0.92
8	3.8	8.8	8.4	162.1	2.19	0.79	0.94
9	3.7	8.8	8.5	153.3	2.05	0.78	0.86
10	3.8	8.8	8.4	153.5	2.08	0.78	0.97
Average	3.8	8.9	8.3	157.2	2.15	0.78	0.96

Table 4.5. Floating and sliding depths calculated for clearance $C = 0$ to 4 cm.

Block No.	Floating depth h_f (cm)					Sliding depth h_s (cm)				
	$C=0$	$C=1$	$C=2$	$C=3$	$C=4$	$C=0$	$C=1$	$C=2$	$C=3$	$C=4$
1	2.1	3.1	4.1	5.1	6.1	1.4	2.2	3.1	3.9	4.8
2	2.1	3.1	4.1	5.1	6.1	1.4	2.2	3.1	3.9	4.8
3	2.0	3.0	4.0	5.0	6.0	1.4	2.2	3.1	3.9	4.8
4	2.4	3.4	4.4	5.4	6.4	1.5	2.4	3.2	4.1	4.9
5	2.1	3.1	4.1	5.1	6.1	1.4	2.2	3.1	3.9	4.8
6	2.1	3.1	4.1	5.1	6.1	1.4	2.2	3.1	4.0	4.8
7	2.4	3.4	4.4	5.4	6.4	1.5	2.4	3.2	4.1	4.9
8	2.2	3.2	4.2	5.2	6.2	1.4	2.3	3.1	4.0	4.9
9	2.0	3.0	4.0	5.0	6.0	1.4	2.2	3.1	3.9	4.8
10	2.1	3.1	4.1	5.1	6.1	1.4	2.2	3.1	3.9	4.8
Average	2.1	3.1	4.1	5.1	6.1	1.4	2.3	3.1	4.0	4.9

Table 4.6. Sliding depth h_s (cm) calculated using measured C , LL.

Run	Block Number									
	1	2	3	4	5	6	7	8	9	10
LL1	5.4	5.4	4.9	5.1	4.6	4.6	4.9	4.9	4.8	4.8
LL2	6.1	6.1	5.1	5.3	4.2	4.2	4.9	4.8	4.7	4.8
LL3	6.3	6.3	5.3	5.4	3.8	3.9	4.7	4.7	4.6	4.7
LL4	6.6	6.6	5.3	5.4	3.5	3.6	4.7	4.7	4.6	4.7
LL5	6.6	6.6	5.2	5.4	3.3	3.4	4.5	4.6	4.5	4.6
LL6	6.6	6.6	5.2	5.3	3.2	3.3	4.5	4.5	4.4	4.5
LL7	6.7	6.7	5.1	5.2	3.0	3.1	4.4	4.5	4.3	4.4
LL8	7.0	7.0	5.2	5.2	3.0	3.0	4.3	4.4	4.3	4.4
LL9	7.1	7.1	5.3	5.2	2.9	2.8	4.1	4.3	4.2	4.3
LL10	7.1	7.0	5.3	5.2	2.8	2.7	4.0	4.2	4.1	4.3

Table 4.7. Sliding depth h_s (cm) calculated using measured C , ML.

Run	Block Number									
	1	2	3	4	5	6	7	8	9	10
ML1	7.1	7.1	5.3	5.2	2.8	2.6	3.9	4.1	4.0	4.2
ML2	7.5	7.4	5.3	5.3	2.8	2.5	3.7	3.8	3.9	4.0
ML3	7.7	7.7	5.6	5.6	3.0	2.6	3.6	3.6	3.9	3.9
ML4	7.8	7.8	5.8	5.7	3.2	2.8	3.4	3.5	3.8	3.9
ML5	7.9	7.9	6.0	5.9	3.4	3.0	3.3	3.4	3.8	3.8
ML6	8.0	8.0	6.0	6.0	3.4	3.0	3.2	3.2	3.7	3.7
ML7	7.9	7.9	6.0	5.9	3.5	3.0	3.1	3.0	3.6	3.6
ML8	8.0	8.0	6.2	6.1	3.7	3.1	3.0	2.9	3.6	3.6
ML9	8.1	8.1	6.3	6.3	3.8	3.3	2.9	2.8	3.6	3.6
ML10	8.2	8.2	6.4	6.5	3.9	3.4	2.8	2.7	3.6	3.5

Table 4.8. Sliding depth h_s (cm) calculated using measured C , HL.

Run	Block Number									
	1	2	3	4	5	6	7	8	9	10
HL1	8.6	8.6	6.7	6.7	4.1	3.6	2.8	2.7	3.5	3.4
HL2	9.1	9.1	7.2	7.3	4.6	4.2	2.8	2.6	3.4	3.2
HL3	9.3	9.3	7.8	7.7	5.3	4.9	2.8	2.4	3.3	3.1
HL4	9.5	9.5	8.2	8.0	6.1	5.7	2.8	2.5	3.4	3.1
HL5	9.8	9.8	8.5	8.5	6.7	6.5	3.1	2.8	3.5	3.1
HL6	10.1	10.1	8.9	8.9	7.3	6.9	3.5	3.3	3.5	3.3
HL7	NR	NR	9.4	9.1	7.7	7.2	3.8	3.8	3.5	3.4
HL8	NR	NR	9.5	9.3	8.1	7.6	4.3	4.2	3.7	3.4
HL9	NR	NR	9.7	9.7	8.5	8.0	4.9	4.6	3.8	3.5
HL10	NR	NR	9.9	9.9	8.9	8.3	5.4	5.0	3.9	3.6

NR implies "not reliable" data

Table 4.9. Sliding depth h_s (cm) calculated using measured C , LS.

Run	Block Number									
	1	2	3	4	5	6	7	8	9	10
LS1	3.6	3.7	3.1	3.2	2.9	2.9	3.2	3.1	3.0	3.0
LS2	4.3	4.4	3.2	3.3	2.6	2.5	3.1	3.0	2.9	2.9
LS3	4.5	4.6	3.3	3.4	2.3	2.3	2.9	2.9	2.8	2.8
LS4	4.6	4.8	3.4	3.3	2.2	2.1	2.8	2.8	2.7	2.7
LS5	4.8	4.8	3.4	3.4	2.1	2.0	2.8	2.7	2.6	2.6
LS6	4.8	4.8	3.3	3.4	1.8	1.8	2.7	2.7	2.6	2.6
LS7	4.9	4.8	3.1	3.2	1.6	1.6	2.7	2.7	2.5	2.5
LS8	4.9	4.8	3.2	3.2	1.5	1.4	2.6	2.6	2.5	2.5
LS9	4.9	4.9	3.3	3.3	1.4	1.3	2.5	2.6	2.4	2.5
LS10	5.1	5.1	3.4	3.3	1.3	1.4	2.4	2.6	2.3	2.4

Table 4.10. Sliding depth h_s (cm) calculated using measured C , MS.

Run	Block Number									
	1	2	3	4	5	6	7	8	9	10
MS1	5.5	5.4	3.7	3.6	1.3	1.5	2.2	2.4	2.2	2.3
MS2	5.7	5.7	4.0	3.9	1.5	1.6	2.1	2.1	2.1	2.1
MS3	6.0	6.0	4.1	4.0	1.8	1.7	2.0	2.0	2.0	2.0
MS4	6.2	6.2	4.3	4.2	2.0	1.9	2.0	1.9	2.0	1.9
MS5	6.3	6.2	4.4	4.3	2.1	2.0	1.8	1.8	2.0	1.8
MS6	6.4	6.4	4.6	4.5	2.3	2.2	1.7	1.6	2.0	1.7
MS7	6.8	6.6	4.8	4.7	2.6	2.4	1.8	1.5	2.2	2.1

Table 4.11. Floating depth h_f (cm) calculated using measured C , LL.

Run	Block Number									
	1	2	3	4	5	6	7	8	9	10
LL1	6.7	6.7	6.1	6.5	5.9	5.9	6.4	6.2	6.0	6.1
LL2	7.4	7.5	6.4	6.8	5.3	5.4	6.3	6.1	5.9	6.0
LL3	7.7	7.7	6.5	6.9	4.9	5.0	6.2	6.0	5.8	5.9
LL4	8.0	8.0	6.5	6.9	4.6	4.7	6.1	5.9	5.8	5.9
LL5	8.0	8.0	6.5	6.9	4.4	4.5	6.0	5.8	5.7	5.8
LL6	8.0	8.0	6.4	6.8	4.2	4.3	5.9	5.8	5.6	5.7
LL7	8.1	8.1	6.3	6.7	4.0	4.1	5.8	5.7	5.5	5.6
LL8	8.4	8.4	6.4	6.7	3.9	4.0	5.6	5.7	5.4	5.6
LL9	8.5	8.5	6.5	6.7	3.9	3.8	5.5	5.6	5.3	5.5
LL10	8.5	8.5	6.6	6.7	3.8	3.6	5.4	5.5	5.2	5.5

Table 4.12. Floating depth h_f (cm) calculated using measured C , ML.

Run	Block Number									
	1	2	3	4	5	6	7	8	9	10
ML1	8.6	8.6	6.6	6.7	3.8	3.6	5.2	5.3	5.1	5.4
ML2	8.9	8.9	6.6	6.8	3.8	3.5	5.0	5.0	5.0	5.2
ML3	9.2	9.2	6.8	7.1	4.0	3.5	4.8	4.7	4.9	5.1
ML4	9.2	9.2	7.1	7.2	4.3	3.7	4.7	4.6	4.9	5.0
ML5	9.4	9.4	7.3	7.4	4.4	4.0	4.6	4.5	4.9	4.9
ML6	9.5	9.5	7.3	7.5	4.5	4.1	4.4	4.2	4.8	4.8
ML7	9.4	9.4	7.3	7.5	4.6	4.1	4.3	4.0	4.7	4.7
ML8	9.5	9.5	7.5	7.6	4.8	4.2	4.2	3.9	4.6	4.7
ML9	9.6	9.6	7.6	7.9	4.9	4.3	4.1	3.8	4.6	4.6
ML10	9.7	9.7	7.7	8.1	5.0	4.4	4.0	3.7	4.6	4.6

Table 4.13. Floating depth h_f (cm) calculated using measured C , HL.

Run	Block Number									
	1	2	3	4	5	6	7	8	9	10
HL1	10.1	10.1	8.0	8.3	5.3	4.7	3.9	3.7	4.5	4.4
HL2	10.6	10.6	8.6	8.9	5.8	5.4	3.9	3.5	4.4	4.2
HL3	10.8	10.8	9.2	9.3	6.6	6.2	3.9	3.4	4.3	4.1
HL4	11.1	11.1	9.7	9.7	7.4	7.0	4.0	3.4	4.4	4.1
HL5	11.3	11.3	10.0	10.2	8.1	7.9	4.2	3.8	4.5	4.2
HL6	11.7	11.7	10.4	10.7	8.7	8.4	4.7	4.4	4.6	4.3
HL7	NR	NR	10.9	10.8	9.1	8.7	5.1	4.9	4.6	4.5
HL8	NR	NR	11.1	11.1	9.5	9.1	5.7	5.4	4.7	4.5
HL9	NR	NR	11.2	11.5	10.0	9.5	6.3	5.9	4.8	4.6
HL10	NR	NR	11.4	11.7	10.4	9.9	7.0	6.4	5.0	4.7

NR implies "not reliable" data

Table 4.14. Floating depth h_f (cm) calculated using measured C , LS.

Run	Block Number									
	1	2	3	4	5	6	7	8	9	10
LS1	4.7	4.8	4.1	4.4	3.9	3.9	4.4	4.1	4.0	4.0
LS2	5.5	5.6	4.2	4.5	3.6	3.5	4.2	4.0	3.8	3.9
LS3	5.7	5.8	4.3	4.6	3.2	3.2	4.1	3.9	3.7	3.8
LS4	5.8	6.0	4.4	4.5	3.1	2.9	4.0	3.8	3.6	3.6
LS5	6.0	6.1	4.5	4.6	2.9	2.7	3.9	3.7	3.5	3.6
LS6	6.1	6.0	4.3	4.6	2.5	2.5	3.8	3.7	3.5	3.5
LS7	6.1	6.0	4.1	4.4	2.3	2.3	3.8	3.7	3.4	3.5
LS8	6.2	6.1	4.2	4.4	2.1	2.0	3.7	3.6	3.3	3.4
LS9	6.2	6.1	4.3	4.5	2.0	1.9	3.6	3.6	3.2	3.4
LS10	6.4	6.3	4.4	4.5	1.9	2.0	3.5	3.6	3.1	3.3

Table 4.15. Floating depth h_f (cm) calculated using measured C , MS.

Run	Block Number									
	1	2	3	4	5	6	7	8	9	10
MS1	6.8	6.7	4.8	4.8	1.9	2.1	3.2	3.3	3.0	3.1
MS2	7.0	7.1	5.1	5.2	2.2	2.3	3.0	2.9	2.9	2.9
MS3	7.3	7.3	5.3	5.3	2.5	2.5	3.0	2.8	2.8	2.8
MS4	7.6	7.5	5.5	5.5	2.8	2.7	2.9	2.7	2.8	2.7
MS5	7.7	7.6	5.6	5.7	2.9	2.9	2.7	2.5	2.8	2.5
MS6	7.8	7.7	5.8	5.8	3.1	3.0	2.6	2.3	2.7	2.5
MS7	8.2	8.0	6.0	6.1	3.5	3.3	2.7	2.2	3.0	2.9

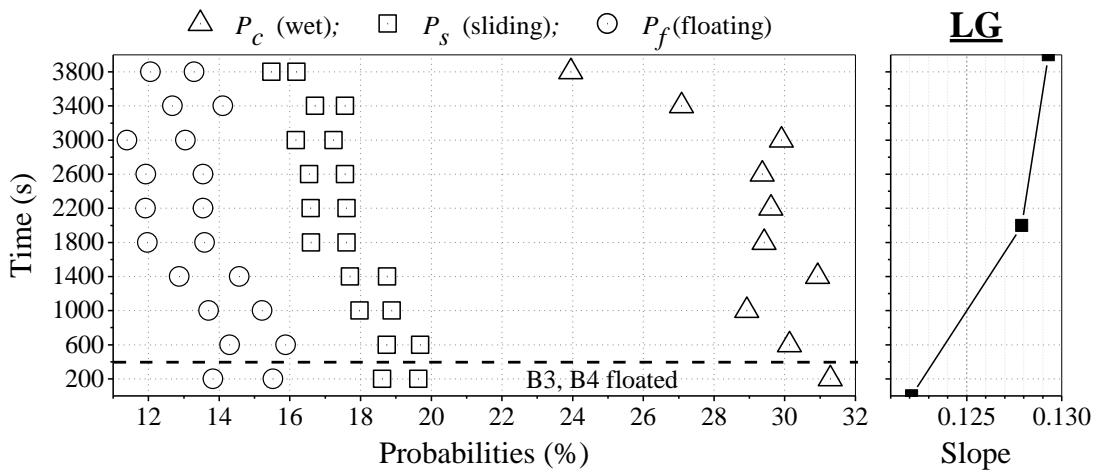


Figure 4.3. Estimated floating (P_f), sliding (P_s), and wetting (P_c) probabilities for blocks 3 and 4 (left), and slope change (right) during test LG.

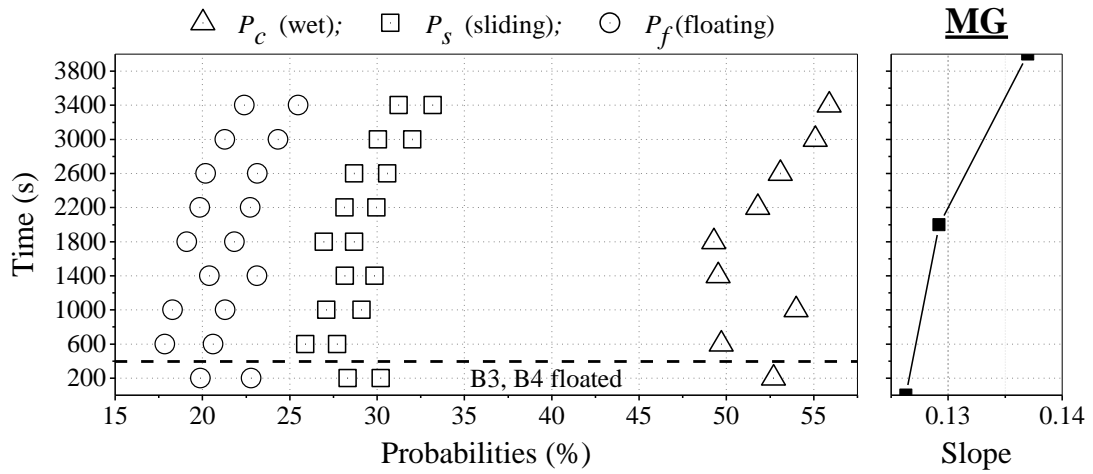


Figure 4.4. Estimated floating (P_f), sliding (P_s), and wetting (P_c) probabilities for blocks 3 and 4 (left), and slope change (right) during test MG.

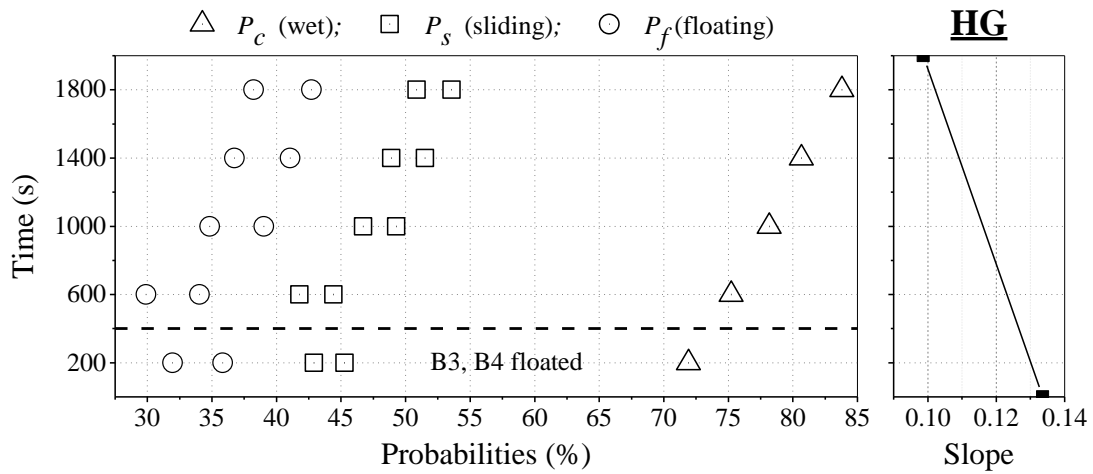


Figure 4.5. Estimated floating (P_f), sliding (P_s), and wetting (P_c) probabilities for blocks 3 and 4 (left), and slope change (right) during test HG.

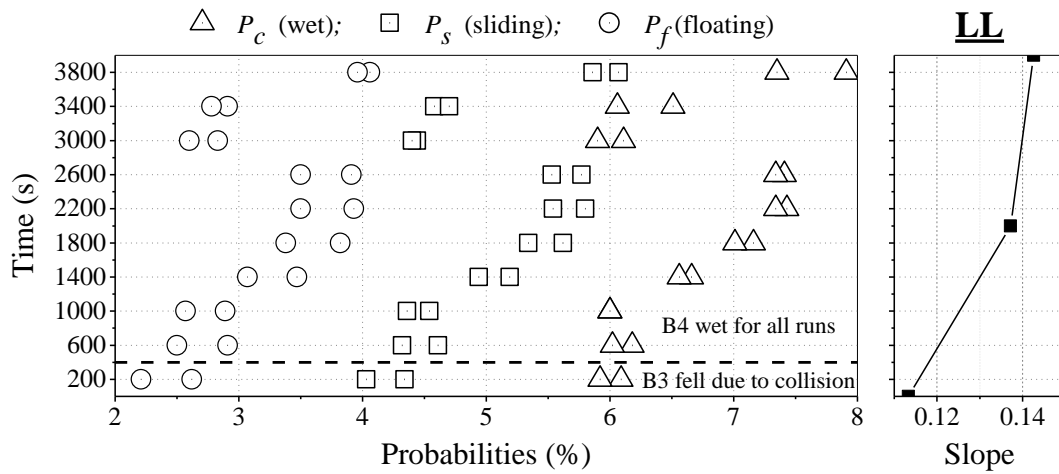


Figure 4.6. Estimated floating (P_f), sliding (P_s), and wetting (P_c) probabilities for blocks 3 and 4 (left), and slope change (right) during the test LL.

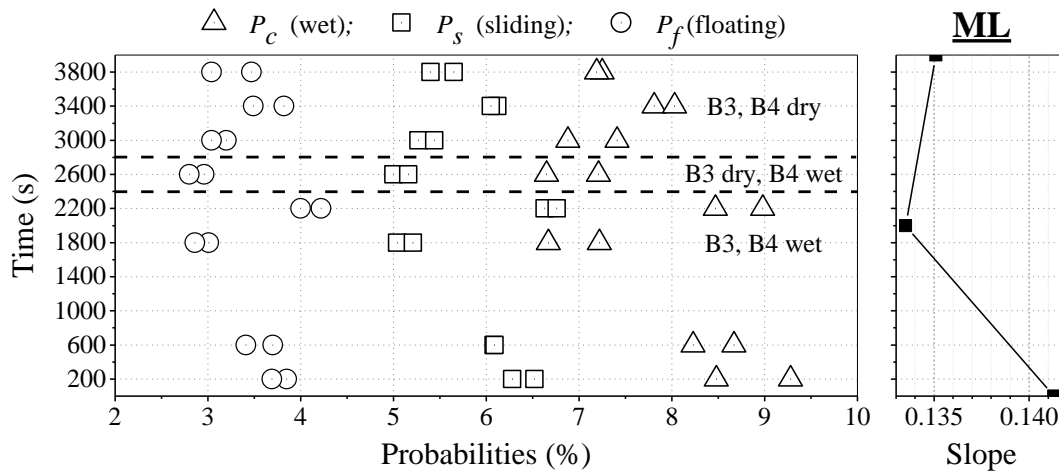


Figure 4.7. Estimated floating (P_f), sliding (P_s), and wetting (P_c) probabilities for blocks 3 and 4 (left), and slope change (right) during test ML.

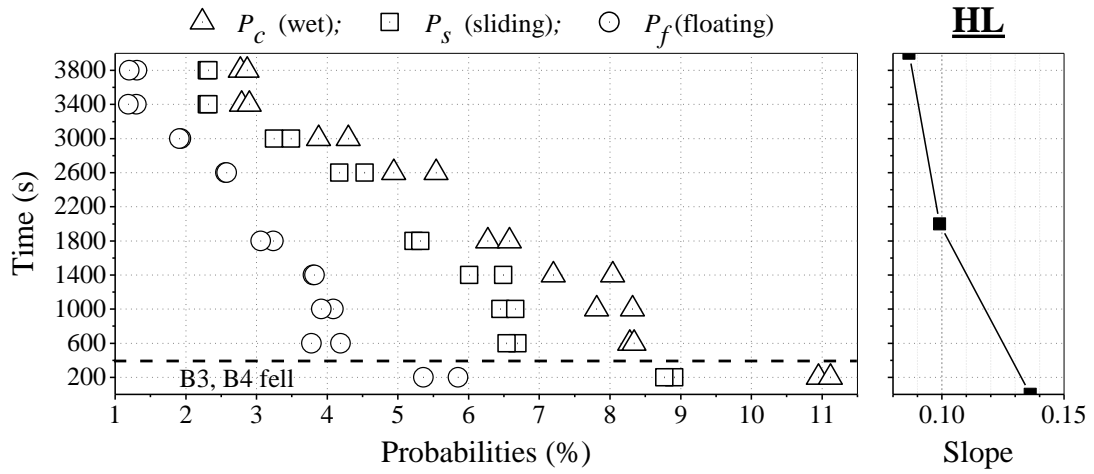


Figure 4.8. Estimated floating (P_f), sliding (P_s), and wetting (P_c) probabilities for blocks 3 and 4 (left), and slope change (right) during test HL.

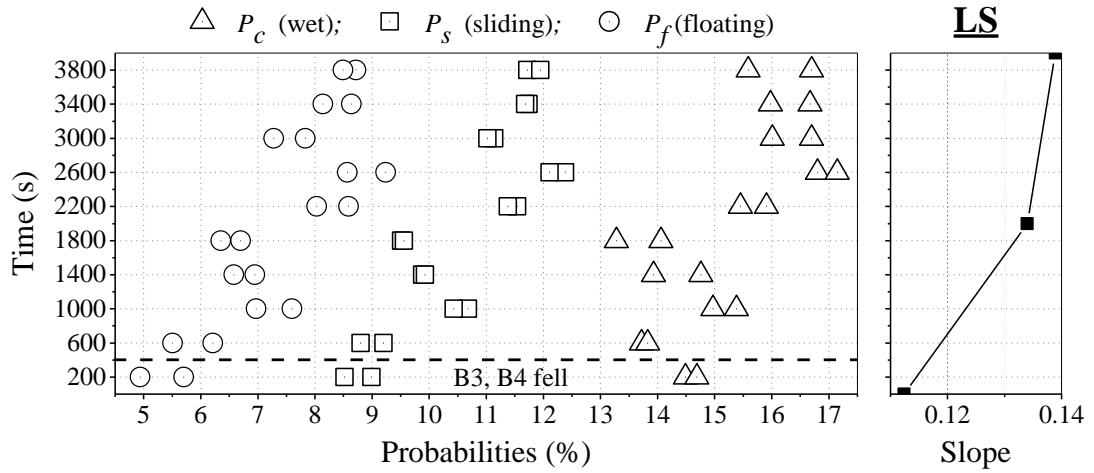


Figure 4.9. Estimated floating (P_f), sliding (P_s), and wetting (P_c) probabilities for blocks 3 and 4 (left), and slope change (right) during test LS.

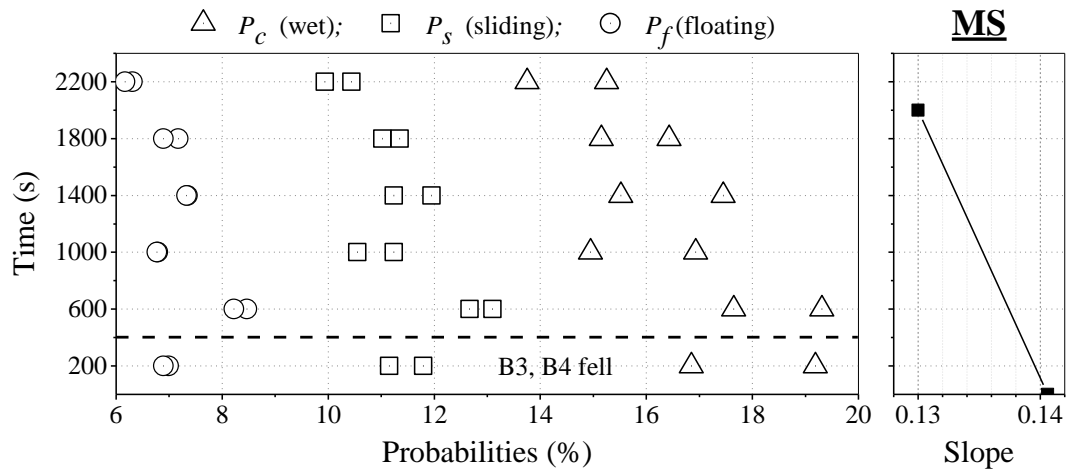


Figure 4.10. Estimated floating (P_f), sliding (P_s), and wetting (P_c) probabilities for blocks 3 and 4 (left), and slope change (right) during test MS.

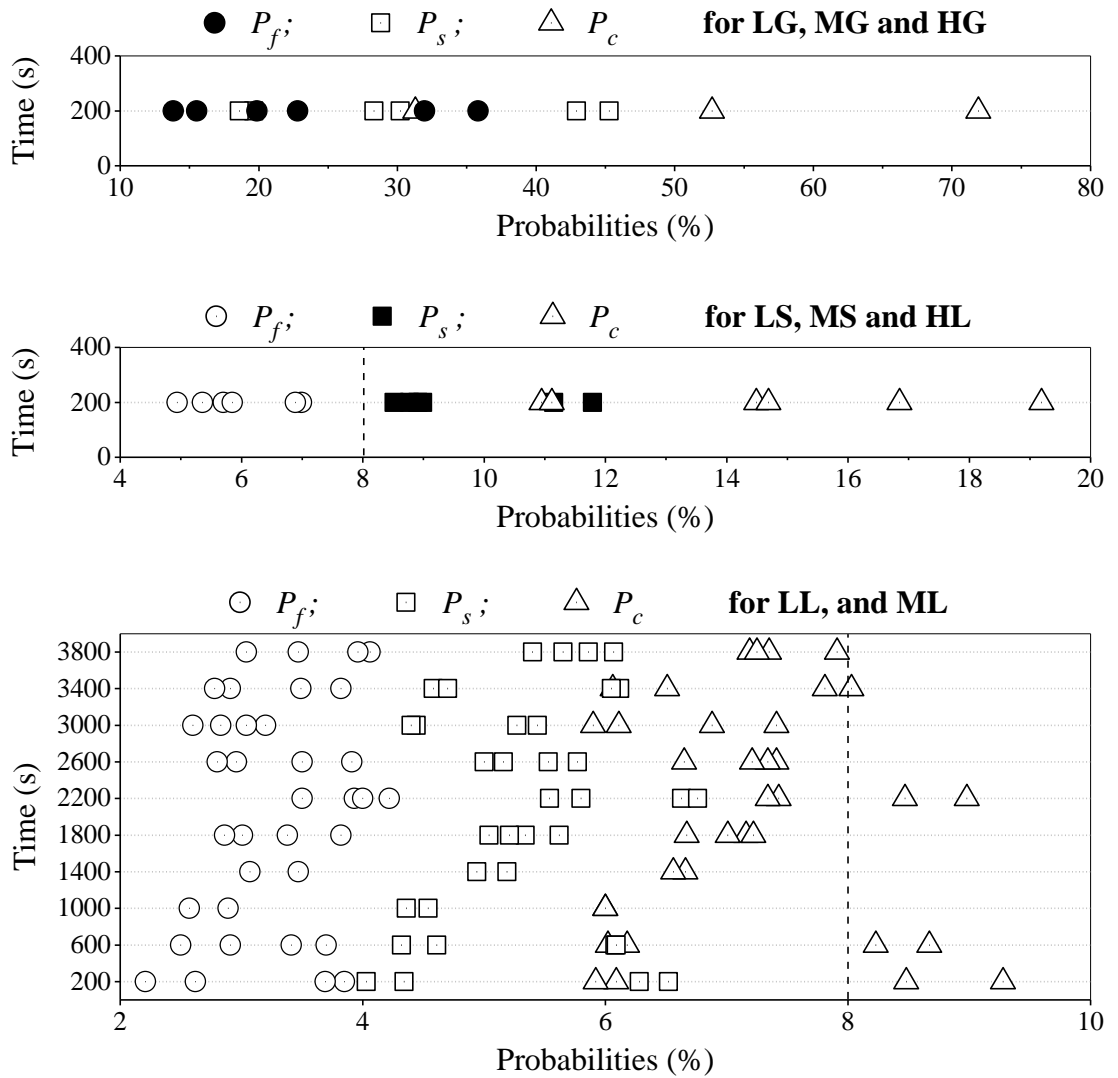


Figure 4.11. Estimated floating (P_f), sliding (P_s), and wetting (P_c) probabilities for blocks 3 and 4 for tests LG, MG, and HG (blocks 3 and 4 floated in run 1), for tests LS, MS, and HL (blocks 3 and 4 fell in run 1), and for tests LL and ML (blocks 3 and 4 did not fall during run 1-10).

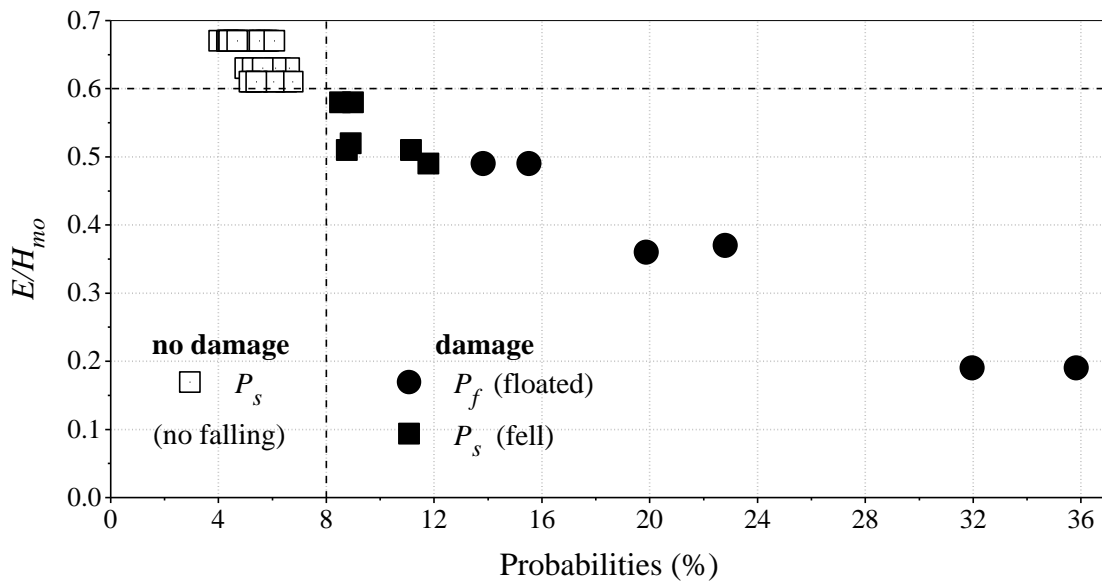


Figure 4.12. Estimated probabilities (P_f for blocks on ground and P_s for blocks on pilings) compared with normalized block elevation E/H_{m0} for blocks 3 and 4.

Chapter 5

CONCLUSIONS

A laboratory experiment consisting of eight tests was conducted in a wave flume with a sand beach to examine the movement of 10 wooden blocks placed on the foreshore and berm as well as on short and long pilings. The still water level was varied to create accretional and erosional profile changes on the foreshore and berm. The cross-shore wave transformation was measured using eight wave gauges and three velocimeters in a 400-s run of irregular waves. The wave overtopping rate and sand overwash rate in each run were measured at the landward end of the berm in 71 runs. The initial block elevation above the sand surface is shown to have little effect on the cross-shore wave transformation and overtopping and the beach profile evolution and sand overwash in this experiment with two blocks blocking $1/6.5$ of the flume width. This finding is convenient for the prediction of the width-averaged hydrodynamics, sediment transport, and morphology apart from local scour around the blocks and pilings.

The block floating and sliding on the sand surface and the block falling from the pilings depended partly on the block elevation above the still water level but on the swash hydrodynamics and the block clearance above the foreshore and berm whose profile varied during each test. A simple probabilistic model is developed to estimate the wetting, sliding, and floating probabilities for the block in the swash zone using the water depth measured in the vicinity of the block. The damage threshold probability of 8% is shown to explain the observed block floating and falling in this limited experiment. The data will be used to extend the cross-shore numerical model CSHORE (Figlus *et al.*, 2011; Kobayashi *et al.*, 2013; Ayat and Kobayashi, 2015) for the

prediction of damage on residential buildings during a storm. Existing methods such as those in Coastal Construction Manual (U.S. Department of Homeland Security, Federal Emergency Management Agency, 2011) do not account for morphology evolution and building damage progression during a storm.

REFERENCES

- Ayat, B. and Kobayashi, N., 2015. Vertical cylinder density and toppling effects on dune erosion and overwash. *Journal of Waterway, Port, Coastal, Ocean Engineering*, 141(1), 04014026, 1-10.
- Edge, B.L.; Ewing, L.; Dean, R.G.; Kaihatu, J.M.; Overton, M.; Rogers, S.M., and Work, P.A., 2010. Immediate impacts of Hurricane Ike on the Texas coast. *Proceedings of 32nd Coastal Engineering Conference, Management 14*, 1-16, <http://journals.tdl.org/icce>.
- Figlus, J.; Kobayashi, N., and Gralher, C., 2012. Onshore migration of emerged ridge and ponded runnel. *Journal of Waterway, Port, Coastal, Ocean Engineering*, 138(5), 331-338.
- Figlus, J.; Kobayashi, N.; Gralher, C., and Iranzo, V., 2011. Wave overtopping and overwash of dunes. *Journal of Waterway, Port, Coastal, Ocean Engineering*, 137(1), 26-33.
- Kobayashi, N.; Farhadzadeh, A.; Melby, J.A.; Johnson, B., and Gravens, M. 2010. Wave overtopping of levees and overwash of dunes. *Journal of Coastal Research*, 26(5), 888-900.
- Kobayashi, N., and Otta, A.K., 1987. Hydraulic stability analysis of armor units. *Journal of Waterway, Port, Coastal, Ocean Engineering*, 113(2), 171-186.
- Kobayashi, N.; Pietropaolo, J.A., and Melby, J.A., 2013. Wave transformation and runup on dikes and gentle slopes. *Journal of Coastal Research*, 29(3), 615-623.

- Tomiczek, K.T.; Kennedy, A., and Rogers, S., 2014. Collapse limit state fragilities of wood-framed residences from storm surge and waves during Hurricane Ike. *Journal of Waterway, Port, Coastal, Ocean Engineering*, 140(1), 43-55.
- Walling, K.; Miller, J.K.; Herrington, T.O., and Eble, A., 2014. Comparison of Hurricane Sandy impacts in three New Jersey coastal communities. *Proceedings of 34th Coastal Engineering Conference, Management 38*, 1-14, <http://journals.tdl.org/icce>.
- United States Department of Homeland Security, Federal Emergency Management Agency. 2011. *Coastal Construction Manual: Principles and practices of planning, siting, designing, constructing, and maintaining residential buildings in coastal areas*, 4th edition, FEME P-55, Volume 1.

Appendix

ADDITIONAL DATA

Table A. 1. Still water shoreline location (m) for 8 tests: before run 1 (X_{S0}), after run 5 (X_{S5}) and after run 10 (X_{S10}).

Test	X_{S0}	X_{S5}	X_{S10}
LG	17.88	17.96	17.96
MG	18.13	18.22	18.26
HG	18.40	18.58	-
LL	17.86	18.00	18.05
ML	18.19	18.26	18.26
HL	18.40	18.55	18.65
LS	17.84	18.02	18.06
MS	18.20	18.30	18.31*

* After run 7 (X_{S7}) (large wave)

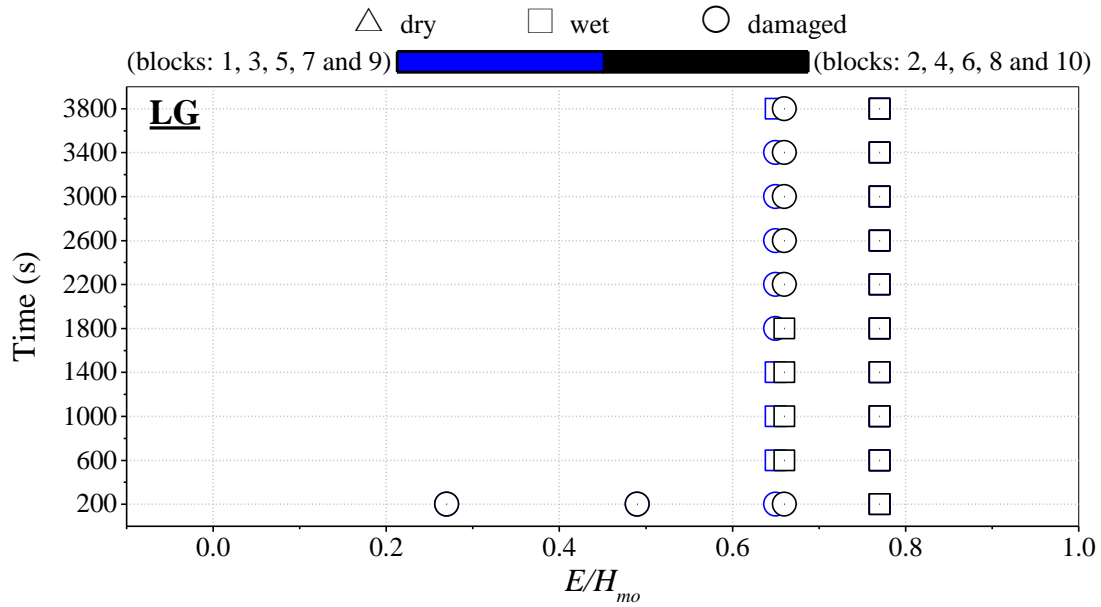


Figure A. 1. Comparisons of response (damaged, wet, and dry) of 10 blocks during test LG using block elevation E above SWL normalized by incident wave height H_{m0} .

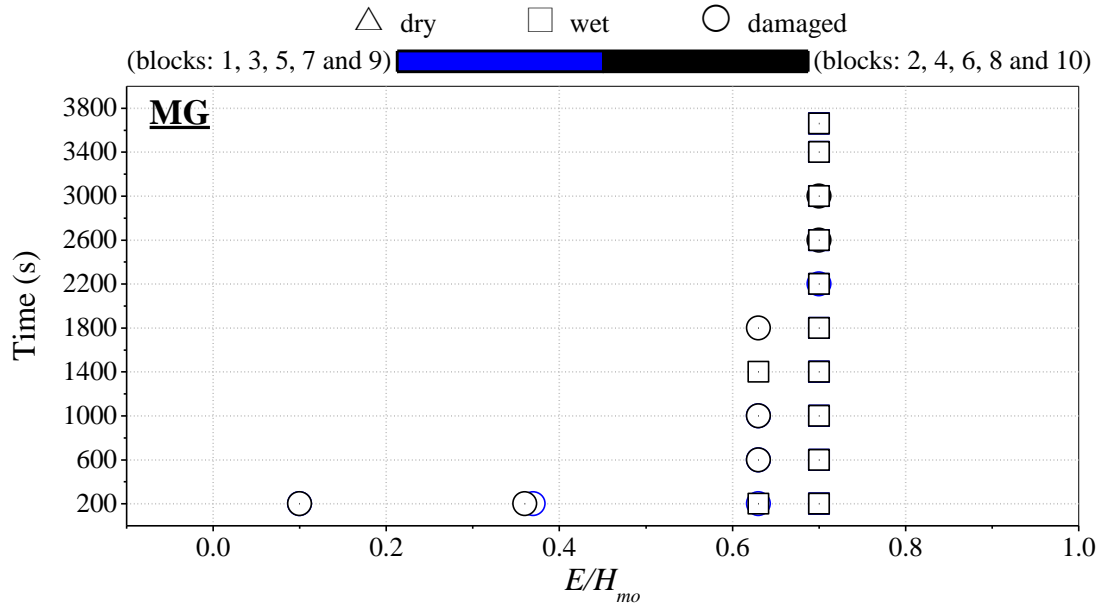


Figure A. 2. Comparisons of response (damaged, wet, and dry) of 10 blocks during test MG using block elevation E above SWL normalized by incident wave height H_{m0} .

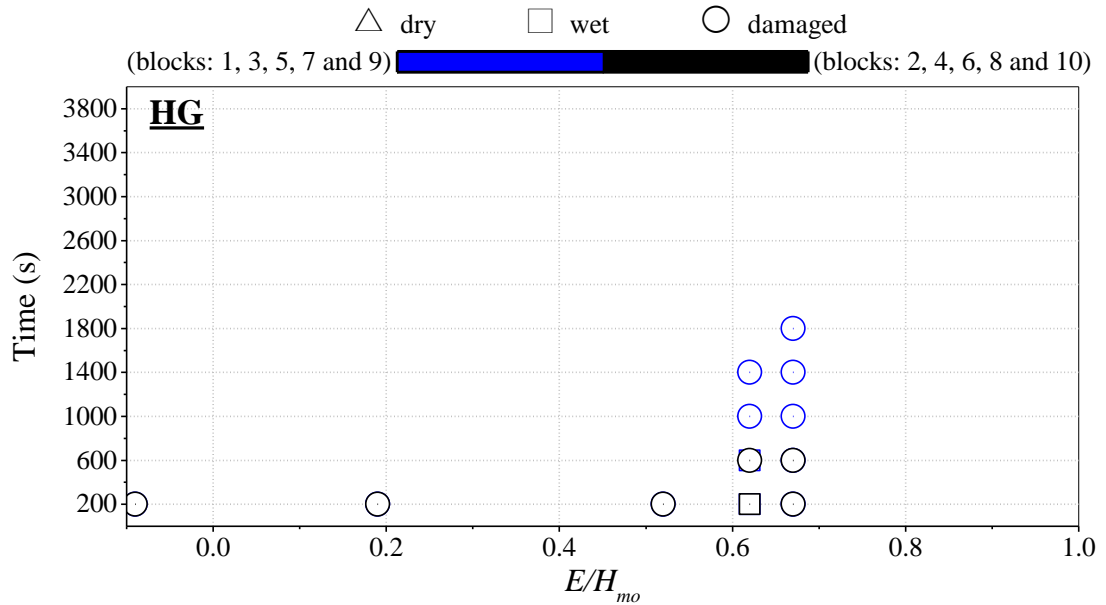


Figure A. 3. Comparisons of response (damaged, wet, and dry) of 10 blocks during test HG using block elevation E above SWL normalized by incident wave height H_{m0} .

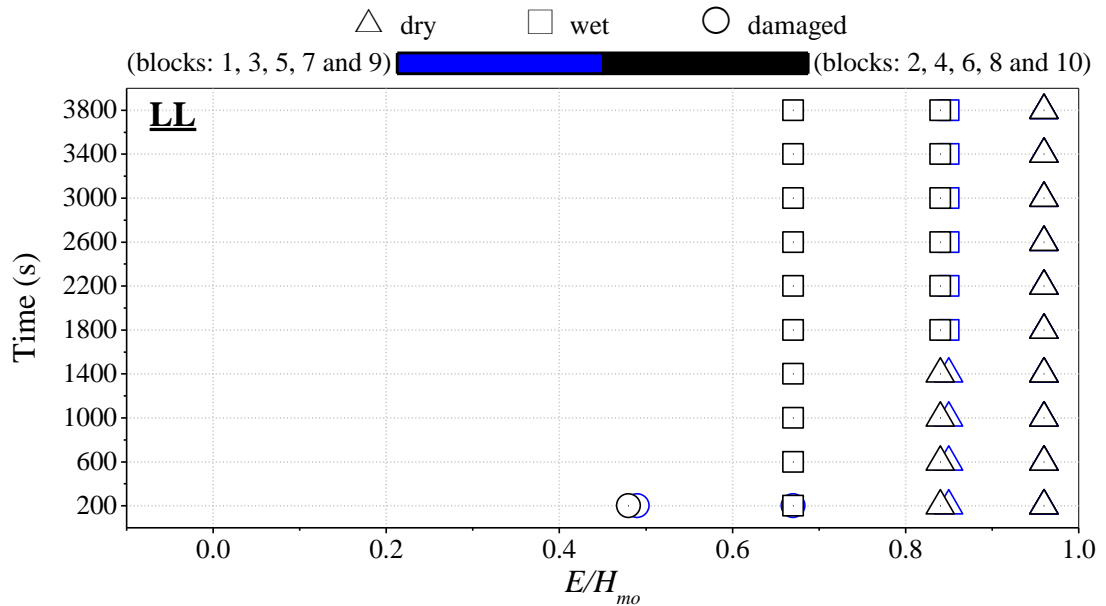


Figure A. 4. Comparisons of response (damaged, wet, and dry) of 10 blocks during test LL using block elevation E above SWL normalized by incident wave height H_{m0} .

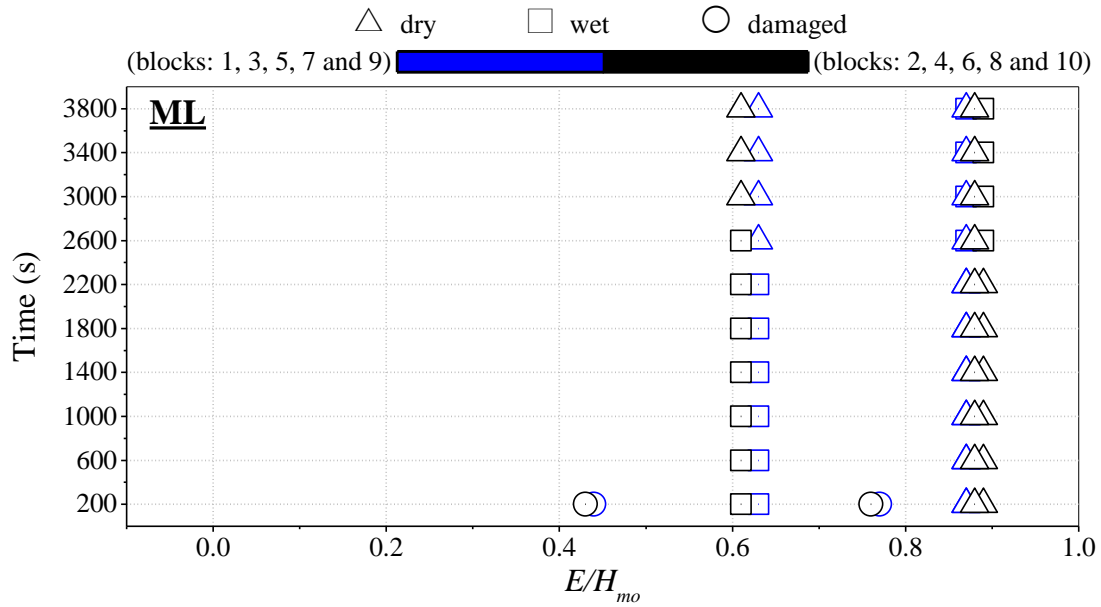


Figure A. 5. Comparisons of response (damaged, wet, and dry) of 10 blocks during test ML using block elevation E above SWL normalized by incident wave height H_{m0} .

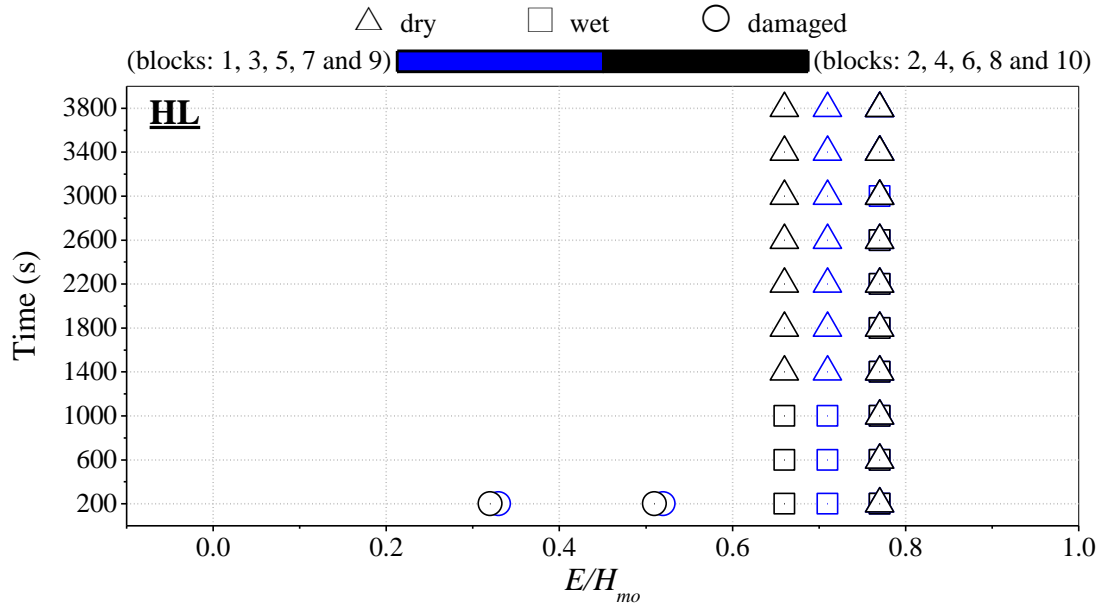


Figure A. 6. Comparisons of response (damaged, wet, and dry) of 10 blocks during test HL using block elevation E above SWL normalized by incident wave height H_{m0} .

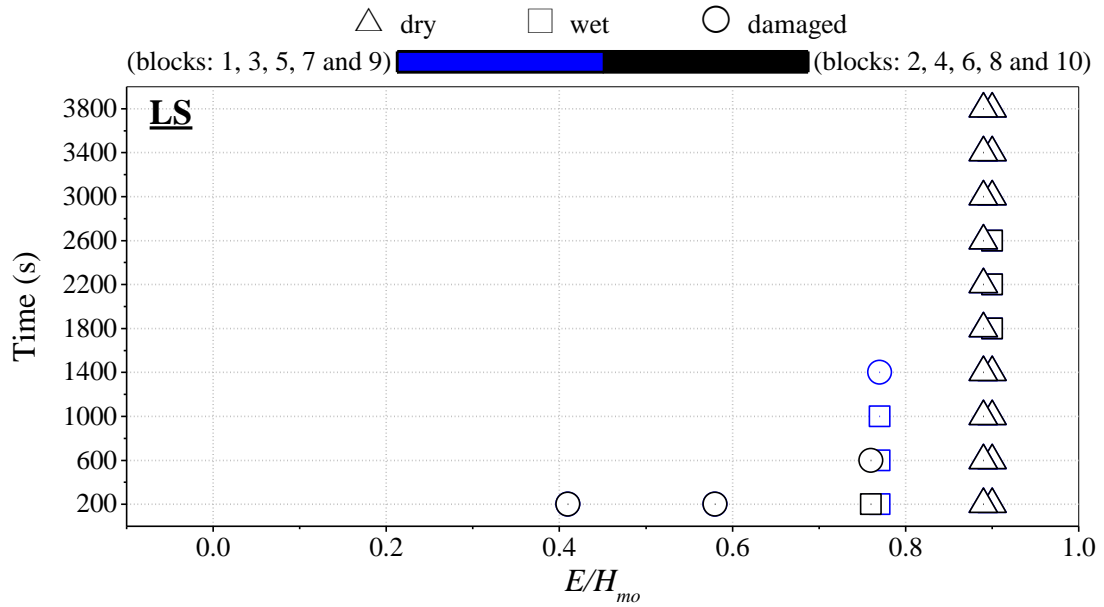


Figure A. 7. Comparisons of response (damaged, wet, and dry) of 10 blocks during test LS using block elevation E above SWL normalized by incident wave height H_{m0} .

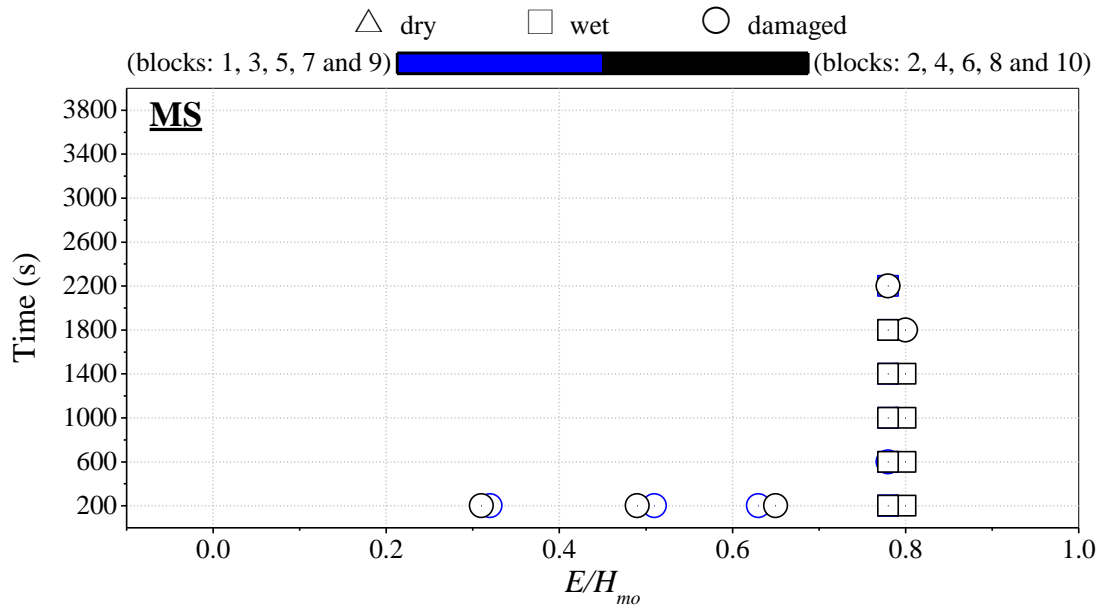


Figure A. 8. Comparisons of response (damaged, wet, and dry) of 10 blocks during test MS using block elevation E above SWL normalized by incident wave height H_{m0} .

Table A. 2. Wetting probability P_c , sliding probability P_s , and floating probability P_f of blocks 3 and 4, LG.

Run	\bar{h} (cm)	σ_η (cm)	P_w	P_c (%)	h_s (cm)		h_f (cm)		P_s (%)			P_f (%)		
	WG 8				B3	B4	B3	B4	B3	B4	Average	B3	B4	Average
LG1	0.91	0.62	0.31	31.29	1.4	1.5	2.0	2.4	19.64	18.61	19.12	15.52	13.83	14.67
LG2	0.96	0.66	0.30	30.14	1.4	1.5	2.0	2.4	19.69	18.74	19.22	15.88	14.30	15.09
LG3	0.92	0.66	0.29	28.93	1.4	1.5	2.0	2.4	18.88	17.97	18.43	15.22	13.70	14.46
LG4	0.84	0.65	0.31	30.93	1.4	1.5	2.0	2.4	18.75	17.70	18.23	14.57	12.87	13.72
LG5	0.77	0.68	0.29	29.42	1.4	1.5	2.0	2.4	17.61	16.60	17.10	13.59	11.97	12.78
LG6	0.77	0.66	0.30	29.61	1.4	1.5	2.0	2.4	17.61	16.59	17.10	13.55	11.92	12.73
LG7	0.77	0.67	0.29	29.37	1.4	1.5	2.0	2.4	17.56	16.55	17.06	13.55	11.93	12.74
LG8	0.73	0.67	0.30	29.91	1.4	1.5	2.0	2.4	17.24	16.17	16.71	13.05	11.39	12.22
LG9	0.85	0.71	0.27	27.08	1.4	1.5	2.0	2.4	17.56	16.71	17.13	14.11	12.68	13.40
LG10	0.83	0.74	0.24	23.95	1.4	1.5	2.0	2.4	16.19	15.48	15.83	13.29	12.06	12.67

Table A. 3. Wetting probability P_c , sliding probability P_s , and floating probability P_f of blocks 3 and 4, MG.

Run	\bar{h}	σ_η	P_w	P_c	h_s (cm)				P_s (%)			P_f (%)		
	(cm)	(cm)			B3	B4	B3	B4	B3	B4	Average	B3	B4	Average
	WG 8				B3	B4	B3	B4	B3	B4	Average	B3	B4	Average
MG1	1.28	0.82	0.53	52.70	1.4	1.5	2.0	2.4	30.21	28.32	29.27	22.80	19.88	21.34
MG2	1.15	0.85	0.50	49.71	1.4	1.5	2.0	2.4	27.71	25.89	26.80	20.62	17.85	19.23
MG3	1.18	0.87	0.54	53.99	1.4	1.5	2.0	2.4	29.11	27.10	28.11	21.31	18.29	19.80
MG4	1.32	0.85	0.50	49.53	1.4	1.5	2.0	2.4	29.85	28.15	29.00	23.12	20.40	21.76
MG5	1.23	0.88	0.49	49.29	1.4	1.5	2.0	2.4	28.69	26.95	27.82	21.83	19.10	20.46
MG6	1.28	0.91	0.52	51.79	1.4	1.5	2.0	2.4	29.97	28.14	29.05	22.74	19.86	21.30
MG7	1.30	0.92	0.53	53.09	1.4	1.5	2.0	2.4	30.58	28.68	29.63	23.14	20.19	21.66
MG8	1.37	0.94	0.55	55.09	1.4	1.5	2.0	2.4	32.01	30.06	31.03	24.33	21.28	22.80
MG9	1.45	0.96	0.56	55.89	1.4	1.5	2.0	2.4	33.18	31.24	32.21	25.49	22.41	23.95
MG10	NR	NR	NR	NR	1.4	1.5	2.0	2.4	NR	NR	NR	NR	NR	NR

NR implies "not reliable" data

Table A. 4. Wetting probability P_c , sliding probability P_s , and floating probability P_f of blocks 3 and 4, HG.

Run	\bar{h} (cm)	σ_h (cm)	P_w	P_c (%)	h_s (cm)		h_f (cm)		P_s (%)			P_f (%)		
	WG 8				B3	B4	B3	B4	B3	B4	Average	B3	B4	Average
HG1	2.10	1.34	0.72	71.92	1.4	1.5	2.0	2.4	45.27	42.91	44.09	35.83	31.96	33.89
HG2	1.93	1.44	0.75	75.22	1.4	1.5	2.0	2.4	44.42	41.79	43.10	34.04	29.89	31.96
HG3	2.29	1.53	0.78	78.16	1.4	1.5	2.0	2.4	49.28	46.71	47.99	39.03	34.83	36.93
HG4	2.43	1.60	0.81	80.67	1.4	1.5	2.0	2.4	51.50	48.90	50.20	41.06	36.75	38.90
HG5	2.53	1.67	0.84	83.80	1.4	1.5	2.0	2.4	53.56	50.85	52.20	42.72	38.24	40.48

Table A. 5. Wetting probability P_c , sliding probability P_s , and floating probability P_f of blocks 3 and 4, LL.

Run	\bar{h}	σ_η	P_w	C (cm)		h_s (cm)		h_f (cm)		P_c (%)			P_s (%)			P_f (%)		
	(cm)	(cm)		B3	B4	B3	B4	B3	B4	B3	B4	Average	B3	B4	Average	B3	B4	Average
LL1	0.8	0.61	0.33	4.1	4.2	4.9	5.1	6.1	6.5	6.09	5.92	6.00	4.34	4.03	4.19	2.62	2.21	2.41
LL2	0.83	0.68	0.31	4.3	4.4	5.1	5.3	6.4	6.8	6.18	6.02	6.10	4.61	4.32	4.47	2.91	2.50	2.71
LL3	0.84	0.71	0.30	4.5	4.5	5.3	5.4	6.5	6.9	6.00	6.00	6.00	4.54	4.36	4.45	2.89	2.57	2.73
LL4	0.88	0.72	0.28	4.5	4.6	5.3	5.4	6.5	6.9	6.66	6.56	6.61	5.19	4.94	5.06	3.47	3.07	3.27
LL5	0.92	0.72	0.28	4.5	4.5	5.2	5.4	6.5	6.9	7.16	7.01	7.09	5.62	5.34	5.48	3.82	3.38	3.60
LL6	0.93	0.73	0.29	4.4	4.4	5.2	5.3	6.4	6.8	7.43	7.34	7.39	5.80	5.54	5.67	3.93	3.50	3.71
LL7	0.91	0.73	0.29	4.3	4.3	5.1	5.2	6.3	6.7	7.41	7.34	7.37	5.77	5.53	5.65	3.91	3.50	3.71
LL8	0.8	0.78	0.29	4.4	4.3	5.2	5.2	6.4	6.7	5.90	6.11	6.00	4.44	4.40	4.42	2.83	2.60	2.71
LL9	0.85	0.8	0.31	4.5	4.3	5.3	5.2	6.5	6.7	6.06	6.51	6.28	4.58	4.70	4.64	2.91	2.78	2.85
LL10	0.95	0.83	0.28	4.6	4.3	5.3	5.2	6.6	6.7	7.35	7.91	7.63	5.86	6.07	5.96	4.06	3.96	4.01

Table A. 6. Wetting probability P_c , sliding probability P_s , and floating probability P_f of blocks 3 and 4, ML.

Run	\bar{h}	σ_η	P_w	C (cm)		h_s (cm)		h_f (cm)		P_c (%)			P_s (%)			P_f (%)		
	(cm)	(cm)		B3	B4	B3	B4	B3	B4	B3	B4	Average	B3	B4	Average	B3	B4	Average
ML1	1.27	0.82	0.49	4.5	4.3	5.3	5.2	6.6	6.7	8.48	9.28	8.88	6.28	6.52	6.40	3.85	3.69	3.77
ML2	1.27	0.87	0.50	4.6	4.5	5.3	5.3	6.6	6.8	8.23	8.67	8.45	6.08	6.09	6.09	3.70	3.41	3.55
ML3	NR	NR	NR	4.8	4.7	5.6	5.6	6.8	7.1	NR	NR	NR	NR	NR	NR	NR	NR	NR
ML4	NR	NR	NR	5.1	4.9	5.8	5.7	7.1	7.2	NR	NR	NR	NR	NR	NR	NR	NR	NR
ML5	1.35	0.93	0.53	5.3	5.1	6.0	5.9	7.3	7.4	6.67	7.22	6.94	5.04	5.21	5.12	3.01	2.86	2.93
ML6	1.52	0.92	0.52	5.3	5.1	6.0	6.0	7.3	7.5	8.47	8.98	8.73	6.63	6.76	6.70	4.22	4.00	4.11
ML7	1.38	0.94	0.55	5.3	5.1	6.0	5.9	7.3	7.5	6.65	7.21	6.93	5.00	5.16	5.08	2.96	2.80	2.88
ML8	1.42	0.95	0.53	5.5	5.3	6.2	6.1	7.5	7.6	6.88	7.41	7.14	5.27	5.44	5.35	3.20	3.04	3.12
ML9	1.58	0.95	0.56	5.6	5.5	6.3	6.3	7.6	7.9	7.81	8.03	7.92	6.12	6.05	6.08	3.82	3.49	3.66
ML10	1.57	0.96	0.57	5.7	5.7	6.4	6.5	7.7	8.1	7.25	7.19	7.22	5.65	5.40	5.52	3.47	3.04	3.25

NR implies "not reliable" data

Table A. 7. Wetting probability P_c , sliding probability P_s , and floating probability P_f of blocks 3 and 4, HL.

Run	\bar{h}	σ_η	P_w	C (cm)		h_s (cm)		h_f (cm)		P_c (%)			P_s (%)			P_f (%)		
	(cm)	(cm)		B3	B4	B3	B4	B3	B4	B3	B4	Average	B3	B4	Average	B3	B4	Average
HL1	2.26	1.36	0.70	6.0	6.0	6.7	6.7	8.0	8.3	10.95	11.12	11.04	8.91	8.77	8.84	5.85	5.36	5.60
HL2	2.22	1.46	0.74	6.6	6.5	7.2	7.3	8.6	8.9	8.28	8.34	8.31	6.69	6.54	6.61	4.19	3.78	3.98
HL3	2.41	1.51	0.77	7.2	7.0	7.8	7.7	9.2	9.3	7.81	8.32	8.06	6.45	6.66	6.56	4.09	3.92	4.01
HL4	2.53	1.54	0.79	7.7	7.3	8.2	8.0	9.7	9.7	7.20	8.04	7.62	6.01	6.49	6.25	3.80	3.82	3.81
HL5	2.54	1.6	0.82	8.0	7.8	8.5	8.5	10.0	10.2	6.27	6.58	6.42	5.22	5.32	5.27	3.24	3.06	3.15
HL6	NR	NR	NR	8.4	8.3	8.9	8.9	10.4	10.7	NR	NR	NR	NR	NR	NR	NR	NR	NR
HL7	2.66	1.65	0.86	8.8	8.5	9.4	9.1	10.9	10.8	4.94	5.54	5.24	4.17	4.53	4.35	2.56	2.58	2.57
HL8	2.53	1.7	0.87	9.0	8.7	9.5	9.3	11.1	11.1	3.88	4.30	4.09	3.25	3.49	3.37	1.93	1.91	1.92
HL9	2.35	1.72	0.88	9.2	9.1	9.7	9.7	11.2	11.5	2.79	2.90	2.84	2.30	2.32	2.31	1.30	1.19	1.25
HL10	2.42	1.73	0.89	9.4	9.3	9.9	9.9	11.4	11.7	2.77	2.87	2.82	2.30	2.32	2.31	1.31	1.20	1.25

NR implies "not reliable" data

Table A. 8. Wetting probability P_c , sliding probability P_s , and floating probability P_f of blocks 3 and 4, LS.

Run	\bar{h}	σ_η	P_w	C (cm)		h_s (cm)		h_f (cm)		P_c (%)			P_s (%)			P_f (%)		
	(cm)	(cm)		B3	B4	B3	B4	B3	B4	B3	B4	Average	B3	B4	Average	B3	B4	Average
LS1	0.82	0.62	0.38	2.1	2.1	3.1	3.2	4.1	4.4	14.49	14.69	14.59	8.99	8.52	8.75	5.70	4.94	5.32
LS2	0.83	0.7	0.32	2.2	2.2	3.2	3.3	4.2	4.5	13.72	13.83	13.78	9.20	8.80	9.00	6.21	5.51	5.86
LS3	0.96	0.75	0.32	2.3	2.2	3.3	3.4	4.3	4.6	14.97	15.38	15.18	10.68	10.43	10.56	7.60	6.97	7.29
LS4	0.91	0.74	0.31	2.4	2.2	3.4	3.3	4.4	4.5	13.93	14.76	14.35	9.88	9.93	9.90	6.95	6.58	6.77
LS5	0.9	0.78	0.30	2.5	2.3	3.4	3.4	4.5	4.6	13.28	14.06	13.67	9.51	9.56	9.54	6.70	6.35	6.52
LS6	1.04	0.78	0.30	2.3	2.2	3.3	3.4	4.3	4.6	15.45	15.91	15.68	11.54	11.38	11.46	8.59	8.03	8.31
LS7	1.06	0.81	0.31	2.1	2.0	3.1	3.2	4.1	4.4	16.80	17.15	16.98	12.38	12.11	12.25	9.24	8.57	8.91
LS8	0.97	0.83	0.34	2.2	2.0	3.2	3.2	4.2	4.4	16.01	16.70	16.36	11.14	11.02	11.08	7.83	7.28	7.56
LS9	1.04	0.83	0.31	2.2	2.1	3.3	3.3	4.3	4.5	15.98	16.67	16.32	11.74	11.68	11.71	8.64	8.14	8.39
LS10	1.08	0.84	0.31	2.4	2.2	3.4	3.3	4.4	4.5	15.59	16.70	16.14	11.72	11.95	11.84	8.72	8.49	8.60

Table A. 9. Wetting probability P_c , sliding probability P_s , and floating probability P_f of blocks 3 and 4, MS.

Run	\bar{h}	σ_η	P_w	C (cm)		h_s (cm)		h_f (cm)		P_c (%)			P_s (%)			P_f (%)		
	(cm)	(cm)		B3	B4	B3	B4	B3	B4	B3	B4	Average	B3	B4	Average	B3	B4	Average
MS1	1.28	0.88	0.55	2.8	2.5	3.7	3.6	4.8	4.8	16.85	19.19	18.02	11.15	11.79	11.47	6.99	6.89	6.94
MS2	1.47	0.93	0.53	3.1	2.8	4.0	3.9	5.1	5.2	17.65	19.31	18.48	12.67	13.10	12.88	8.47	8.22	8.35
MS3	1.36	0.96	0.53	3.3	2.9	4.1	4.0	5.3	5.3	14.95	16.93	15.94	10.55	11.24	10.89	6.79	6.77	6.78
MS4	1.5	0.99	0.55	3.5	3.1	4.3	4.2	5.5	5.5	15.52	17.45	16.48	11.24	11.95	11.60	7.35	7.33	7.34
MS5	1.52	0.99	0.56	3.6	3.3	4.4	4.3	5.6	5.7	15.15	16.43	15.79	11.02	11.35	11.18	7.17	6.89	7.03
MS6	1.51	1.02	0.58	3.8	3.5	4.6	4.5	5.8	5.8	13.75	15.25	14.50	9.94	10.44	10.19	6.31	6.17	6.24